

Washington University in St. Louis

Washington University Open Scholarship

All Theses and Dissertations (ETDs)

5-24-2009

Uropathogenic E. coli Employ a Conserved Intracellular Infection Pathway that can be Inhibited by Novel Anti-Virulence Therapeutics

Corinne Cusumano

Washington University in St. Louis

Follow this and additional works at: <https://openscholarship.wustl.edu/etd>

Recommended Citation

Cusumano, Corinne, "Uropathogenic E. coli Employ a Conserved Intracellular Infection Pathway that can be Inhibited by Novel Anti-Virulence Therapeutics" (2009). *All Theses and Dissertations (ETDs)*. 884. <https://openscholarship.wustl.edu/etd/884>

This Dissertation is brought to you for free and open access by Washington University Open Scholarship. It has been accepted for inclusion in All Theses and Dissertations (ETDs) by an authorized administrator of Washington University Open Scholarship. For more information, please contact digital@wumail.wustl.edu.

WASHINGTON UNIVERSITY IN ST. LOUIS
Division of Biology and Biomedical Sciences
Molecular Microbiology and Microbial Pathogenesis

Dissertation Examination Committee:
Scott J. Hultgren, Ph.D., Chair
John P. Atkinson, M.D.
Tamara L. Doering, M.D., Ph.D.
Daniel E. Goldberg, M.D., Ph.D.
David A. Hunstad, M.D.
Jeffrey S. McKinney, M.D., Ph.D.

UROPATHOGENIC *ESCHERICHIA COLI* EMPLOY A CONSERVED INTRACELLULAR
INFECTION PATHWAY THAT CAN BE INHIBITED BY NOVEL ANTI-VIRULENCE
THERAPEUTICS

by

Corinne Katherine Cusumano

A dissertation presented to the
Graduate School of Arts and Sciences
of Washington University in
partial fulfillment of the
requirements for the degree
of Doctor of Philosophy

August 2009

Saint Louis, Missouri

copyright by
Corinne Katherine Cusumano
2009

ABSTRACT OF THE DISSERTATION

Uropathogenic *Escherichia coli* Employ a Conserved Intracellular Infection Pathway that
can be Inhibited by Novel Anti-Virulence Therapeutics

By

Corinne Katherine Cusumano

Doctor of Philosophy in Biology and Biomedical Sciences
(Molecular Microbiology and Microbial Pathogenesis)

Washington University in St. Louis, 2009

Professor Scott J. Hultgren, Chairperson

Urinary tract infections (UTIs) affect 13 million women annually in the United States and are predominately caused by uropathogenic *Escherichia coli* (UPEC). In a murine cystitis model, UPEC utilize a multistep pathogenic pathway in which they invade and form intracellular bacterial communities (IBCs) within bladder facet cells. Type 1 pili expressing the adhesin, FimH, are necessary for UPEC binding and invasion of urothelial cells and formation of IBCs. UPEC ultimately disperse from the IBC, many with filamentous morphology, and infect other host urothelial cells. Using a panel of UPEC clinical isolates, this work evaluates the conservation of the IBC pathway across UPEC, the function of a UPEC pathogenicity island (PAI) in the UPEC pathway, and the therapeutic effect of inhibition of FimH.

Investigation of 18 clinical isolates revealed that the majority of isolates proceed through the IBC cascade confirming its relevance in UPEC infection. Due to the commonality of the UPEC pathway, this panel of clinical isolates was used to investigate other determinants important in UPEC infection. One potential virulence determinant is pUTI89, isolated from UTI89. pUTI89 has many characteristics of a PAI thus it was evaluated for its presence in UPEC isolates and its role in pathogenesis. Evidence of

pUTI89 was found in 67% of UPEC isolates tested. Studies revealed that while there was no observable phenotype *in vitro* in the absence of pUTI89, there was a significant defect in binding, invasion and colonization at early time points post-infection, however, infection levels were restored by 24h post-infection. Since pUTI89 is not essential to UPEC infection, type 1 pili were used to develop a therapeutic against UPEC infection. Binding and invasion are critical to the UPEC pathway, thus inhibition of these early steps could result in unsuccessful colonization of the bladder. Knowledge of the FimH mannose-binding pocket enabled the rational development of mannosides that competitively inhibit binding to mannosylated uroplakins on the bladder surface.

These studies demonstrated the commonality of the IBC pathway among UPEC isolates as well as the importance of pUTI89 in early stages of UPEC infection. Knowledge of the UPEC pathway facilitated the development of novel therapeutics to inhibit binding and invasion and reduce infection.

ACKNOWLEDGEMENTS

This work was supported by NIH grants:
NIH DK64540, DK51406, AI029549 (S.J.H.)

and by Washington University in St. Louis:
Infectious Diseases/Basic Microbial Pathogenesis Mechanisms training grant (C.K.C.)

Thank you to my thesis committee and my mentor, Scott Hultgren. This thesis would not be possible without his advice, guidance and unequivocal understanding.

A special thanks to my friends and family, especially my husband and parents, for all they have taught me both in science and outside of science.

TABLE OF CONTENTS

Abstract of the Dissertation.....	ii
Acknowledgements.....	iv
Table of Contents.....	v
List of Tables, Figures, Illustrations.....	vii
Chapter One: Introduction to the Dissertation.....	1
Urinary tract infections.....	1
Recurrent infection.....	1
UPEC pathogenic cycle.....	3
UPEC clinical isolates and the UPEC pathogenic cycle.....	4
Urovirulence determinants.....	6
Pathogenicity islands.....	6
pUTI89.....	8
Type 1 pili.....	10
FimH.....	11
Small molecule inhibitors.....	12
Chaperone-Usher pathway.....	13
Chaperones.....	14
Subunits.....	14
Tip adhesins.....	15
Ushers.....	15
Pilicides.....	16
Summary.....	17
References.....	22
Chapter Two: <i>Escherichia coli</i> from Urine of Female Patients with Urinary Tract Infections is Competent for Intracellular Bacterial Community Formation.....	32
Abstract.....	33
Introduction.....	33
Materials and Methods.....	35
Results.....	40
Discussion.....	47
Acknowledgements.....	51
References.....	59
Chapter Three: The Plasmid pUTI89 from the Uropathogenic <i>Escherichia coli</i> strain, UTI89, has Virulence Properties	

Important for UTI Pathogenesis	63
Abstract.....	63
Introduction.....	64
Materials and Methods.....	68
Results.....	73
Discussion.....	80
Acknowledgements.....	85
References.....	95
Chapter Four: Intervening with Urinary Tract Infections Using Anti-Adhesives Based on the Crystal Structure of the FimH- Oligomannose-3 Complex	104
Abstract.....	105
Introduction.....	106
Materials and Methods.....	112
Results.....	117
Discussion.....	124
Acknowledgements.....	130
References.....	142
Chapter Five: Future Directions and Concluding Remarks	152
Conservation of the IBC pathogenic pathway among UPEC.....	152
Evaluation of the co-infection phenotype.....	154
pUTI89 as a virulence factor.....	157
Immune response in the absence of pUTI89.....	159
Functional <i>tra</i> operon.....	160
pUTI89 has an effect on chromosomal genes.....	162
Type 1 pili as a virulence factor.....	163
Treatment of UTIs.....	165
Mannosides.....	166
Pilicides.....	168
Concluding remarks.....	171
References.....	188
Appendix 1: Bacterial Adhesion – A Source of Alternative Antibiotic Targets	195
Abstract.....	195
Introduction.....	196
Rising antibiotic resistance.....	196
Alternative antibiotic targets.....	197
Pili in bacteria.....	198
Pili in UTI.....	199
New drug development strategies to inhibit pilus mediated function.....	201
Conclusion.....	205
Further reading.....	209

LIST OF TABLES, FIGURES, ILLUSTRATIONS

Chapter One: Introduction to the Dissertation

Figure 1	UPEC pathogenesis pathway.....	19
Figure 2	Type 1 pili interact with uroplakins on the bladder surface.....	20
Figure 3	UPEC type 1 pili encoded by the <i>fim</i> operon.....	20
Figure 4	The FimH adhesin accommodates mannose in its binding pocket..	21
Figure 5	Chaperone/usher mediated pilus biogenesis as shown for the P pilus system.....	21

Chapter Two: *Escherichia coli* from Urine of Female Patients with Urinary Tract Infections is Competent for Intracellular Bacterial Community Formation

Table 1	Characterization of UTI isolates collected.....	52
Table 2	Virulence genotypes and hemagglutination titers of clinical isolates.....	53
Table 3	IBC formation at different time points.....	54
Figure 1	Immunoblot of pyelonephritis isolates with antibodies against P pili.....	54
Figure 2	UTI89 and CFT073 formed IBCs in multiple mouse strains.....	55
Figure 3	IBCs were formed by UPEC strains isolated from women.....	56
Figure 4	The three non-IBC-forming isolates, rUTI1, acute4, and pyelo3, were deficient in invasion <i>in vivo</i>	57
Figure 5	Co-infection with a clinical isolate and UTI89 altered the behavior of bacteria.....	58

Chapter Three: The Plasmid pUTI89 from the Uropathogenic *Escherichia coli* strain, UTI89, has Virulence Properties Important for UTI Pathogenesis

Table 1	Primers for plasmid PCR.....	86
Table 2	Evidence of pUTI89 in a panel of clinical isolates.....	87

Table 3	Directed knock-outs of pUTI89.....	87
Figure 1	pUTI89 diagram.....	88
Figure 2	Confirmation of pUTI89 curing by PCR.....	89
Figure 3	<i>In vitro</i> characteristics of pUTI89.....	90
Figure 4	<i>In vivo</i> timecourse of UTI89 and Δ pUTI89.....	91
Figure 5	Colonization and invasion of UTI89 versus Δ pUTI89.....	92
Figure 6	Confocal microscopy and LacZ staining for IBCs.....	93
Figure 7	Identification of virulence factors on pUTI89.....	94

Chapter Four: Intervening with Urinary Tract Infections Using Anti-Adhesives Based on the Crystal Structure of the FimH-Oligomannose-3 Complex

Figure 1	Oligomannose-3 as part of the high-mannose glycans.....	131
Figure 2	Crystal structure of FimH in complex with oligomannose-3.....	132
Figure 3	Panel of FimH lectin domain interactions along the oligomannose-3 chain.....	133
Figure 4	Scheme of the interactions in the extended FimH receptor-binding pocket.....	134
Figure 5	Specificity spots for interaction with FimH.....	135
Figure 6	Inhibition of bacterial adhesion to 5637 bladder cells by mannose or heptyl α -D-mannose.....	136
Figure 7	Bacterial load in the mouse bladder at 6 hours post-infection.....	137
Figure 8	Gentamicin protection assay to determine luminal versus intracellular bacterial population.....	138
Figure 9	Biofilm formation in the presence of methyl or heptyl α -D-mannose.....	139
Figure S1	Crystals of the FimH receptor-binding domain in complex with oligomannose-3.....	140
Table S1	Data collection and processing, refinement statistics and model quality.....	141

Chapter Five: Future Directions and Concluding Remarks

Table 1	Chromosomal genes demonstration a twofold or greater Transcript differential via microarray analysis.....	173
Table 2	Alignment of FimH sequences.....	173
Table 3	Structure activity relationship.....	174
Figure 1	Bacterial load in the bladder and kidney of UTI89 and pyelo3 in single and mixed infections.....	175
Figure 2	Cytokine levels in the kidney of UTI89, pyelo3 and co-infections....	176
Figure 3	Immune response at 6h in UTI89 and Δ pUTI89 infected bladders...	177
Figure 4	Biofilm formation in the presence or absence of pUTI89.....	178
Figure 5	Bacterial load in the bladder of clinical isolates with and without pUTI89.....	179
Figure 6	Plasmid genes demonstrating greater than two-fold change in Δ pUTI89 signal compared to UTI89 signal.....	180
Figure 7	Chromosomal genes demonstrating greater than two-fold change in Δ pUTI89 signal compared to UTI89 signal.....	181
Figure 8	FimH residues under positive selection.....	182
Figure 9	Quantification of IBCs at 6h post-infection from bladders infected with clinical isolates.....	183
Figure 10	acute4 + UTI89 FimH alters colonization but not IBC formation.....	184
Figure 11	Mannosides ZFH177 and ZFH253 reduced intracellular bacteria at 1 hour post-infection.....	185
Figure 12	Mannosides ZFH177 and ZFH253 reduce infection capacity <i>in vivo</i>	186
Figure 13	Structures of 2-pyridone compounds.....	186
Figure 14	FN075 has an effect on UTI89 bladder colonization <i>in vivo</i>	187

Appendix 1: Bacterial Adhesion – A Source of Alternate Antibiotic Targets

Table 1	Representative adhesive fibers, fiber classification and disease association.....	206
---------	---	-----

Figure 1	Two strategies to inhibit bacterial binding to host cells.....	207
Figure 2	Chaperone-subunit donor strand exchange (DSE) and donor strand complementation (DSC).....	208

CHAPTER ONE

INTRODUCTION TO THE DISSERTATION

Urinary Tract Infections

The urinary tract is a common site of infection in women, resulting in an estimated 8 million outpatient visits yearly in the U.S. with an estimated cost exceeding \$2.5 billion (22). It is thought that acute urinary tract infections (UTI) develop when bacteria from the fecal flora colonize the vaginal and periurethral areas and are subsequently introduced into the bladder by ascension via the urethra. The vast majority of patients are female. Women have a 50% chance of developing an acute UTI within their lifetime (45, 51). This gender difference in UTI is presumed to be due to the anatomical differences between males and females, with females having a relatively short urethra as well as a shorter distance between the urethral opening and the anus. In addition, higher rates of infection are associated with some subpopulations, such as the elderly, diabetics, those with anatomical abnormalities and pregnant women (4, 49). UTI can lead to a number of serious sequelae including renal scarring and premature birth (4, 49). Nosocomial infection is extremely common and can result in sepsis with significant morbidity and mortality particularly for elderly patients (18). Uropathogenic *Escherichia coli* (UPEC) is the leading causative agent of UTI, responsible for up to 85% of community-acquired UTI and 25% of nosocomial UTI (50).

Recurrent infection

Recurrence is a serious problem for many women. Women who present with an initial episode of acute UTI have a 25-44% chance of developing a second and a 3% chance

of experiencing three episodes within six months of the initial UTI (19). Recurrence occurs despite appropriate antibiotic treatment and clearance of the initial infection from the urine. A large percentage of recurrent UTI (rUTI) are caused by the same strain of bacteria as the initial infection. One study followed 58 women and found that 68% of recurrences were caused by the same initial index strain of UPEC as determined by restriction fragment length polymorphism (RFLP) analysis (54). In a separate study, 50% of recurrent strains isolated from female college students appeared genotypically identical to the bacterial strain corresponding to the initial UTI (20). Another long-term prospective study demonstrated that the same strain of UPEC can cause a rUTI up to 3 years later (9). The high frequency of same-strain recurrences supports the notion that a UPEC reservoir can exist in the affected individual. The current dogma is that all rUTI result from the re-inoculation of the urinary tract with bacteria originating from a reservoir within the gastrointestinal tract (GIT) and/or vagina (26). Consistent with this idea, it has been demonstrated that the GIT and the vagina/periurethral areas can support UPEC reservoirs (54, 64). In addition, vaginal epithelial cells from women that are prone to rUTIs tend to support higher levels of bacterial adherence, as compared to cells from healthy control patients (59). However, the presence of perineal bacterial or GIT colonization does not explain how a first time urinary tract infection predisposes for the risk of recurrence in girls or women with anatomically normal urinary tracts (61, 62). Furthermore, daily application of antibacterial ointment to the perineal area fails to prevent recurrent infections, even though such a treatment would be expected to block fecal/vaginal-to-urinary tract transmission (11). Women who get frequent rUTIs have been offered a variety of prevention strategies. Often these women are given antibiotics to take upon first presentation of symptoms, after sexual intercourse, or daily as UTI prophylaxis (42, 65, 66). These courses, however, promote uropathogen antibiotic resistance. Additional studies have looked at cranberry products (5), *Lactobacillus*

probiotic therapy (70), and vaccination against bacterial adhesins (35, 36). While many of these strategies are promising, they have yet to be validated in large-scale clinical trials.

UPEC Pathogenic Cycle

Clinically, it has been presumed that UPEC infection consists of a relatively simple extracellular colonization of the luminal surface after inoculation of fecal flora into the bladder via the urethra. In contrast, using a murine model of UPEC infection of the urinary tract, we have detailed an unexpectedly complex UPEC pathogenesis cycle that involves both intracellular and extracellular niches (Figure 1). Using genetic, biochemical and cell biological approaches together with a variety of imaging techniques including transmission, quick freeze-deep etch and scanning electron microscopy, as well as confocal and time lapse video microscopy, it has been discovered that UPEC invade bladder facet cells via a FimH-dependent mechanism (2, 31, 40). After invasion, cytoplasmic intracellular bacterial communities (IBCs) are formed. Rapid replication of the initial invading bacteria results in the formation of an early IBC of loosely-packed rod-shaped bacteria (31). The bacteria continue to replicate and progress to form a large densely packed mid-stage IBC of morphologically coccoid bacteria (31), with biofilm-like characteristics including positive periodic acid-Schiff (PAS) staining (3) and differential gene expression throughout the community (3, 73). After the IBC matures, bacteria detach from the biomass, often become filamentous, and spread to neighboring cells forming new generation IBCs. Filamentous bacteria are more resistant to neutrophil killing resulting in evasion of neutrophil phagocytosis and promoting bacterial survival. Thus, the IBC pathway facilitates massive expansion of the invading bacteria in a niche protected from host defenses. Population dynamic studies using *ex vivo* gentamicin

protection assays demonstrated that $\sim 10^4$ UPEC of an initial 10^7 inoculum invaded the bladder tissue within 15 minutes after infection and that one percent of the invaded bacteria went on to form IBCs, resulting in an average of 100 IBCs per infected mouse bladder. If this is extrapolated to the human situation, innate defenses in the bladder most likely prevent the majority of bacterial inoculation events into the bladder from leading to disease. However, the ramifications of the IBC cascade are striking. Invasion of a single infecting bacterium can lead to rapid expansion of the infection via IBC formation, replicating within hours to 10^4 bacteria and even higher numbers followed by dispersal of the bacteria from the biomass and spreading to neighboring cells to reinitiate the IBC cascade. This process allows the bacteria to gain a critical foothold. Bacterial descendants of the acute IBC cascade have been shown using our murine model, to be able to form a quiescent intracellular reservoir (QIR) that can persist, protected from antibiotics and seemingly undetected by the host immune system even after the acute infection is resolved and bacteria are no longer detectable in the urine (41, 60). Bacteria in the QIR can later seed a recurrent infection (60), manifested by IBC formation, bacteriuria and inflammation. Growing understanding of the bacterial mechanisms of virulence and the subsequent host responses have led to new avenues of research and identification of powerful new therapeutic targets, diagnostic regimens, and the design of anti-virulence compounds.

UPEC Clinical Isolates and the UPEC Pathogenic Cycle

Due to the unique nature of the UPEC pathogenic cycle in UTI89, translational studies were performed in an effort to show that the majority of UPEC isolates form IBCs when introduced into the murine bladder and that IBCs and filamentous bacteria occur in the urine of human UTI patients (21, 52). The study began with the enrollment of hundreds

of women into three different studies to obtain the four different clinical syndromes of UTI. The four common syndromes of UTI are asymptomatic bacteriuria (ASB), acute cystitis, recurrent cystitis (rUTI) and pyelonephritis. ASB is clinically defined as greater than 10^5 bacteria present in the urine without symptoms of UTI such as dysuria, frequency and/or urgency. Acute cystitis is a one-time UTI event without a subsequent UTI event during the course of the study, whereas, rUTI requires recurrent events within 3 months of the initial UTI. Lastly, pyelonephritis was defined as fever, back pain and/or costovertebral angle tenderness (CVAT) as well as a positive urine culture as with acute UTI. In an effort to determine if a specific genotype would associate with a specific clinical syndrome, putative UPEC virulence factors were examined by PCR. Not surprising, there was no correlation between clinical syndrome and virulence genotype. Since the study enrolled human subjects, genetic backgrounds and pain thresholds are different between subjects likely contributing to the difference in clinical manifestation of different isolates. To confirm the UPEC pathogenic cycle is common among UPEC isolates, strains from the study were inoculated in the mouse model of UTI and IBC formation was evaluated at 3, 6 and 24 hours post-infection. Results revealed that IBC formation is an almost universal characteristic of UPEC isolates. Fifteen of 18 isolates formed IBCs and the 3 isolates that were unsuccessful at IBC formation had evidence of the UPEC pathogenic cycle upon co-inoculation with UTI89. Additionally, another study was performed to identify hallmarks of the UPEC pathogenic cycle within human urine. This study revealed the presence of exfoliated umbrella cells containing IBCs and filamentous bacteria present in the urine of human subjects. Also, evidence of IBCs were seen significantly more often in Gram-negative isolates than Gram-positive isolates. These two studies demonstrated that IBC formation is common among UPEC and evident within humans. Now that a panel of UPEC isolates that proceed through the IBC cascade is available, perhaps this will facilitate the development of a virulence

profile identifying *E. coli* isolates as UPEC. This will enable rational drug design to target virulence factors essential for UPEC infection.

Urovirulence Determinants

E. coli is an incredibly diverse bacterial species that can colonize numerous niches in the environment and the animal host. Generally, *E. coli* within the intestinal flora exist as commensals that form a beneficial symbiotic relationship with their host (75). However, some strains of *E. coli* can diverge from their commensal cohorts and cause disease within the intestinal tract and elsewhere within the host. These pathogenic strains are broadly characterized as either diarrheagenic *E. coli* or extraintestinal pathogenic *E. coli* (ExPEC) (32, 53). ExPEC have maintained the ability to exist in the gut without consequence, but have the capacity to disseminate and colonize other host niches resulting in disease. Among ExPEC, strains of UPEC are most commonly associated with human disease. Despite the well-studied nature of UPEC, especially in regards to virulence factors and colonization strategies, no single feature accurately defines an isolate as UPEC. All UPEC isolates contain the *fim* operon encoding type 1 pili, which is necessary for binding and invasion within the urinary tract. However, since the majority of *E. coli* strains possess this operon, it cannot define an *E. coli* as UPEC. A better understanding of UPEC-associated virulence factors and the coordination of their activities during the course of a UTI might significantly enhance our ability to both predict and rationally redirect disease outcome. The most likely place to discover UPEC-associated virulence factors is within pathogenicity islands.

Pathogenicity Islands

Compared to K12 lab strains and commensal *E. coli* isolates, UPEC harbor more genes encoding virulent capsule antigens, iron acquisition systems, adhesins, and secreted toxins. These genes are often encoded within regions referred to as pathogenicity islands (PAIs). PAIs were first described in pathogenic *E. coli*, but have now been discovered in pathogenic bacteria of species other than *E. coli*, both Gram-positive and Gram-negative. PAIs possess most, if not all, of the following characteristics: they (i) carry genes encoding one or more virulence factors, (ii) are present in the genomes of pathogenic organisms but absent from the genomes of nonpathogenic organisms of the same or closely related species, (iii) occupy relatively large genomic regions, (iv) often consist of DNA regions that differ from the core genome in G+C content and in different codon usage, (v) are often flanked by small directly repeated (DR) sequences, (vi) are often associated with transfer RNA (tRNA) genes, (vii) often carry cryptic or functional genes encoding mobility factors such as integrases, transposases, and insertion sequence (IS) elements or parts of these elements, and (viii) often represent unstable DNA regions (23). Due to mobility factors, PAIs often do not represent homogeneous pieces of DNA but rather are made up of mosaic-like structures which have been generated by a multistep process of genomic acquisition, loss, and rearrangement. PAIs frequently contain genes encoding regulators of virulence factor genes located on the same island. However, various arrangements of regulators and regulatory factors are possible, including PAI-encoded regulators that are specific for PAI genes, PAI-encoded regulators that also regulate genes located outside the PAI, and regulators encoded outside the PAI that regulate genes encoded on the PAI.

The analysis of the structure of PAIs revealed that these genetic elements have been generated after lateral gene transfer processes. The acquisition of new genes following horizontal gene transfer either directly by transformation with naked DNA, transduction with phages, or uptake of plasmids or chromosomal fragments by

conjugation, results in the generation of new variants of pathogens. Thus, PAIs contributed to the development of pathogenic variants, preferentially in macroevolution. The ongoing processes of rearrangements, deletions, and transfer of PAIs, however, also have a strong impact on microevolution and adaptation of pathogenic microbes during acute infectious processes. In organisms such as UPEC, whole PAI elements can be deleted. It is suggested that the deletion processes may play a role in the adaptation of pathogenic microbes during certain stages of infection. Therefore, genetic flexibility of pathogenic microbes may create selection advantages over other, less flexible organisms and may finally result in proper replication in host organisms or other ecological niches.

pUTI89

The majority of PAIs are located on the chromosome; however, they can also be part of bacterial plasmids, considered 'PAI precursors' or 'Pre-PAIs' (37). UPEC PAIs encode adherence factors, toxins and iron uptake systems. Interestingly, these same virulence factors can be plasmid or phage encoded on intestinal *E. coli* isolates whereas in UPEC they are located chromosomally, i.e. alpha-hemolysin. Thus UPEC PAIs could represent former plasmid-derived sequences. UTI89 carries a large extrachromosomal element with many characteristics of UPEC PAIs, however it is not incorporated into the chromosome suggesting that it may be a 'PAI precursor'. This plasmid, pUTI89, is approximately 114 kb and like plasmid F, contains the *tra* operon, as well as genes from known virulence plasmids. Due to the potential of pUTI89 to be a 'pre-PAI' and the need to identify genes encoding UPEC-specific virulence factors most likely present on PAIs, this plasmid could provide a snapshot for the acquisition of this PAI among future

bacteria and enable identification of novel virulence factors. Thus a study was done to determine if pUTI89 is important for virulence of UPEC.

Evidence of pUTI89 is present in the majority of clinical isolates tested suggesting maintenance within the community and importance in some aspect of virulence. To assess its role in pathogenesis, pUTI89 was cured from UTI89 to obtain a plasmid-less strain. The *in vitro* characteristics of UTI89 and Δ pUTI89 were then evaluated. Based on growth, type 1 pili expression and function, and biofilm formation, the two isolates were virtually indistinguishable suggesting that pUTI89 is not involved in these *in vitro* characteristics which are used to mimic *in vivo* virulence capabilities. However, it has been shown that in the absence of a *Chlamydia trachomatis* plasmid there was no observable phenotype *in vitro*, yet *in vivo* experiments revealed significantly lower ID₅₀ and lack of glycogen accumulation (10). Thus, the plasmid-less strain was tested *in vivo* to see if a similar phenomenon existed. Using the mouse model of UTI, bacterial load, IBC formation and intracellular and extracellular survival were examined. All of these parameters of infectivity, revealed a significant defect in the Δ pUTI89 strain to colonize the bladder at early timepoints post-infection. Interestingly, within 24 hours post-infection, normal infection was restored as measured by bacterial titers in the bladder. Through selected deletions of operons on pUTI89, the *cjr* operon was implicated in the observed defect. The *cjr* operon, studied in enteroinvasive *E. coli* (EIEC), encodes for CjrA, CjrB and CjrC, is regulated by iron and is involved in uptake of colicin Js, although this is likely not its primary function. Similar to EIEC, a putative iron regulation *fur* box was located upstream of pUTI89 *cjrA*. UTI89 CjrB is homologous to the TonB protein present in many Gram-negative bacteria which has been implicated in energy translocation between the inner and outer membrane. Furthermore, UTI89 CjrC shows homology to putative outer membrane siderophore receptors. Many studies have shown iron's importance in survival within the urinary tract (24, 38, 48). Due to the

necessity of iron acquisition, many systems are redundant in bacteria explaining the lack of complete infection inhibition in the absence of CjrB and CjrC. This study revealed that pUTI89 is very likely a 'PAI precursor' and may be incorporated into the genomes of future UPEC. Horizontal gene transfer by pUTI89 may therefore play a role in the creation of new pathogenic variants.

While it is not essential for virulence in UTI89, perhaps in less virulent UPEC isolates, pUTI89 will facilitate greater invasion efficiency. Thus, strains that otherwise may not cause disease, with the help of genes on pUTI89, will survive within the urinary tract. Through this work a virulence enhancer has been identified, however, since it is not present in all UPEC isolates it cannot, by definition, be added to the urovirulence profile. One virulence factor that is present in all UPEC isolates is type 1 pili. Thus an understanding of this adhesive fiber could ultimately lead to a treatment for UTIs.

Type 1 pili

Type 1 pili are essential cystitis virulence determinants (6, 39, 40, 74). Using EM and the mouse cystitis model, it has been shown that adhesive type 1 piliated bacteria are able to bind and invade host superficial umbrella cells, while UPEC lacking type 1 pili are not. Colonization and invasion of the bladder epithelium is dependent on the FimH adhesin located at the distal end of the pilus which interacts directly with receptors on the luminal surface of the bladder (Figure 2). Once inside the cell, type 1 pili are expressed within IBCs as shown by pilus-like fibers radiating from bacteria and interacting with matrix material (3). Further work confirmed that not only are type 1 pili essential for binding and invasion, they are required for the survival and proliferation of UPEC within superficial facet cells, making type 1 pili arguably the most important virulence factor of UPEC.

FimH

The proteins involved in biogenesis and composition of type 1 pili are encoded by *fimA-H* of the *fim* operon (Figure 3), the expression of which is regulated by an invertible promoter switch element (often termed *fimS*). Type 1 pili consist of a thicker pilus rod, composed of FimA, and a thinner tip fibrillum, composed of FimF, FimG and the adhesin, FimH. The FimH adhesin is a two domain protein, with a receptor binding domain linked to a typical pilin domain that joins the adhesin to the pilus fiber. Binding of FimH to its receptor, mannose, initiates a critical initial event in UTI pathogenesis (27). The mannose binding site of FimH is a deep and negatively charged pocket at the tip of its receptor-binding domain (Figure 4). The FimH pocket engages in extensive hydrogen bonding to mannose, which are abundant in the oligosaccharide moieties of uroplakins that coat the luminal surface of the bladder epithelium. A hydrophobic ridge surrounds the mannose binding pocket in a manner that may facilitate polar interactions within the FimH pocket. Mutational studies revealed that each residue is critical in mannose binding and pathogenesis, emphasizing why the pocket is invariant among UPEC isolates (12, 27). While the mannose-binding pocket is invariant, residues outside the binding pocket are not. The panel of 18 clinical isolates described above was used to assess the role of these variant amino acids. Three of the 18 clinical isolates did not form IBCs and five more did so poorly. Through FimH sequence alignment it was identified that the majority of the poor IBC-formers contained a valine at position 27 which was a residue shown to be under positive selection (12). In an effort to understand the role of FimH in the pathogenic cycle, the clinical isolates with poor ability to form IBCs were manipulated to contain the FimH of UTI89 in the place of their FimH on the chromosome, thus under the same regulation and expression. The hypothesis

being that despite the genetic background, with UTI89 FimH, the clinical isolates will be able to form IBCs. One isolate, acute4, was tested and while it still did not form IBCs, it did colonize the bladder significantly better with UTI89 FimH. This result suggests that there is more to FimH than IBC formation. Additional functions of FimH make it an extremely enticing drug target.

Small molecule inhibitors

The FimH-mannose interaction was further investigated in an effort to develop potential ligand-based antagonists of UTIs. The chitobiose unit on oligomannose was found to bridge various mannose derivatives to the asparagine in the Asn-X-Ser/Thr motif of FimH resulting in higher affinity binding (71). Crystallization of FimH in complex with oligomannose-3 revealed the mechanism of this higher affinity binding. The non-reducing Man4 anchors into the mannose-binding pocket while the GlcNAc folds over Thr51 allowing specific interactions with a hydrophobic tyrosine gate. Heptyl mannoside mimics the GlcNAc tail of oligomannose-3 and extends it further to increase interactions outside the binding pocket resulting in high affinity binding ($K_d = 5$ nM). Based on the high affinity of heptyl mannose for FimH, its ability to reduce bacterial infection in the mouse model of UTI was tested. Biofilm formation was evaluated as a surrogate for IBCs formed in the bladder. Heptyl mannose at 1 mM inhibited UPEC biofilm formation *in vitro* suggesting that the mannose binding properties of the FimH adhesin is required for biofilm formation. Thus, UPEC strain UTI89 was incubated with heptyl mannose prior to inoculation into the bladders of mice. This resulted in a significant attenuation of virulence at 6 hours post-infection at 5 mM heptyl mannose. The ability of these compounds to significantly attenuate virulence establishes mannosides as a potential treatment for UTI. More potent mannosides can now be developed that mimic the

natural receptor for FimH but with increased affinity and avidity in order to ultimately block bacterial colonization, invasion, IBC formation and disease. The ramifications of this work are immense, since, if effective, these carbohydrate inhibitors of disease can be translated to multiple organisms. Sugars, such as mannose, are the molecules most commonly involved in cell recognition playing an important role in microbial adherence. Thus, carbohydrate derivatives of host ligands can block the adhesive properties of pili on a multitude of bacterial organisms. In the face of antibiotic resistance, this novel drug development could treat otherwise resistant infections. While this strategy for bacterial binding inhibition focuses on occupying the receptor binding pocket with carbohydrates mimicking host ligands, a second strategy could eliminate pilus formation all together by blocking the chaperone-usher pathway.

Chaperone-Usher Pathway

Adhesive type 1 pili are prototypic structures of a family of adhesive fibers produced by diverse Gram-negative bacteria via the chaperone/usher assembly pathway (Figure 5) (57, 69). The chaperone/usher molecular machine functions to regulate the ordered secretion, folding and assembly of hundreds of thousands of subunits into defined architectures on the surface of a bacterium. Hundreds of these operons have been reported with as many as twelve encoded in one organism. UTI89 encodes 10 chaperone/usher pilus biogenesis systems (13) each encoded by a distinct gene cluster, which contains a dedicated chaperone and usher. Type 1 and P pilus systems are prototypes for understanding secretion and assembly via the chaperone/usher pathway.

Chaperones

Periplasmic chaperones function to fold their corresponding subunits, shield interactive subunit surfaces and deliver the subunits to their outer membrane usher in a process

termed donor strand complementation (DSC) (55). The highly homologous chaperones (~25 to 30 kDa) consist of two immunoglobulin-like (Ig-like) domains stabilized by a conserved salt-bridge in an overall boomerang shape as seen in the crystal structures of PapD, FimC and SfaE (14, 25, 33, 46). Periplasmic peptidyl-prolyl isomerases and DsbA were found to facilitate chaperone folding (7, 8, 30, 76). Each chaperone contains a conserved subunit binding site (29) consisting of two positively charged cleft residues that hydrogen bond to their target subunits (34, 63) and solvent exposed hydrophobic residues that participate in DSC (28). In addition to the conserved subunit-binding surface, each chaperone contains a conserved patch of solvent exposed residues on the back side of domain 2 (28, 29) shown to be important for usher binding as well as for subsequent events leading to subunit polymerization (43, 47).

Subunits

Single domain subunits share a homologous structure consisting of an incomplete Ig-like fold and an N-terminal extension (Nte). The body of each subunit consists of six of the seven strands of a standard Ig fold. In order to form a stable structure, the corresponding chaperone for each subunit donates structural information to compensate for the missing seventh strand of the subunit thereby completing the hydrophobic core in a process known as donor strand complementation (DSC) (14, 55). During pilus assembly, the free Nte of one subunit displaces the chaperone bound to another subunit and serves as the seventh strand of the Ig-like fold, in a process called donor strand exchange (DSE) (55, 56). While all subunits share an overall structure and mechanism of polymerization, each subunit is adapted for a particular role, which have been identified in both the *pap* and *fim* systems. Pilin subunits require the function of the chaperone for folding due to the absence of the seventh C-terminal strand which is

transiently donated by the chaperone. In the absence of chaperone, subunits misfold into conformations that drive them 'OFF-pathway', resulting in non-productive interactions and their eventual proteolytic degradation.

Tip adhesins

Unlike the single domain subunits described above, tip adhesins contain two domains. The C terminal domain is homologous to the single domain subunits (14). The N terminal domain folds into a ligand binding structure. Crystal structures of PapG and FimH reveal each adhesin has a unique positioning of the ligand-binding site (17, 27). These binding domains serve as the functional end of the pilus, recognizing specific host ligands and influencing bacterial tropism for host tissues.

Ushers

The ushers (~90 kDa) share homology and serve as assembly sites in the outer membrane for polymerization of the resulting fibers. In the absence of the usher the corresponding chaperone/subunit complexes accumulate in the periplasm, but are not assembled into the final fiber (44). Ushers also serve as pores (~2 nm) allowing export of the growing fiber to the surface of the cell (68). Ushers PapC and FimD have been shown to discriminately bind the different chaperone/subunit complexes of their respective systems (16, 58). Once bound by initiating chaperone/subunit complexes, ushers undergo a conformational change (displacement of the β sandwich plug domain), which is then maintained throughout fiber assembly such that the polymerized subunits can transit the channel.

Pilicides

The chaperone/usher system has been cited as the most mechanistically understood assembly/translocation process at a structural level (15). The vast understanding of the molecular structure and function of chaperones important in bacterial pathogenesis facilitates the development of therapeutics capable of targeting and inhibiting the formation of these adhesive structures associated with virulence. Increasing antibiotic resistance among chronic bacterial infections necessitates the identification of new therapeutic options. Combinatorial chemistry has identified small molecule inhibitors of pilus biogenesis. The inhibitors were rationally designed based on the knowledge that thiazolo ring-fused 2-pyridones are highly useful as scaffolds for the development of compounds that inhibit protein-protein interactions in bacteria (1, 47, 67). The synthetic pilicides disrupt an essential protein-protein interaction between the chaperone and usher at a site that has been identified by x-ray crystallography resulting in 'bald' bacteria. Lack of type 1 pili production results in inhibition of biofilm formation and hemagglutination (HA) titer. Considering type 1 pili are essential for colonization of the murine urinary tract, bacteria grown in the presence of pilicide, FN075, failed to establish a robust infection *in vivo* as identified by IBC formation and were significantly reduced in bacterial colonization (Cegelski *et al*, submitted). Thus, FN075 was successful at inhibiting urinary tract infection within the mouse. The efficacy of FN075 within the mouse model suggests it could be used as a therapeutic against UTIs in humans. Furthermore, pyridinones are already advantageous because they avoid severe drawbacks observed upon use of peptides as drugs such as poor absorption after oral administration, rapid enzymatic degradation and quick excretion (67). This work identifies a compound that selectively disrupts protein-protein interactions with a strong potential for therapeutic effects on infection, which due to the ubiquitous nature of

chaperone-usher systems in Gram-negative bacteria may serve as a broader-range therapeutic.

Summary

The high prevalence of UTIs necessitates understanding of the molecular mechanisms associated with virulence and infection. As described above, a multitude of work has been done to elucidate the pathway of infection within the bladder. Discovery of the UPEC pathogenic pathway in a multitude of clinical isolates confirmed the relevancy of this pathway and its importance in persistence. Furthermore, identification of hallmarks of the UPEC pathway in human urine confirmed that this is not an enigma of the murine urinary tract. Now that it is clear that UPEC proceed through a surprisingly complex pathway consisting of extracellular and intracellular niches, one can evaluate each aspect of infection to determine if certain virulence factors are important to one or a multitude of components within the UPEC pathway. For example, by examining binding and invasion, IBC formation, extracellular filaments and reservoir formation and knowing what enables their development, one can start to target these components to disrupt the UPEC pathway. Based on this idea, an extrachromosomal element termed pUTI89 was examined to determine its role in the UPEC pathway. pUTI89 has many characteristics of a PAI and was, in fact, shown to play a role in virulence. The *cjr* operon on pUTI89 was implicated in this role in UTI89 infection. Based on the lack of extracellular filaments and gentamicin protection assays, it appears that Cjr proteins may enhance or facilitate extracellular survival. Work is underway to understand the role of Cjr proteins and their expression profile. While a new potential virulence factor, pUTI89, was discovered, it has long been known that type 1 pili are an essential virulence factor. Without these adhesive fibers, infection is severely depressed. Thus, due to the

necessary function of type 1 pili in infection, they were targeted for development of therapeutics. At the tip of the type 1 pilus is the FimH adhesin. This molecule selectively binds mannosylated residues exposed by uroplakins that coat the surface of the bladder. Due to the necessity of this interaction for binding and invasion and its essential role in IBC formation, exogenous carbohydrates were used to prevent binding. The rational development of the highest affinity mannose derivatives proved to be successful at reducing infection load in the bladder. Additionally, understanding of the chaperone/usher system led to the rational design of 2-pyridone compounds termed pilicides. Testing *in vitro* and *in vivo* revealed that these compounds can eliminate pilus expression and thus reduce bacterial infection. Thus, the work described above has enhanced our understanding of UPEC infection which led to the development of therapeutics to inhibit type 1 pili and reduce infection *in vivo*. Further work will continue to evaluate even more potent type 1 pili inhibitors. New mannosides have been synthesized with much greater affinity for FimH relative to heptyl mannose and preliminary experiments have shown promising results at infection reduction. Additionally, one can imagine using a mannoside and a pilicide in synergy: the mannoside preventing binding to uroplakins by occupying the FimH binding pocket while the pilicide enters the bacterial cell and prevents future pilus production thus eliminating adherence to urothelial cells and promoting clearance of the bacteria. We are now beginning to deliver compounds to the mouse prior to or during infection to test efficacy in a more clinically relevant situation. Ultimately, we hope that our knowledge of UTIs will lead to the severe reduction in prevalence of this disease.

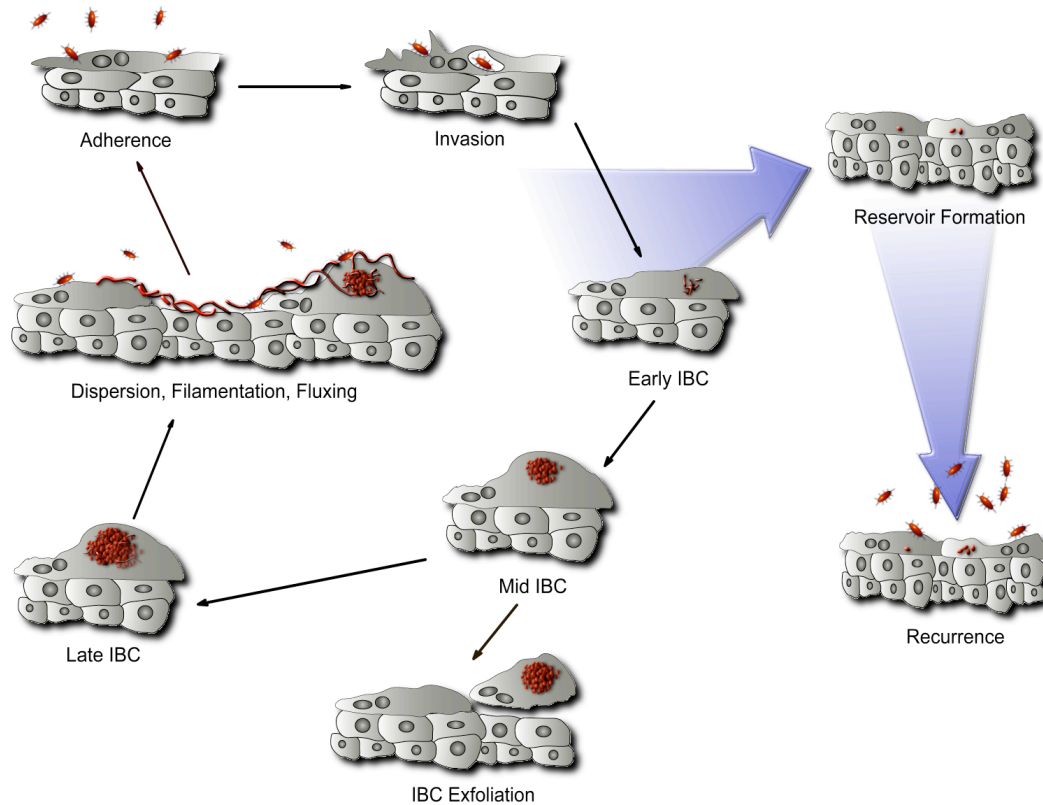


Figure 1. UPEC pathogenesis pathway. UPEC utilize a multi-step pathogenic pathway in a murine cystitis model. Upon introduction into the bladder, UPEC bind to the host urothelium via type 1 pili and an invasion event ensues. UPEC escape into the facet cell cytoplasm and replicate to form loosely-packed early IBCs and ultimately tightly packed mid and late IBCs. Bacteria disperse from the IBC, many in filamentous morphology, bind to another host cell and can ultimately reenter this developmental pathway. In addition, UPEC are able to form intracellular reservoirs within different layers of the urothelium that may lead to recurrent bacteriuria.

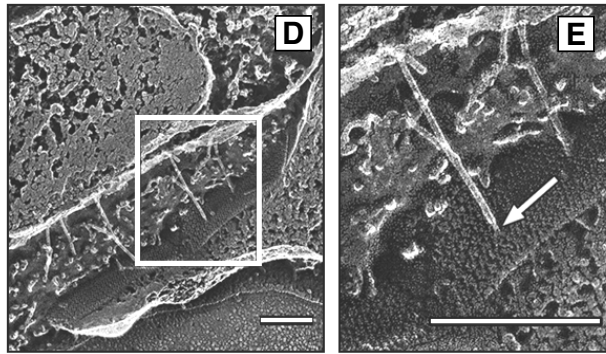


Figure 2. Type 1 pili interact with uroplakins on the bladder surface. EM reveals pilated bacteria interacting with hexameric uroplakins on the surface of bladder tissue. This interaction results in the subsequent invasion of the bacterium into the host cell. The FimH adhesin on the tip of type 1 pili is required for the binding of mannose exposed by the uroplakins. Figure adapted from (40).

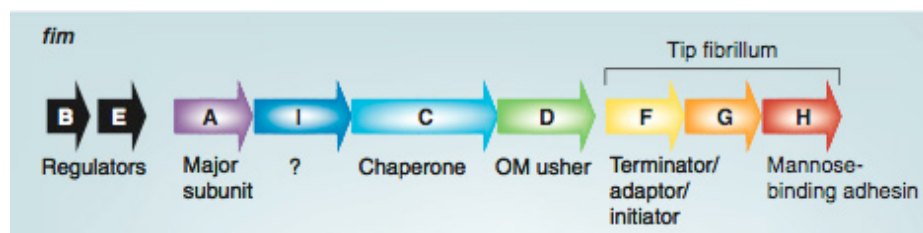


Figure 3. UPEC type 1 pili encoded by the *fim* operon. This schematic representation shows the UPEC *fim* operon. FimB and FimE are regulatory recombinases controlling the expression of *fimA-H*. FimA is the major subunit of type 1 pili and forms the helical rod. FimC acts as a chaperone, stabilizing subunits prior to secretion through FimD, the outer membrane usher. FimF, FimG, and FimH form the distal tip fibrillum. The adhesin FimH is composed of a pilin domain and an adhesin or receptor binding domain. Figure adapted from (72).

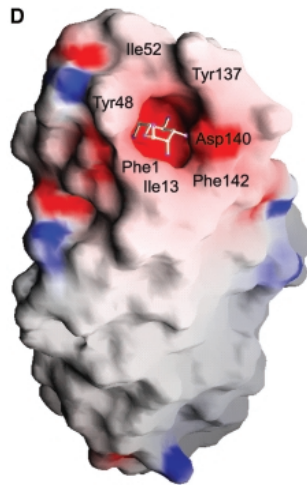


Figure 4. The FimH adhesin accommodates mannose in its binding pocket. The receptor binding domain of FimH has a deep negatively charged pocket that binds mannose. Outside the binding pocket are hydrophobic residues making up the hydrophobic ridge. Positively charged residues shown in blue, negatively charged residues in red, and neutral and hydrophobic residues in white. Adapted from (27).

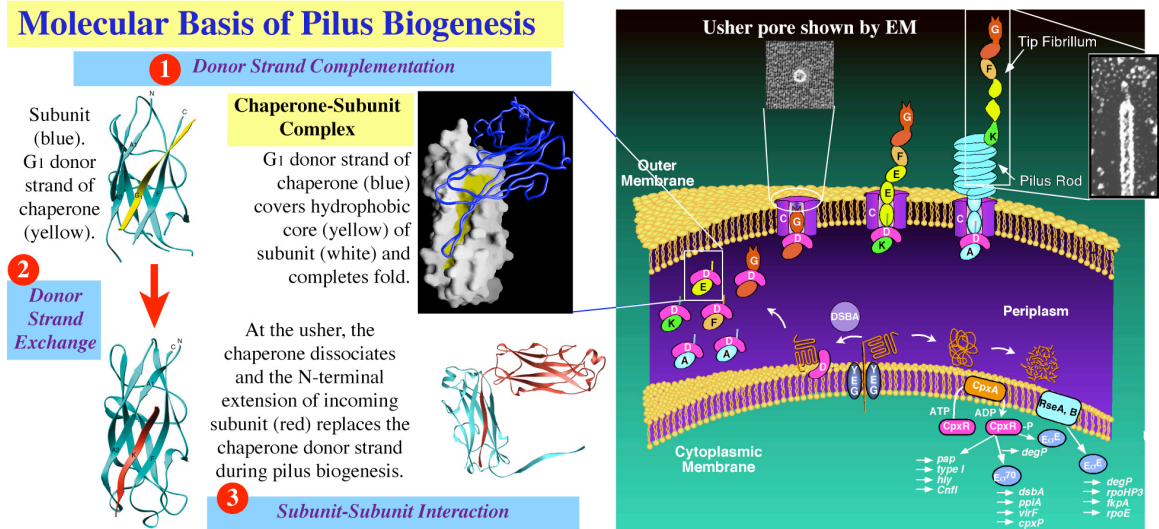


Figure 5. Chaperone/usher mediated pilus biogenesis as shown for the P pilus system.

References

1. **Aberg, V., F. Norman, E. Chorell, A. Westermark, A. Olofsson, A. E. Sauer-Eriksson, and F. Almqvist.** 2005. Microwave-assisted decarboxylation of bicyclic 2-pyridone scaffolds and identification of Abeta-peptide aggregation inhibitors. *Org Biomol Chem* **3**:2817-2823.
2. **Anderson, G. G., S. M. Martin, and S. J. Hultgren.** 2004. Host subversion by formation of intracellular bacterial communities in the urinary tract. *Microbes Infect* **6**:1094-1101.
3. **Anderson, G. G., J. J. Palermo, J. D. Schilling, R. Roth, J. Heuser, and S. J. Hultgren.** 2003. Intracellular bacterial biofilm-like pods in urinary tract infections. *Science* **301**:105-107.
4. **Andriole, V. T., and T. F. Patterson.** 1991. Epidemiology, natural history, and management of urinary tract infections in pregnancy. *Med Clin North Am* **75**:359-373.
5. **Avorn, J., M. Monane, J. H. Gurwitz, R. J. Glynn, I. Choodnovskiy, and L. A. Lipsitz.** 1994. Reduction of bacteriuria and pyuria after ingestion of cranberry juice. *JAMA* **271**:751-754.
6. **Bahrani-Mougeot, F. K., E. L. Buckles, C. V. Lockett, J. R. Hebel, D. E. Johnson, C. M. Tang, and M. S. Donnenberg.** 2002. Type 1 fimbriae and extracellular polysaccharides are preeminent uropathogenic *Escherichia coli* virulence determinants in the murine urinary tract. *Mol Microbiol* **45**:1079-1093.
7. **Bann, J. G., and C. Frieden.** 2004. Folding and domain-domain interactions of the chaperone PapD measured by 19F NMR. *Biochemistry* **43**:13775-13786.
8. **Bann, J. G., J. S. Pinkner, C. Frieden, and S. J. Hultgren.** 2004. Catalysis of protein folding by chaperones in pathogenic bacteria. *Proc Natl Acad Sci U S A* **101**:17389-17393.

9. **Brauner, A., S. H. Jacobson, and I. Kuhn.** 1992. Urinary Escherichia coli causing recurrent infections--a prospective follow-up of biochemical phenotypes. Clin Nephrol **38**:318-323.
10. **Carlson, J. H., W. M. Whitmire, D. D. Crane, L. Wicke, K. Virtaneva, D. E. Sturdevant, J. J. Kupko, 3rd, S. F. Porcella, N. Martinez-Orengo, R. A. Heinzen, L. Kari, and H. D. Caldwell.** 2008. The Chlamydia trachomatis plasmid is a transcriptional regulator of chromosomal genes and a virulence factor. Infect Immun **76**:2273-2283.
11. **Cass, A. S., and G. W. Ireland.** 1985. Antibacterial perineal washing for prevention of recurrent urinary tract infections. Urology **25**:492-494.
12. **Chen, S. L., C. Hung, J. Pinkner, J. N. Walker, C. K. Cusumano, Z. Li, J. Bouckaert, J. I. Gordon, and S. J. Hultgren.** 2009. Positive selection identifies an in vivo role for FimH during urinary tract infection in addition to mannose binding. Proc Natl Acad Sci U S A **Accepted**.
13. **Chen, S. L., C. S. Hung, J. Xu, C. S. Reigstad, V. Magrini, A. Sabo, D. Blasiar, T. Bieri, R. R. Meyer, P. Ozersky, J. R. Armstrong, R. S. Fulton, J. P. Latreille, J. Spieth, T. M. Hooton, E. R. Mardis, S. J. Hultgren, and J. I. Gordon.** 2006. Identification of genes subject to positive selection in uropathogenic strains of Escherichia coli: a comparative genomics approach. Proc Natl Acad Sci U S A **103**:5977-5982.
14. **Choudhury, D., A. Thompson, V. Stojanoff, S. Langermann, J. Pinkner, S. J. Hultgren, and S. D. Knight.** 1999. X-ray structure of the FimC-FimH chaperone-adhesin complex from uropathogenic Escherichia coli. Science **285**:1061-1066.
15. **Daniels, R., and S. Normark.** 2008. Twin ushers guide pili across the bacterial outer membrane. Cell **133**:574-576.

16. **Dodson, K. W., F. Jacob-Dubuisson, R. T. Striker, and S. J. Hultgren.** 1993. Outer-membrane PapC molecular usher discriminately recognizes periplasmic chaperone-pilus subunit complexes. *Proc Natl Acad Sci U S A* **90**:3670-3674.
17. **Dodson, K. W., J. S. Pinkner, T. Rose, G. Magnusson, S. J. Hultgren, and G. Waksman.** 2001. Structural basis of the interaction of the pyelonephritic *E. coli* adhesin to its human kidney receptor. *Cell* **105**:733-743.
18. **Emori, T. G., D. H. Culver, T. C. Horan, W. R. Jarvis, J. W. White, D. R. Olson, S. Banerjee, J. R. Edwards, W. J. Martone, R. P. Gaynes, and et al.** 1991. National nosocomial infections surveillance system (NNIS): description of surveillance methods. *Am J Infect Control* **19**:19-35.
19. **Foxman, B.** 2003. Epidemiology of urinary tract infections: incidence, morbidity, and economic costs. *Dis Mon* **49**:53-70.
20. **Foxman, B., L. Zhang, P. Tallman, K. Palin, C. Rode, C. Bloch, B. Gillespie, and C. F. Marrs.** 1995. Virulence characteristics of *Escherichia coli* causing first urinary tract infection predict risk of second infection. *J Infect Dis* **172**:1536-1541.
21. **Garofalo, C. K., T. M. Hooton, S. M. Martin, W. E. Stamm, J. J. Palermo, J. I. Gordon, and S. J. Hultgren.** 2007. *Escherichia coli* from urine of female patients with urinary tract infections is competent for intracellular bacterial community formation. *Infect Immun* **75**:52-60.
22. **Griebing, T. L.** 2007. Urinary tract infection in women. In: *Urologic Diseases in America*, M.S. Litwin and C.S. Saigal, Editors., p. p. 587-620. U.S. Government Printing Office: Washington, D.C.
23. **Hacker, J., and J. B. Kaper.** 2000. Pathogenicity islands and the evolution of microbes. *Annu Rev Microbiol* **54**:641-679.
24. **Henderson, J. P., J. R. Crowley, J. S. Pinkner, J. N. Walker, P. Tsukayama, W. E. Stamm, T. M. Hooton, and S. J. Hultgren.** 2009. Quantitative

- metabolomics reveals an epigenetic blueprint for iron acquisition in uropathogenic *Escherichia coli*. *PLoS Pathog* **5**:e1000305.
25. **Holmgren, A., and C. I. Branden.** 1989. Crystal structure of chaperone protein PapD reveals an immunoglobulin fold. *Nature* **342**:248-251.
 26. **Hooton, T. M.** 2001. Recurrent urinary tract infection in women. *Int J Antimicrob Agents* **17**:259-268.
 27. **Hung, C. S., J. Bouckaert, D. Hung, J. Pinkner, C. Widberg, A. DeFusco, C. G. Auguste, R. Strouse, S. Langermann, G. Waksman, and S. J. Hultgren.** 2002. Structural basis of tropism of *Escherichia coli* to the bladder during urinary tract infection. *Mol Microbiol* **44**:903-915.
 28. **Hung, D. L., S. D. Knight, and S. J. Hultgren.** 1999. Probing conserved surfaces on PapD. *Mol Microbiol* **31**:773-783.
 29. **Hung, D. L., S. D. Knight, R. M. Woods, J. S. Pinkner, and S. J. Hultgren.** 1996. Molecular basis of two subfamilies of immunoglobulin-like chaperones. *EMBO J* **15**:3792-3805.
 30. **Jacob-Dubuisson, F., J. Pinkner, Z. Xu, R. Striker, A. Padmanabhan, and S. J. Hultgren.** 1994. PapD chaperone function in pilus biogenesis depends on oxidant and chaperone-like activities of DsbA. *Proc Natl Acad Sci U S A* **91**:11552-11556.
 31. **Justice, S. S., C. Hung, J. A. Theriot, D. A. Fletcher, G. G. Anderson, M. J. Footer, and S. J. Hultgren.** 2004. Differentiation and developmental pathways of uropathogenic *Escherichia coli* in urinary tract pathogenesis. *Proc Natl Acad Sci U S A* **101**:1333-1338.
 32. **Kaper, J. B., J. P. Nataro, and H. L. Mobley.** 2004. Pathogenic *Escherichia coli*. *Nat Rev Microbiol* **2**:123-140.

33. **Knight, S. D., D. Choudhury, S. Hultgren, J. Pinkner, V. Stojanoff, and A. Thompson.** 2002. Structure of the S pilus periplasmic chaperone SfaE at 2.2 Å resolution. *Acta Crystallogr D Biol Crystallogr* **58**:1016-1022.
34. **Kuehn, M. J., D. J. Ogg, J. Kihlberg, L. N. Slonim, K. Flemmer, T. Bergfors, and S. J. Hultgren.** 1993. Structural basis of pilus subunit recognition by the PapD chaperone. *Science* **262**:1234-1241.
35. **Langermann, S., R. Mollby, J. E. Burlein, S. R. Palaszynski, C. G. Auguste, A. DeFusco, R. Strouse, M. A. Schenerman, S. J. Hultgren, J. S. Pinkner, J. Winberg, L. Guldevall, M. Soderhall, K. Ishikawa, S. Normark, and S. Koenig.** 2000. Vaccination with FimH adhesin protects cynomolgus monkeys from colonization and infection by uropathogenic *Escherichia coli*. *J Infect Dis* **181**:774-778.
36. **Langermann, S., S. Palaszynski, M. Barnhart, G. Auguste, J. S. Pinkner, J. Burlein, P. Barren, S. Koenig, S. Leath, C. H. Jones, and S. J. Hultgren.** 1997. Prevention of mucosal *Escherichia coli* infection by FimH-adhesin-based systemic vaccination. *Science* **276**:607-611.
37. **Lee, C. A.** 1996. Pathogenicity islands and the evolution of bacterial pathogens. *Infect Agents Dis* **5**:1-7.
38. **Lloyd, A. L., D. A. Rasko, and H. L. Mobley.** 2007. Defining genomic islands and uropathogen-specific genes in uropathogenic *Escherichia coli*. *J Bacteriol* **189**:3532-3546.
39. **Martinez, J. J., M. A. Mulvey, J. D. Schilling, J. S. Pinkner, and S. J. Hultgren.** 2000. Type 1 pilus-mediated bacterial invasion of bladder epithelial cells. *EMBO J* **19**:2803-2812.

40. **Mulvey, M. A., Y. S. Lopez-Boado, C. L. Wilson, R. Roth, W. C. Parks, J. Heuser, and S. J. Hultgren.** 1998. Induction and evasion of host defenses by type 1-piliated uropathogenic *Escherichia coli*. *Science* **282**:1494-1497.
41. **Mulvey, M. A., J. D. Schilling, and S. J. Hultgren.** 2001. Establishment of a persistent *Escherichia coli* reservoir during the acute phase of a bladder infection. *Infect Immun* **69**:4572-4579.
42. **Nicolle, L. E., and A. R. Ronald.** 1987. Recurrent urinary tract infection in adult women: diagnosis and treatment. *Infect Dis Clin North Am* **1**:793-806.
43. **Nishiyama, M., R. Horst, O. Eidam, T. Herrmann, O. Ignatov, M. Vetsch, P. Bettendorff, I. Jelesarov, M. G. Grutter, K. Wuthrich, R. Glockshuber, and G. Capitani.** 2005. Structural basis of chaperone-subunit complex recognition by the type 1 pilus assembly platform FimD. *EMBO J* **24**:2075-2086.
44. **Norgren, M., M. Baga, J. M. Tennent, and S. Normark.** 1987. Nucleotide sequence, regulation and functional analysis of the *papC* gene required for cell surface localization of Pap pili of uropathogenic *Escherichia coli*. *Mol Microbiol* **1**:169-178.
45. **Patton, J. P., D. B. Nash, and E. Abrutyn.** 1991. Urinary tract infection: economic considerations. *Med Clin North Am* **75**:495-513.
46. **Pellecchia, M., P. Guntert, R. Glockshuber, and K. Wuthrich.** 1998. NMR solution structure of the periplasmic chaperone FimC. *Nat Struct Biol* **5**:885-890.
47. **Pinkner, J. S., H. Remaut, F. Buelens, E. Miller, V. Aberg, N. Pemberton, M. Hedenstrom, A. Larsson, P. Seed, G. Waksman, S. J. Hultgren, and F. Almqvist.** 2006. Rationally designed small compounds inhibit pilus biogenesis in uropathogenic bacteria. *Proc Natl Acad Sci U S A* **103**:17897-17902.
48. **Reigstad, C. S., S. J. Hultgren, and J. I. Gordon.** 2007. Functional genomic studies of uropathogenic *Escherichia coli* and host urothelial cells when

- intracellular bacterial communities are assembled. *J Biol Chem* **282**:21259-21267.
49. **Ronald, A., and E. Ludwig.** 2001. Urinary tract infections in adults with diabetes. *Int J Antimicrob Agents* **17**:287-292.
 50. **Ronald, A. R., L. E. Nicolle, E. Stamm, J. Krieger, J. Warren, A. Schaeffer, K. G. Naber, T. M. Hooton, J. Johnson, S. Chambers, and V. Andriole.** 2001. Urinary tract infection in adults: research priorities and strategies. *Int J Antimicrob Agents* **17**:343-348.
 51. **Ronald, A. R., and A. L. Pattullo.** 1991. The natural history of urinary infection in adults. *Med Clin North Am* **75**:299-312.
 52. **Rosen, D. A., T. M. Hooton, W. E. Stamm, P. A. Humphrey, and S. J. Hultgren.** 2007. Detection of intracellular bacterial communities in human urinary tract infection. *PLoS Med* **4**:e329.
 53. **Russo, T. A., and J. R. Johnson.** 2000. Proposal for a new inclusive designation for extraintestinal pathogenic isolates of *Escherichia coli*: ExPEC. *J Infect Dis* **181**:1753-1754.
 54. **Russo, T. A., A. Stapleton, S. Wenderoth, T. M. Hooton, and W. E. Stamm.** 1995. Chromosomal restriction fragment length polymorphism analysis of *Escherichia coli* strains causing recurrent urinary tract infections in young women. *J Infect Dis* **172**:440-445.
 55. **Sauer, F. G., K. Futterer, J. S. Pinkner, K. W. Dodson, S. J. Hultgren, and G. Waksman.** 1999. Structural basis of chaperone function and pilus biogenesis. *Science* **285**:1058-1061.
 56. **Sauer, F. G., J. S. Pinkner, G. Waksman, and S. J. Hultgren.** 2002. Chaperone priming of pilus subunits facilitates a topological transition that drives fiber formation. *Cell* **111**:543-551.

57. **Sauer, F. G., H. Remaut, S. J. Hultgren, and G. Waksman.** 2004. Fiber assembly by the chaperone-usher pathway. *Biochim Biophys Acta* **1694**:259-267.
58. **Saulino, E. T., D. G. Thanassi, J. S. Pinkner, and S. J. Hultgren.** 1998. Ramifications of kinetic partitioning on usher-mediated pilus biogenesis. *EMBO J* **17**:2177-2185.
59. **Schaeffer, A. J., J. M. Jones, and J. K. Dunn.** 1981. Association of vitro *Escherichia coli* adherence to vaginal and buccal epithelial cells with susceptibility of women to recurrent urinary-tract infections. *N Engl J Med* **304**:1062-1066.
60. **Schilling, J. D., R. G. Lorenz, and S. J. Hultgren.** 2002. Effect of trimethoprim-sulfamethoxazole on recurrent bacteriuria and bacterial persistence in mice infected with uropathogenic *Escherichia coli*. *Infect Immun* **70**:7042-7049.
61. **Schlager, T. A., J. O. Hendley, J. A. Lohr, and T. S. Whittam.** 1993. Effect of periurethral colonization on the risk of urinary tract infection in healthy girls after their first urinary tract infection. *Pediatr Infect Dis J* **12**:988-993.
62. **Scholes, D., T. M. Hooton, P. L. Roberts, A. E. Stapleton, K. Gupta, and W. E. Stamm.** 2000. Risk factors for recurrent urinary tract infection in young women. *J Infect Dis* **182**:1177-1182.
63. **Slonim, L. N., J. S. Pinkner, C. I. Branden, and S. J. Hultgren.** 1992. Interactive surface in the PapD chaperone cleft is conserved in pilus chaperone superfamily and essential in subunit recognition and assembly. *EMBO J* **11**:4747-4756.
64. **Stamey, T. A., and C. C. Sexton.** 1975. The role of vaginal colonization with enterobacteriaceae in recurrent urinary infections. *J Urol* **113**:214-217.

65. **Stamm, W. E.** 2002. Scientific and clinical challenges in the management of urinary tract infections. *Am J Med* **113 Suppl 1A**:1S-4S.
66. **Stamm, W. E., and T. M. Hooton.** 1993. Management of urinary tract infections in adults. *N Engl J Med* **329**:1328-1334.
67. **Svensson, A., A. Larsson, H. Emtenas, M. Hedenstrom, T. Fex, S. J. Hultgren, J. S. Pinkner, F. Almqvist, and J. Kihlberg.** 2001. Design and evaluation of pilicides: potential novel antibacterial agents directed against uropathogenic *Escherichia coli*. *Chembiochem* **2**:915-918.
68. **Thanassi, D. G., E. T. Saulino, M. J. Lombardo, R. Roth, J. Heuser, and S. J. Hultgren.** 1998. The PapC usher forms an oligomeric channel: implications for pilus biogenesis across the outer membrane. *Proc Natl Acad Sci U S A* **95**:3146-3151.
69. **Thanassi, D. G., C. Stathopoulos, A. Karkal, and H. Li.** 2005. Protein secretion in the absence of ATP: the autotransporter, two-partner secretion and chaperone/usher pathways of gram-negative bacteria (review). *Mol Membr Biol* **22**:63-72.
70. **Triezenberg, D. J.** 2001. Can regular intake of either cranberry juice or a drink containing *Lactobacillus* bacteria prevent urinary tract infection (UTI) recurrence in women after an initial episode? *J Fam Pract* **50**:841.
71. **Wellens, A., C. Garofalo, H. Nguyen, N. Van Gerven, R. Slattegard, J. P. Hernalsteens, L. Wyns, S. Oscarson, H. De Greve, S. Hultgren, and J. Bouckaert.** 2008. Intervening with urinary tract infections using anti-adhesives based on the crystal structure of the FimH-oligomannose-3 complex. *PLoS ONE* **3**:e2040.
72. **Wright, K. J., and S. J. Hultgren.** 2006. Sticky fibers and uropathogenesis: bacterial adhesins in the urinary tract. *Future Microbiol* **1**:75-87.

73. **Wright, K. J., P. C. Seed, and S. J. Hultgren.** 2005. Uropathogenic Escherichia coli flagella aid in efficient urinary tract colonization. *Infect Immun* **73**:7657-7668.
74. **Wu, X. R., T. T. Sun, and J. J. Medina.** 1996. In vitro binding of type 1-fimbriated Escherichia coli to uroplakins Ia and Ib: relation to urinary tract infections. *Proc Natl Acad Sci U S A* **93**:9630-9635.
75. **Yan, F., and D. B. Polk.** 2004. Commensal bacteria in the gut: learning who our friends are. *Curr Opin Gastroenterol* **20**:565-571.
76. **Zav'yalov, V. P., T. V. Chernovskaya, D. A. Chapman, A. V. Karlyshev, S. MacIntyre, A. V. Zavialov, A. M. Vasiliev, A. I. Denesyuk, G. A. Zav'yalova, I. V. Dudich, T. Korpela, and V. M. Abramov.** 1997. Influence of the conserved disulphide bond, exposed to the putative binding pocket, on the structure and function of the immunoglobulin-like molecular chaperone Caf1M of Yersinia pestis. *Biochem J* **324 (Pt 2)**:571-578.

CHAPTER TWO

ESCHERICHIA COLI FROM URINE OF FEMALES SUFFERING FROM URINARY TRACT INFECTIONS ARE COMPETENT FOR IBC-FORMATION

Modified from: Garofalo *et al.* (2007) *Infect immun.*

Corinne K. Garofalo¹, Thomas M. Hooton^{2†}, Steven M. Martin^{1‡}, Walter E. Stamm²,
Joseph J. Palermo¹, Jeffrey I. Gordon³, Scott J. Hultgren^{1*}

Department of Molecular Microbiology and Microbial Pathogenesis¹, Washington
University School of Medicine, St. Louis, Missouri 63110

Division of Allergy and Infectious Diseases, Department of Medicine², University of
Washington School of Medicine, Seattle, Washington 98195

Center for Genome Sciences³, Washington University School Medicine, St. Louis,
Missouri 63108

†Present address: Department of Medicine, University of Miami Miller School of
Medicine, Miami, FL 33136

‡Present address: Sequoia Sciences, 1912 Innerbelt Business Center Dr., St. Louis,
MO 63114

*Corresponding author. Mailing address: Department of Molecular Microbiology, Box
8230, Washington University School of Medicine, 660 S. Euclid Ave., St. Louis, MO
63110. Phone: (314) 362-6772. Fax: (314) 362-1998. E-mail:
hultgren@borcim.wustl.edu.

Author contributions: CKG, TMH, WES, JJP and SJH conceived and designed the experiments; CKG and SMM performed the experiments; CKG and SJH analyzed the data; CKG, TMH, WES and JIG contributed reagents/materials/analysis tools; and CKG and SJH wrote the paper.

Abstract

Nearly 50% of women experience at least one UTI in their lifetime. Studies in mice have revealed that uropathogenic *E. coli* (UPEC) invade superficial umbrella cells that line the bladder, allowing them to find a safe haven and subvert clearance by innate host responses. Rapid intracellular replication results in the formation of distinctive intracellular bacterial communities (IBCs). In this study, we evaluated whether UPEC strains, cultured from the urine of women and classified as causing acute cystitis, recurrent cystitis, asymptomatic bacteriuria (ASB), or pyelonephritis, could progress through the IBC cascade in a well-characterized mouse model of cystitis. Of 18 UPEC isolates collected from women, 15 formed IBCs. Variations in the size, number, and kinetics of IBC formation were observed with strains isolated from women with different clinical syndromes. Two of the three isolates that did not form IBCs when inoculated alone, were able to do so when co-inoculated with an isolate that was capable of generating IBCs. The mixed infections dramatically altered the behavior of the co-infecting bacteria relative to their behavior in a single infection. The study also showed that mice with five different genetic backgrounds can support IBC formation. Although UPEC differ genetically in their virulence factors, the majority of UPEC from different syndromes of UTI proceed through the IBC pathway confirming the universality of IBCs in UTI pathogenesis in mice.

Introduction

Urinary tract infections (UTIs) account for nearly 7 million office visits per year in the United States and cost \$2 billion annually (4). The majority of community acquired UTIs occur in women and are caused by uropathogenic *Escherichia coli* (UPEC) (7). Greater than 40% of women who experience acute cystitis develop recurrent UTIs (rUTIs) (12). Uropathogens causing UTIs as well as asymptomatic bacteriuria (ASB) are generally thought to emanate from the distal gut, colonize the vagina, and ascend to the bladder via the urethra (4). Likewise, acute pyelonephritis is assumed to be the result of an ascending infection from the bladder to the kidney. However, this widely accepted paradigm does not adequately address questions raised by epidemiologic data. Why does an initial UTI predispose a woman to an increased likelihood of a recurrent infection? Why are up to 68% of rUTIs caused by *E. coli* identical to the original infecting strain (23)? Why are recurrent uropathogens not more representative of the diversity of *E. coli* present within an individual's gastrointestinal tract (2, 21)?

Although it is believed that bladder infection in humans does not involve the bladder wall, previous studies of human bladders indicated a potential intracellular component of UTI (3). Cultures of bladder biopsies taken from women with sterile urine cultures with various urinary tract symptoms revealed the presence of bacteria. Studies in mice have revealed that bacterial invasion of the epithelium lining the bladder lumen (urothelium) is an essential component of lower UTI.

In mice, adhesive bacterial fibers known as type 1 pili are necessary for invasion into the superficial umbrella cells of the urothelium (17, 18). Entry into these host cells initiates a program that has been extensively characterized in mice using the human cystitis isolate UTI89 and that results in formation of intracellular bacterial communities (IBCs). Early IBCs are seen within 6 hours of infection and consist of loosely packed rod-shaped bacteria (19). Over the next 6 hours, they expand into tightly packed consortia of coccoid-shaped bacteria (mid IBC) (15). Sixteen hours after infection,

bacteria detach from the late IBC, elongate into a filamentous form, escape from the host epithelial cell, and spread in the bladder to re-initiate the IBC cascade in other host superficial umbrella cells (15, 19). Subsequent rounds of IBC formation allow *E. coli* to build up large populations within the bladder. Interestingly, within 12 hours of infection, virtually all bacteria in the bladder are intracellular, implying that luminal bacteria are rapidly eliminated (18). One consequence of bacterial invasion is establishment of a quiescent intracellular reservoir (QIR) in the bladder that can persist for months even in the face of antibiotic therapy (25). In addition, bacteria in this QIR can revert to an active metabolic state that is initiated by unknown signals: rapid intracellular bacterial replication ensues, re-initiating additional rounds of IBC formation, inflammation, and spread of bacterial infection throughout the urinary tract (20). This model argues that a portion of rUTIs in humans could be seeded from bacteria present in a QIR in the bladder.

In this study, we investigated the ability of multiple clinical isolates to form IBCs in the mouse model. We found that (i) the majority of UPEC isolates proceed through the IBC pathway; (ii) although isolates from women with ASB, acute UTI, rUTI, and pyelonephritis all form IBCs, IBCs from acute UTI isolates are significantly smaller; and (iii) isolates unable to form IBCs alone are able to do so in mixed infections where the second isolate was an IBC-competent strain. Together, these results confirm that the ability to form IBCs is a common attribute of UPEC isolates.

Materials and Methods

Patients and strains.

Clinical studies were approved by the University of Washington Institutional Review Board and written informed consent was obtained from all participants.

Five isolates causing ASB and four causing first-episode acute cystitis (acute UTI) were collected from women enrolled in a previously described study at the University of Washington (5). Briefly, healthy women between 18 and 40 years old who were about to start or had started a new method of contraception and had no more than one UTI in the previous year were eligible for enrollment. The study excluded a woman if she was pregnant, planned to become pregnant, had a chronic illness, had used systemic antimicrobial agents within 14 days, or had a known anatomical or functional abnormality of the urinary tract. Enrollees were monitored for 6 months, during which time urine was collected at monthly clinic visits and whenever patients had symptoms suggestive of a UTI. Asymptomatic bacteriuria was defined as $>10^5$ CFU of a uropathogen per milliliter of midstream urine documented in at least two separate cultures obtained at least 24 h apart. A symptomatic, culture-confirmed episode of cystitis was defined as $\geq 10^2$ CFU of a uropathogen per milliliter of midstream urine from a patient with dysuria, frequency, and/or urgency.

E. coli isolates from five women with recurrent cystitis were collected from another study of healthy women between 18 and 45 years of age who had acute cystitis and a history of at least one previous UTI in the past year, who were not pregnant and did not plan to become pregnant, and who had no chronic health problems (T. M. Hooton, unpublished data). Approximately 110 women have been enrolled in this ongoing prospective study investigating the temporal associations between bacteriuria and clinical manifestations of recurrent UTI. The women are being treated and then followed with daily urine cultures for 3 months, during which time they are seen in the clinic on a regular basis and whenever they have symptoms suggestive of a UTI. rUTI isolates used in this study were the initial isolate from a women with same-strain recurrence. 'Same strain' isolates were identified by chromosomal restriction fragment

length polymorphism (RFLP) analysis using pulsed-field gel electrophoresis (PFGE) (23).

E. coli isolates collected from four women between 18 and 45 years old who had a clinical diagnosis of pyelonephritis were also included in our analysis (T. M. Hooton and W. E. Stamm, unpublished data). Women were eligible for this study if they had fever, back pain and/or costovertebral angle tenderness (CVAT), and a positive urine culture, as defined above.

Virulence factor PCR.

Bacterial chromosomal DNA was isolated using the Wizard[®] genomic DNA purification kit (Promega) from each UPEC strain after growth overnight in Luria Broth (LB). PCR reactions to detect virulence factors were performed as described in Johnson *et al.* (14).

Western blotting for detecting PapA and FimH protein.

For immunoblot analysis to detect PapA protein in the pyelonephritis isolates, bacteria were grown on tryptic soy agar (TSA) plates at 37°C for 36 hours, scraped, and suspended into 1 mL of PBS. Resuspended cells were heated at 65°C to remove bound pili (9), and the supernatants containing pili were heated in SDS sample buffer (0.25 M Tris-HCl (pH 6.8), 4% SDS, 20% glycerol, 50 mM DTT, bromophenol blue), 4 M Urea at 95°C and analyzed by SDS-PAGE followed by immunoblotting with antibodies to the P pilus (11).

For immunoblot analysis of FimH expression, bacteria were grown statically in LB at 37°C for 24 hours. Equivalent numbers of cells ($OD_{600} \sim 1.0$) from each isolate were suspended in SDS sample buffer, 1 M HCl was added dropwise until pH indicator (bromophenol blue) turned yellow, and solution was heated at 95°C for 5 minutes. The samples were then neutralized and analyzed by SDS-PAGE followed by immunoblotting

with antibodies to FimH (raised in rabbits using purified FimH protein). Specific FimH proteins were visualized on nitrocellulose membranes by BCIP/NBT Liquid Substrate System (Sigma), and analyzed for intensity using ImageJ software (rsb.info.nih.gov/ij/).

Hemagglutination assays for detecting bacterial adhesins.

Bacteria were grown statically in LB for 24 hours to induce expression of type 1 pili. Hemagglutination (HA) assays with guinea pig erythrocytes were performed using well-established protocols (10, 26).

Mouse strains and infections.

All studies using mice were approved by the Animal Studies Committee of Washington University. Eight-week-old female mice, belonging to the inbred C3H/HeN strain, were anesthetized and inoculated with a 50 ml suspension of $\sim 10^7$ CFUs of a given clinical isolate (in PBS) via transurethral catheterization (19). Three, 6, 12, 16 and/or 24 h after inoculation, animals were euthanized, and their bladders harvested, divided in half, opened, and pinned on dissecting wax. Bladders were washed three times with PBS to eliminate loosely associated bacteria not likely involved in infection. The splayed bladders were then incubated for 20 min at room temperature with (i) wheat germ agglutinin (WGA) (Molecular Probes; 1:1000 in PBS) to stain their luminal surfaces and (ii) SYTO[®] 61 red (Molecular Probes; 1:1000 in PBS) to stain IBCs as well as host urothelial cell nuclei. (Individual bacteria could be visualized in the densely packed IBCs, thus distinguishing them from the nuclei). Trolox (10 μ M; Fluka) was added to the splayed bladders to reduce photobleaching (24). The total number of IBCs was scored by confocal microscopy (see below). If all infections were not successful, 5 successfully infected mice were used for further evaluation. The diameters of a maximum of 25 IBCs (5 IBCs/bladder/isolate [$n = 5$ bladders/isolate]) were measured across the width of each

IBC, averaged, and standard deviations calculated to estimate differences in the sizes of IBCs. If less than 25 IBCs were observed for a given isolate, the total number of IBCs observed were used to calculate the average diameter and standard deviation. If IBCs were not observed in all 5 bladders inoculated with a clinical isolate, more than 5 IBCs were measured per bladder containing IBCs to obtain 25 measurements. After microscopy, bladders were homogenized in 1 mL of 0.025% Triton X-100-PBS and bacterial titers determined by plating serial dilutions of the homogenates on LB agar plates. Standard gentamicin assays were done to define the number of intracellular bacteria in the bladder (19).

For the single infections with the two laboratory strains, UTI89 and CFT073 were genetically engineered to express Green Fluorescent Protein (GFP). Eight-week-old female mice belonging to inbred C3H/HeN, C3H/HeJ, C57BL/6J, CBA/J, and FVB/NJ strains were inoculated with UTI89-GFP and CFT073-GFP as above. At 6 and 24 h after inoculation, bladders were harvested as above, however, the splayed bladders were fixed and visualized without additional staining due to GFP-expressing UTI89 and CFT073.

Co-inoculation of clinical isolate and UTI89.

Equal amounts of each clinical isolate and UTI89-gfp (cystitis strain engineered to express GFP) were mixed to obtain a 50 ml bacterial suspension of $\sim 10^7$ CFUs. The suspension was then inoculated into C3H/HeN mice and infected bladders were harvested and visualized as above. UTI89-gfp contains the kanamycin resistance cassette and thus is Kan^R, whereas the clinical isolate was Kan^S. Serially diluted bladder homogenates were plated on LB agar plates and LB agar plates containing kanamycin (50 μ g/ml) and grown overnight at 37°C. The number of CFU of the clinical

isolate was determined by subtracting the number of the kanamycin-resistant UTI89 from the total number of CFU on LB medium lacking kanamycin.

Confocal scanning laser microscopy.

Bladders were examined with a Zeiss LSM410 confocal laser scanning microscope under a 63X objective. WGA and SYTO[®] 61 were excited at 488- and 633-nm, respectively. In co-inoculation experiments using GFP-expressing UTI89 and a clinical isolate that did not form IBCs alone, GFP was excited at 488-nm, the clinical isolate was stained red by SYTO[®] 61, and wheat germ agglutinin was omitted.

Statistical analysis.

Observed differences in IBC diameter between isolates representing the four different types of UTI were analyzed for significance using the nonparametric Mann-Whitney U test (InStat; GraphPad Software).

Results

Virulence genotypes of the clinical isolates

We studied 18 clinical isolates collected from women enrolled in the three different studies described above (Table 1). To characterize the isolates, they were first analyzed *in vitro* for the presence of 29 putative virulence factors by multiplex PCR, as previously described (14). The level of type 1 pili expression was then assessed with hemagglutination assays and an immunoblot using FimH antisera. The isolates were then analyzed in a murine model to assess their ability to form IBCs within the bladder.

UPEC virulence factors are typically involved in colonization and invasion of the host and evasion of the immune responses. Each isolate had a unique combination of virulence factors and their prevalence was similar to a previous study analyzing 63

UPEC isolates (13), suggesting our small sample size was representative of a larger, diverse UPEC group (Table 2). The most prevalent virulence factors were *fimH* (100% of isolates), *fyuA* (yersiniabactin receptor; 80%), *traT* (serum-resistance; 70%), *PAI* (CFT073 pathogenicity-associated island marker for a series of genes that provide a mechanism for horizontal transfer of virulence factor genes; 70%), *kpsMT II* (group 2 capsule; 70%), *sfa/focDE* (S/F1 fimbriae; 60%), and *hlyA* (hemolysin; 50%). The presence or absence of individual virulence factors could not be correlated with a particular clinical syndrome.

Surprisingly, none of the four pyelonephritis isolates had genes within the *pap* operon which encodes for the production of P pili. Due to the absence of the *pap* operon, anti-P pilus antibodies failed to react with these isolates after growth on TSA, which typically induces P pili production (Figure 1).

Type 1 pilus production in clinical isolates

Hemagglutination (HA) of guinea pig red blood cells (GPRBCs) was performed as previously described (10) to determine the degree of type 1 pilus production by each clinical isolate. Type 1-mediated HA is specifically inhibited by the addition of exogenous mannose and this reaction is referred to as mannose sensitive hemagglutination (MSHA).

For this study, bacteria were grown in static culture at 37°C for 24 hours to enhance type 1 production. After 24 hours of static growth, UTI89, a prototypic cystitis reference strain shown to proceed through the IBC pathway, produced a MSHA titer of 64 (values equal 2^x where x equals the last well of agglutination). Comparable MSHA titers were seen with the ASB isolates, which ranged from 32-128, suggesting a similar level of type 1 production as UTI89 (Table 2). The first event UTI strains (acute UTI isolates) produced MSHA titers ranging from 16-64. The rUTI isolates had HA titers

ranging from 2-8 that could not be entirely inhibited by addition of exogenous mannose. The persisting HA titers in the presence of mannose suggests expression of a mannose resistant (MR) adhesin system under these growth conditions. The pyelonephritis isolates had MRHA titers ranging from 4-16.

To further confirm the results seen with HA titer, anti-FimH antibodies were used in immunoblots to assess the relative levels of FimH in all of the strains after 24-h growth in static broth. The intensity of each band was quantitated and expressed as a value relative to the amount of FimH expressed by UTI89, which was set at 100% (Table 2). MC4100, which does not produce type 1 pili, was used as a negative control. The majority of isolates expressed type 1 pili at levels of 50%-99% of UTI89. Only one isolate, ASB3, expressed type 1 pili at a level substantially higher than UTI89, 150%-199%. Strains acute1, rUTI1, and rUTI4 did not express detectable levels of type 1 pili, and acute3 and CFT073 expressed comparable levels of type 1 pili relative to UTI89 as determined by our immunoblot analysis. These results suggest UPEC isolates from different clinical syndromes produce varying degrees of type 1 pili *in vitro*.

IBC formation by UPEC isolated from women

First the commonality of the IBC pathway in the face of differing host responses was evaluated. To date the IBC pathway has been best described in the C3H/HeN and C3H/HeJ mouse strains with UPEC strains UTI89 and NU14 (1, 15, 18). A previous study evaluated the level of infection and inflammation in different mouse genetic backgrounds, but did not examine the IBC pathway (8). To determine if the cystitis and pyelonephritis isolates, UTI89 and CFT073 respectively, form IBCs in various host genetic backgrounds, three other strains of mice were infected, C57BL/6J, CBA/J, and FVB/NJ. Mouse strains for use in this study were chosen based on their previous use as models for host responses to UPEC infection and/or identification of bacterial virulence

factors (16, 18, 27). At 6 hours post infection, IBCs were detected in all mouse strains tested with both UPEC strains. IBCs from C3H/HeJ (Figure 2D,I) and C3H/HeN (Figure 2E, J) mice showed the expected IBC morphology inside superficial epithelial cells. Early IBCs were readily detected in C57BL/6J, CBA/J, and FVB/NJ (Figure 2A-C,F-H) that were visually indistinguishable from IBCs in C3H genetic background. Occasionally, some IBCs in C57BL/6J mice had more loosely defined edges. The presence of IBCs at six hours post infection in five mice strains after infection with UTI89 and CFT073 suggests that the mechanisms utilized for invasion and intracellular replication *in vivo* are a conserved feature in these strains.

Next, the commonality of IBC formation among different clinical isolates was evaluated. Eighteen clinical isolates recovered from women enrolled in three different UTI studies (Table 1) were evaluated for their ability to form IBCs. Each isolate was inoculated transurethrally into the bladders of young adult female C3H/HeN mice and the bladders harvested at 3, 6, 12, 16, and 24 h post infection ($n=5$ mice/time point/isolate) (Table 3 and Figure 3).

All five ASB isolates formed IBCs although the time course varied: IBCs were observed 6 h and 24 h after inoculation of strains ASB1, ASB2, and ASB3 (Figure 3E, F) while IBCs were only observed at 6 h for ASB4 and at 24 h for ASB5. This suggests that although IBC formation is common, the rate at which the isolates proceed through the pathway is potentially strain specific. In UTI89, first round IBCs are observed at 6 h post-infection and second round IBCs are observed at 24 h post-infection despite asynchronous micturation among the mice. Since IBCs were not observed at 24 h in ASB4, it is possible that the second round IBCs were either earlier or later and thus missed. The fact that ASB5 only formed apparent IBCs 24 h post inoculation suggests that it either proceeds more slowly through the IBC pathway due to slow replication within the umbrella cells, or it invades the urothelium at later time points. ASB5

produces a high MSHA titer (128) and FimH was detectable in the immunoblots (Table 2). These piliation characteristics strongly argue that the observed delay in IBC formation is not related to type 1 pilus expression of the inoculum. The average diameter of ASB IBCs was $51 \pm 20 \mu\text{m}$ (5 IBCs/bladder) which is the same as the prototypic isolate, UTI89, which has an average IBC diameter of $51 \pm 9 \mu\text{m}$ at 6 h post infection.

Three of the four acute UTI isolates formed IBCs at the time points examined. Again, there were isolate-specific differences in the time course. IBCs were only observed at 3 h in acute3 (Figure 3B), 6 h in acute2, and 12 h in acute1 (data not shown) ($n = 5$ mice for each group). IBCs in all acute UTI isolates were small with an average diameter of $20 \pm 8 \mu\text{m}$ ($p < 0.01$ compared to UTI89 and ASB isolates) and sparse (average 3/bladder compared to ~20-100/bladder with UTI89 and ASB isolates, $n = 15$ mice). No IBCs were observed at any of the five time points surveyed for acute4. However, bacteria were visualized on the luminal surface of the bladder and quantitated by tissue titer to be greater than 10^2 CFUs/bladder throughout the time course. With UTI89, by 12 h virtually all of the bacteria have entered an intracellular niche (19). The ability of acute4 to persist extracellularly up to 24 hours emphasizes that different UTI strains may use alternative mechanisms to cause infection. Although acute4 produces type 1 pili *in vitro* it is unable to form IBCs. Thus, additional factors must be critical in IBC formation independent of type 1 piliation. Acute4 is further analyzed in studies described below and in separate studies to investigate the mechanism by which it persists in the urinary tract.

IBCs were observed for four of the five recurrent cystitis isolates. IBCs were only observed at 3 h in rUTI5 (Figure 3A), 6 h in rUTI2 (Figure 3C) and rUTI3, and 24 h in strain rUTI4 ($n = 5$ mice for each group), again showing differences in the IBC pathway.

The diameter of the IBCs observed in all 4 isolates was $41 \pm 14 \mu\text{m}$, a value that is significantly greater compared to acute UTI strain IBCs ($p < 0.05$) but not significantly different compared to UTI89 or the ASB strains ($p = 0.274$). Similar to strain acute4, rUTI1 bacteria were present in the bladders throughout the time course, as evidenced by tissue titers (10^3 - 10^4) but no IBCs were observed by microscopy. However, in contrast to acute4, rUTI1 expressed little to no type 1 pili *in vitro* (Table 2) even though it contains the *fimH* gene. The inability to produce type 1 pili *in vitro* could possibly explain the inability of rUTI1 to invade (see below) and form IBCs at the time points tested. Whether type 1 pilus expression can be induced *in vivo* at later time points and lead to invasion and IBC formation is the subject of future studies.

Of the four pyelonephritis isolates, three formed IBCs and did so by 6 h post-inoculation (Figure 3D) suggesting similar kinetics in their IBC pathway ($n = 5$ mice in each group). IBC diameter ($55 \pm 10 \mu\text{m}$) was significantly larger than in acute UTI strains ($p < 0.01$). IBCs were not observed with pyelo3, and, similar to rUTI1, MSHA was not detected after growth in static broth *in vitro* (Table 2). As seen with the two other strains unable to form IBCs, acute4 and rUTI1, pyelo3 was unable to invade into the superficial umbrella cells of the bladder (see below).

Invasion defects in strains unable to form IBCs

Since invasion is a prerequisite to IBC formation, we performed an *in vivo* gentamicin protection assay to assess whether any of the three isolates that did not form IBCs: acute4, rUTI1, and pyelo3, had invasion defects. PCR demonstrated that the *fimH* gene was present in all three strains and HA assays revealed that acute4 produced type 1 pili while rUTI1 and pyelo3 produced mannose-resistant fibers. The ability of UPEC to invade is thought to be dependant on type 1 pili (17). At 1 hour post infection bladders were removed, bisected, and incubated in gentamicin to kill extracellular bacteria.

Homogenates of the treated bladders were then cultured since intracellular bacteria have been shown to survive this treatment (19). Bacterial titers revealed that the three non-IBC forming isolates were deficient in invasion compared to UTI89 (Figure 4). 4.4% of adherent UTI89 bacteria (defined as bacteria removed from the lumen after multiple washes) were able to invade the urothelium (defined as bacteria surviving the gentamicin treatment). In contrast, the three isolates that did not form IBCs (acute4, rUTI1, and pyelo3) had invasion percentages of 0.3%, 0.5%, and 1.1%, respectively, thus potentially explaining their inability to form IBCs.

Mixed infection model of UTI89 with non-IBC forming isolate

Due to the complex nature of the intestinal, peri-anal, vaginal, and periurethral microbiota, it is likely that the initial inoculum in the human bladder is a mixture of bacterial strains. We sought to investigate whether one isolate could improve the fitness or out-compete another isolate in the bladder. Thus, we investigated the outcome of experiments where UTI89 was genetically engineered to express a readily detectable green fluorescent protein marker and then co-inoculated with each the three non-IBC-forming clinical isolates in equal concentrations. Although IBCs were not observed during single infection with acute4, when it was co-inoculated with UTI89, acute4 was able to participate in IBC formation, but only as a mixed IBC with UTI89-gfp IBCs (Figure 5C, D). When rUTI1 was co-infected with UTI89, rUTI1 formed IBCs at 24 h (Figure 5B) and caused UTI89 to form giant IBCs at 6 h (diameter = $130 \pm 25 \mu\text{m}$) (Figure 5A). Pyelo3 was unable to form IBCs in the presence or absence of UTI89 and even prevented IBC formation in UTI89. In the UTI89/pyelo3 mixed infection, most of the extracellular (luminal) pyelo3 were filamentous and this same overwhelming filamentation phenotype was induced in UTI89 (Figure 5E, F). Interestingly, although two of the three clinical isolates altered the behavior of UTI89, they were present in the

bladder in quantities 100-1000 fold less than UTI89 at each time point tested ($n = 5$ mice in each group). Additionally, all three of the clinical isolates showed altered behavior in the presence of UTI89 relative to their behavior when inoculated individually. Clinically, a UTI is often defined as bacteria in the urine in quantities greater than 10^5 and mixed infections with different UPEC strains would typically not be detected. Thus, small amounts of a competing strain in the bladder could possibly have profound and distinct effects on the outcome of infection.

Discussion

The widely accepted paradigm of acute and recurrent infection is that both are due to the ascension of bacteria from the gut microbiota to the vagina and then the bladder. In addition, UTIs have clinically been thought to be due to simple extracellular colonization of the urothelium by UPEC. However, recently it has been shown in mice that UPEC invade the urothelium in order to subvert innate defenses (15, 17, 18). Likewise, intracellular bacteria have been demonstrated in the human bladder following UTI (3). The discovery and characterization of intracellular bacterial communities (IBCs) in the murine model of cystitis has challenged the traditional clinical paradigm of UTIs and revealed a mechanism by which UPEC are able to build up in numbers in the bladder despite potent innate defenses. The IBC pathway has been well characterized with the cystitis isolate, UTI89, in the C3H mouse model of cystitis. In this study we have demonstrated that the IBC pathway is common to most UPEC strains isolated from humans with different UTI syndromes and in mice of different genetic backgrounds.

We found, through multiplex PCR virulence factor assays, that the isolates chosen for this study were representative of a larger pool of UPEC isolates (13). Surprisingly, none of our pyelonephritis isolates contained any genes within the *pap* operon and thus did not express P pili. The *pap* operon encodes for P pili containing a

distally located PapG adhesin that binds the globoside receptor in the human kidney which has been shown to be critical for the ability of pyelonephritic strains to colonize the kidney (22). The four pyelonephritis strains in this study were obtained from patients that had classic symptoms of pyelonephritis, namely fever and CVAT (Table 1). The absence of the *pap* operon in these strains is intriguing, but given the small sample size, further studies will need to be done to interpret the significance of this finding. In contrast, all of the pyelonephritis isolates, as well as the ASB, acute UTI, and rUTI isolates, had the *fimH* gene. However, expression of type 1 pili after growth in static LB broth differed among the strains. Strains with varying levels of type 1 pili after *in vitro* growth were able to colonize the mouse bladder and form IBCs. It is possible that the *in vivo* environment in the bladder altered the type 1 pilus expression profile after inoculation, thus partially explaining the ability of strains with various levels of type 1 pili to colonize and form IBCs within the bladder.

In our mouse model of UTI, we demonstrated that 15 of 18 clinical isolates from various human clinical syndromes proceeded through the IBC pathway when inoculated as a single strain. However, IBC formation differed among the strains in terms of the kinetics by which bacterial communities formed, the size of the communities, and the number of communities. While isolates from each clinical syndrome formed IBCs, the acute UTI isolates formed significantly smaller and fewer IBCs relative to any other syndrome. In general, ASB, rUTI, and pyelonephritis strains are associated with longer-term persistence in the host. The ASB, rUTI and pyelonephritis strains produced more IBCs/bladder and the IBCs were of increased size compared to acute UTI strains. The differences in IBC behavior of the acute strains compared to the other three groups could potentially explain why the acute strains are less persistent.

The behavior of the three outlying strains (rUTI1, acute4, and pyelo3) required more research to better understand their apparent deviations in IBC behavior with

respect to their group. rUTI1, acute4, and pyelo3 were unable to efficiently invade into the superficial umbrella cells of the bladder and thus were unable to form IBCs. Lack of IBC formation in the three isolates could not be associated with a specific virulence factor due to their differing virulence factor profiles. Likely, there are a multitude of virulence factors contributing to IBC formation and perhaps some redundancy in the necessary factors. rUTI1 did not produce any detectable levels of type 1 pili *in vitro* thus most likely explaining its inability to invade and form IBCs at the time points tested. Acute4 was able to produce type 1 pili *in vitro* at levels equivalent to or better than isolates able to form IBCs suggesting that type 1 pilus expression is not sufficient for IBC formation and implicates the importance of other factors in invasion. Pyelo3 produced a small amount of type 1 as determined by immunoblotting with anti-FimH antisera. No MSHA was detected *in vitro* possibly because of the presence of MRHA adhesins that would potentially mask type 1 mediated hemagglutination. The deficiency of *in vivo* invasion of pyelo3 could suggest that either the MRHA adhesins somehow interfered with the process and/or that pyelo3 lacked other factors involved in invasion.

Given the diverse microbial communities in the rectum and vagina (2, 21), it is likely that multiple strains of bacteria are simultaneously introduced into the urinary tract of a woman during the early events that lead to a UTI, such as sexual intercourse. While mixed infections may select for bacteria with a distinct competitive advantage, they may also allow less virulent bacteria the opportunity to establish a niche in conjunction with more efficient UPEC strains. Co-inoculation of UTI89, a known IBC forming strain, with each of the three isolates that were deficient in IBC formation, resulted in dramatic, synergistic effects. Of the three isolates in which IBC formation was not detected, two were able to do so in mixed infections with UTI89 (rUTI1, acute4). This may explain the seemingly outlying behavior of these strains when analyzed in single infections. The diagnosis of UTIs rarely delineates whether multiple strains of *E. coli* are present. Thus,

strains such as rUTI1 and acute4 could have “piggy-backed” with a more invasive IBC forming strain that went undetected. UTI89 formed significantly larger IBCs in the presence of rUTI1. This may be due to potential host responses induced by rUTI1 that facilitate bacterial replication in the superficial umbrella cells, or possibly that rUTI1 induces signals that prevent or slow the dispersal and fluxing of the bacteria in the IBC. IBC formation is a clonal process in that each IBC arises from a single bacterium (P. C. Seed and S. J. Hultgren, submitted for publication). Surprisingly, the mixed infection with acute4 and UTI89 resulted in non-clonal IBCs. Acute4 only existed as a mixed IBC with UTI89. The bacteria did not inter-mingle in the IBC but instead each strain seemed to group together in patches that melded into one IBC. These results argue that UTI89 was able to provide factors *in trans* that could support acute4 in the intracellular biofilm matrix.

Pyelo3 was the only strain in our study unable to form IBCs under any of the conditions tested. Co-inoculation of UTI89 and pyelo3 resulted in massive filamentation of both isolates. Based on previous work showing that filamentation occurs in response to an inflammatory response (15), further study is required to assess whether pyelo3 is triggering a more robust innate response that leads to the massive filamentation observed. The complexities we have observed with co-infections between the bacteria and with the host might explain the occurrence of different clinical syndromes manifested by the same organism (6) or the differing behavior in single versus mixed infections as described above. Alternatively, it is possible that these isolates could represent a class of strains that do not use the IBC pathway but instead use a different extracellular strategy for persistence.

In summary, 15 of 18 isolates causing different clinical syndromes in humans and possessing various combinations of virulence factors were successful in invading the bladder epithelium of mice to form IBCs. Two of the remaining three isolates were also

able to form IBCs in mixed infections with UTI89. These findings demonstrate that the IBC pathway is common to UPEC pathogenesis. Studies are in progress to determine whether UPEC forms IBCs in humans and whether they contribute to same-strain recurrences of UTI. The murine model of IBC formation will allow investigators the ability to study the intricacies of host-pathogen interactions in the bladder. Understanding the basis of the intracellular niche occupied by UPEC will lead to the better evaluation and treatment of UTIs and will foster the development of new therapeutic strategies.

Acknowledgements

This study was funded by NIH/NIDDKD grant DK 64540 ORWH, DK 51406, DK 40045, DK 47549 and the Infectious Diseases/Basic Microbial Pathogenesis Mechanisms Training Grant.

Tables and Figures

Table 1. Characterization of UTI isolates collected

Strain	Enrollment Study	Duration of Follow-up (weeks)	Clinical Classification	Symptoms	Duration of Symptoms (days)	Age at First UTI	Prior Lifetime UTIs	Age	Demographics§
ASB1	PUTS*	24	ASB	none	NA	NA	0	39	w/sep/15
ASB2	PUTS*	24	ASB	none	NA	NA	0	22	w/nm/16
ASB3	PUTS*	24	ASB	none	NA	NA	0	21	w/nm/13-15
ASB4	PUTS*	20	ASB	none	NA	NA	0	28	w/div/13-15
ASB5	PUTS*	16	ASB	none	NA	NA	0	18	w/nm/12
acute1	PUTS*	24	First Event	d,f,h	NR	NA	0	23	w/nm/17+
acute2	PUTS*	24	First Event	d,f,h	NR	NA	0	23	w/nm/17+
acute3	PUTS*	25	First Event	d,u	4	NA	0	19	w/nm/12
acute4	PUTS*	24	First Event	f,u,n	<1	NA	0	18	hisp/nm/12
rUTI1	TOP†	12	Recurrent	d,f	1	23	5	27	w/nm/17+
rUTI2	TOP†	12	Recurrent	d,f	1	13	10	25	w/nm/17+
rUTI3	TOP†	12	Recurrent	d,f	2	18	3	22	a/nm/13-15
rUTI4	TOP†	12	Recurrent	d,f,u	2	19	1	21	a/nm/12
rUTI5	TOP†	12	Recurrent	d,f,u	1	6	20	23	w/nm/13-15
pyelo1	Pyelo‡	20	Pyelonephritis	f,n,s,o,lbp,fe,c	16	19	3	21	w/nm/15
pyelo2	Pyelo‡	4	Pyelonephritis	d,f,u,n,s,o,lbp,fe,c	1	24	3	24	other/nm/18
pyelo3	Pyelo‡	16	Pyelonephritis	d,f,u,n,s,lbp,fe,lap	3	19	1	25	w/div/21
pyelo4	Pyelo‡	4	Pyelonephritis	u,lbp,fe,c,lap,i	2	NA	0	20	other/nm/13

Abbreviations: d, dysuria; f, frequency; h, hematuria; u, urgency; n, nocturia; s, urinating in small amounts; o, urine odor; lbp, lower back pain; fe, fever; c, chills; lap, lower abdominal pain; i, incontinence; NA, not applicable; NR, not recorded; w, White; hisp, Hispanic; a, Asian; sep, separated; nm, not married; div, divorced

*PUTS enrollment criteria - women age 18-40, starting new birth control method, may be pill, diaphragm, cervical cap, or foam and condoms, no history of >1 UTI in past year

†TOP enrollment criteria - women age 18-45, non-pregnant, contraception, symptoms less than 7 days, no chronic health problems, no costovertebral angle tenderness

‡Pyelo enrollment criteria - women age 18-45, clinical diagnosis of pyelonephritis with fever, back pain and/or costovertebral angle tenderness, and a positive urine culture

§Race/marital status/years of education

Table 2. Virulence Genotypes and Hemagglutination Titers of Clinical Isolates

Strain	papACEFG	sfar/focDE	fimH	hyA	fyuA	itutA	kpsMTII	kpsMTIII	K1	K5	ibeA	traT	PAI	HA*	HA+ mannose	FimH Immunoblot
ASB1	+	+	+	+	+	-	+	-	+	-	+	+	+	128	<2	+
ASB2	-	-	+	-	+	-	-	-	-	-	+	+	+	64	<2	+
ASB3	-	-	+	-	+	+	-	-	-	+	-	+	+	128	<2	+++
ASB4	-	-	+	-	-	-	-	-	-	+	-	-	-	32	<2	+
ASB5	-	+	+	+	+	-	+	-	-	+	-	+	+	128	<2	+
acute1	-	+	+	-	+	+	+	-	+	-	-	+	+	16	<2	0
acute2	-	-	+	-	-	-	+	-	-	+	-	+	-	64	<2	+
acute3	+	+	+	+	+	-	-	+	-	-	-	-	+	64	<2	++
acute4	+	+	+	+	+	-	-	-	-	+	+	-	+	32	<2	+
rUT1	-	-	+	-	-	-	-	-	-	-	-	-	-	8	8	0
rUT2	-	-	+	-	+	-	+	-	-	+	-	+	+	2	<2	+
rUT3	+	+	+	+	+	-	-	+	-	-	-	+	+	8	2	+
rUT4	+	-	+	+	+	+	-	-	-	+	-	+	+	2	<2	0
rUT5	+	+	+	+	+	+	-	-	-	+	-	+	+	8	4	+
pyelo1	-	-	+	+	+	-	-	-	-	-	-	+	-	16	16	+
pyelo2	-	+	+	-	-	-	-	-	-	-	-	-	-	4	2	+
pyelo3	-	+	+	-	+	+	-	-	-	+	-	+	+	8	8	+
pyelo4	-	+	+	-	+	+	-	-	+	-	+	+	-	8	8	+
UTI89	+	+	+	+	+	-	+	+	+	-	+	+	+	64	2	++
CFT073	+	+	+	+	+	+	-	-	-	-	-	-	+	128	4	++
% prevalence	40	60	100	50	80	40	70	10	20	45	25	70	70			

Abbreviation: HA, hemagglutination of guinea pig red blood cells

*Values equal 2^x, where x equals the last well of agglutination

†Percent expression relative to UT189; 0 = 0%-49%, + = 50%-99%, ++ = 100%-149%, +++ = 150%-199%

Table 3. Summary of IBC formation at different time points

	3h	6h	24h	no IBCs	Avg IBC diameter (μm)
ASB isolates	0/5	4/5	4/5	0/5	51 +/- 20
acute isolates	1/4	1/4	0/4	1/4	20 +/- 8
recurrent isolates	1/5	2/5	1/5	1/5	41 +/- 14
pyelonephritis isolates	0/4	3/4	0/4	1/4	55 +/- 10

n = 5 mice/time point
 measured 5 IBCs/bladder/isolate, n = 5 bladders

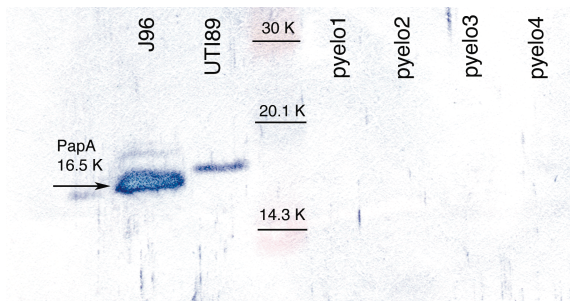


Figure 1. Immunoblot of pyelonephritis isolates with antibodies against P pili. P pilus antibodies were raised against J96 P pili, thus J96 and UT189 were used as positive controls for P pili production. Both isolates are positive for P pili due to a PapA-specific band at 16.5 K. However, the P pilus antibody did not recognize protein at 16.5 K for the four pyelonephritis isolates, confirming the lack of the *pap* operon seen with multiplex PCR. Thus, pyelo1, pyelo2, pyelo3, and pyelo4 do not contain the genes nor produce protein associated with P pili which are thought to be critical in kidney colonization.

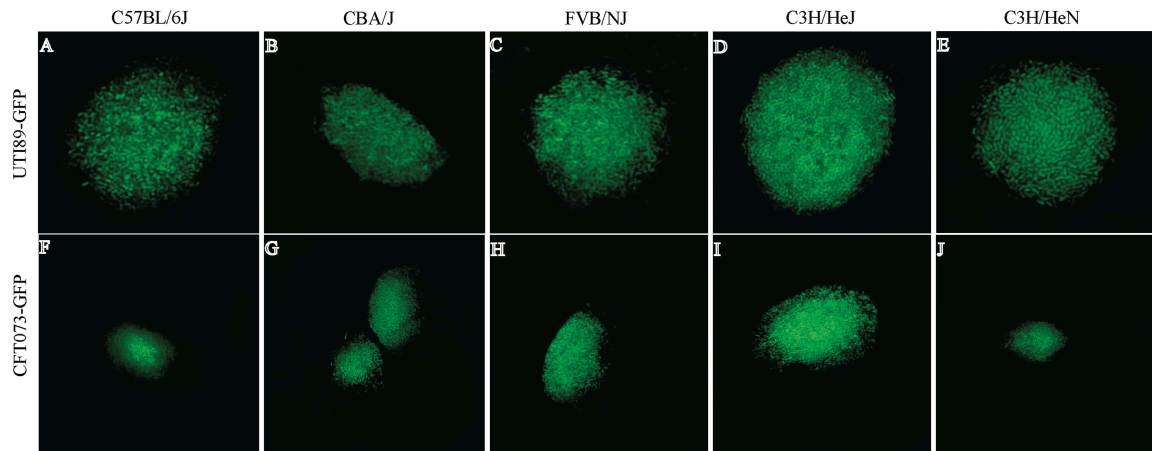


Figure 2. UTI89 and CFT073 formed IBCs in multiple mouse strains. UTI89 and CFT073, two commonly used UTI isolates, were inoculated into 5 different mouse strains. At 6 h post-infection each strain of mice was able to support IBC formation by each UTI isolate. (A-E) represents UTI89 IBCs and (F-J) represents CFT073 IBCs.

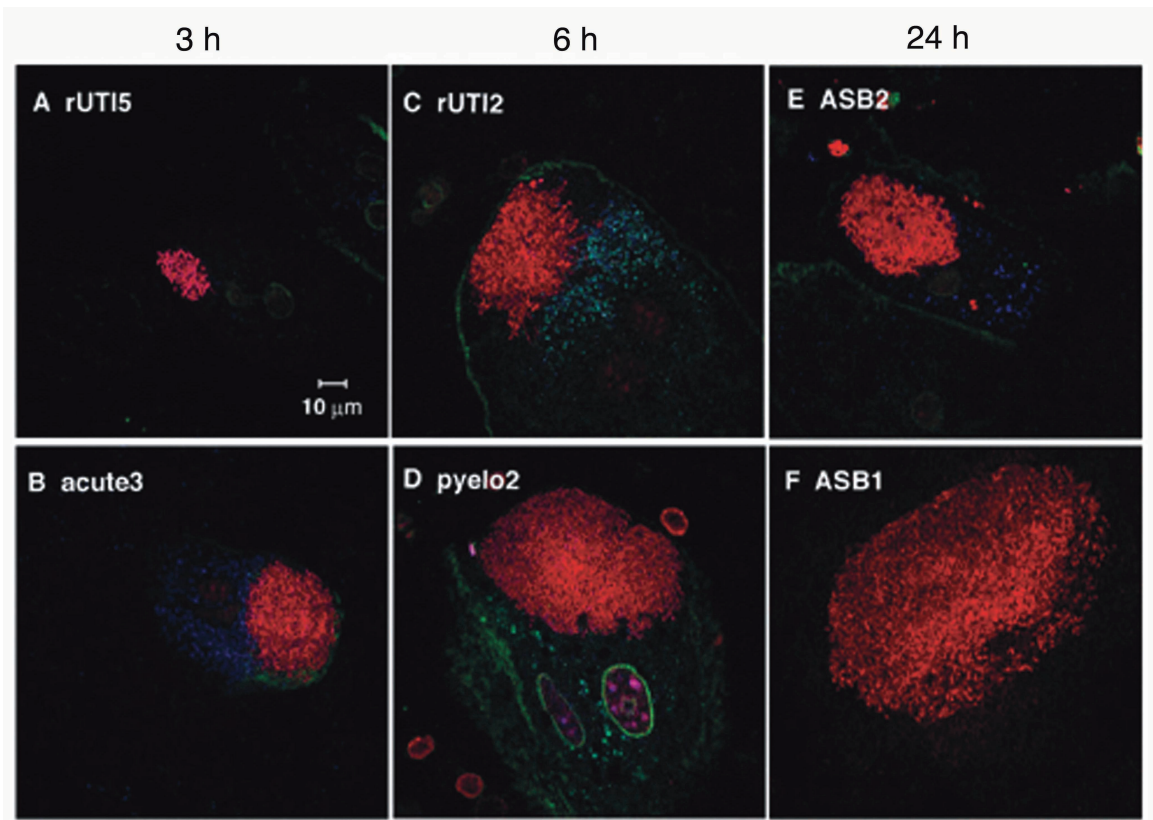


Figure 3. IBCs were formed by UPEC isolated from women. Clinical isolates (red) were inoculated into C3H/HeN female mice and bladders were harvested at 3 h, 6 h, and 24 h. Fifteen isolates produced IBCs at either (A,B) 3 hours, (C,D) 6 hours, or (E,F) 24 hours. Each clinical syndrome is represented above. The cell surface (green) was stained with WGA and in this cross-sectional view can be seen bordering the umbrella cells. While the majority of isolates produced IBCs, size and density of the IBCs varied. Bars = 10 μ m.

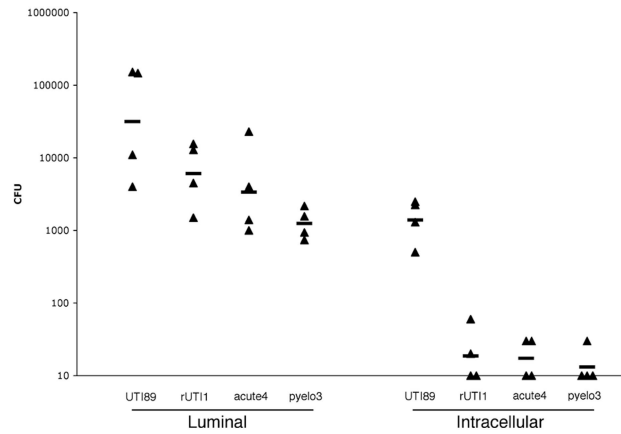


Figure 4. The three non-IBC forming isolates, rUTI1, acute4, and pyelo3, were deficient in invasion *in vivo*. C3H/HeN female mice were inoculated with UTI89, rUTI1, acute4, and pyelo3. At 1 h post-infection bladders were removed and processed. The *Luminal* fraction represents luminal bacteria and the *Intracellular* fraction represents invaded bacteria. One hour after inoculation, 4.4% of UTI89 bacteria invaded whereas for rUTI1, acute4, and pyelo3 only 0.3%, 0.5%, and 1.1% of luminal bacteria invaded, respectively. Thus, the three non-IBC forming isolates invade poorly relative to UTI89.

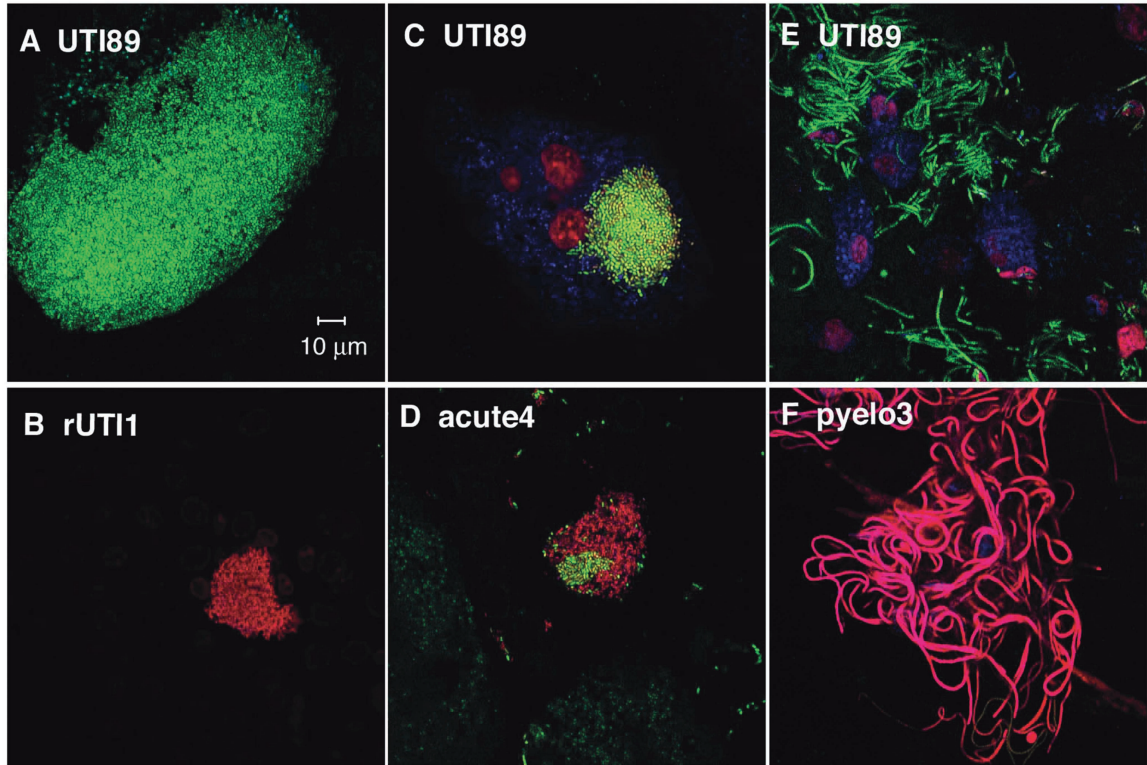


Figure 5. Co-infection with a clinical isolate and UTI89 altered the behavior of the bacteria.

(A,B) rUT11 (red) produced IBCs only when co-infected with UTI89 (green) and caused UTI89 to produce abnormally large IBCs (compare A to C). (C,D) acute4 (red) formed mixed IBCs with UTI89 (green) which also formed normal IBCs. (E,F) pyelo3 (red) formed large collections of filaments, induced UTI89 (green) to do the same, and prevented UTI89 IBCs. Bars = 10 μ m.

References

1. **Anderson, G. G., J. J. Palermo, J. D. Schilling, R. Roth, J. Heuser, and S. J. Hultgren.** 2003. Intracellular bacterial biofilm-like pods in urinary tract infections. *Science* **301**:105-107.
2. **Eckburg, P. B., E. M. Bik, C. N. Bernstein, E. Purdom, L. Dethlefsen, M. Sargent, S. R. Gill, K. E. Nelson, and D. A. Relman.** 2005. Diversity of the human intestinal microbial flora. *Science* **308**:1635-1638.
3. **Elliott, T. S., L. Reed, R. C. Slack, and M. C. Bishop.** 1985. Bacteriology and ultrastructure of the bladder in patients with urinary tract infections. *J Infect* **11**:191-199.
4. **Foxman, B.** 2002. Epidemiology of urinary tract infections: incidence, morbidity, and economic costs. *Am J Med* **113 Suppl 1A**:5S-13S.
5. **Hooton, T. M., D. Scholes, J. P. Hughes, C. Winter, P. L. Roberts, A. E. Stapleton, A. Stergachis, and W. E. Stamm.** 1996. A prospective study of risk factors for symptomatic urinary tract infection in young women. *N Engl J Med* **335**:468-474.
6. **Hooton, T. M., D. Scholes, A. E. Stapleton, P. L. Roberts, C. Winter, K. Gupta, M. Samadpour, and W. E. Stamm.** 2000. A prospective study of asymptomatic bacteriuria in sexually active young women. *N Engl J Med* **343**:992-997.
7. **Hooton, T. M., and W. E. Stamm.** 1997. Diagnosis and treatment of uncomplicated urinary tract infection. *Infect Dis Clin North Am* **11**:551-581.
8. **Hopkins, W. J., A. Gendron-Fitzpatrick, E. Balish, and D. T. Uehling.** 1998. Time course and host responses to *Escherichia coli* urinary tract infection in genetically distinct mouse strains. *Infect Immun* **66**:2798-2802.

9. **Hoschutzky, H., F. Lottspeich, and K. Jann.** 1989. Isolation and characterization of the alpha-galactosyl-1,4-beta-galactosyl-specific adhesin (P adhesin) from fimbriated *Escherichia coli*. *Infect Immun* **57**:76-81.
10. **Hultgren, S. J., J. L. Duncan, A. J. Schaeffer, and S. K. Amundsen.** 1990. Mannose-sensitive haemagglutination in the absence of piliation in *Escherichia coli*. *Mol Microbiol* **4**:1311-1318.
11. **Hung, D. L., T. L. Raivio, C. H. Jones, T. J. Silhavy, and S. J. Hultgren.** 2001. Cpx signaling pathway monitors biogenesis and affects assembly and expression of P pili. *Embo J* **20**:1508-1518.
12. **Ikaheimo, R., A. Siitonen, T. Heiskanen, U. Karkkainen, P. Kuosmanen, P. Lipponen, and P. H. Makela.** 1996. Recurrence of urinary tract infection in a primary care setting: analysis of a 1-year follow-up of 179 women. *Clin Infect Dis* **22**:91-99.
13. **Johnson, J. R., M. A. Kuskowski, A. Gajewski, S. Soto, J. P. Horcajada, M. T. Jimenez de Anta, and J. Vila.** 2005. Extended virulence genotypes and phylogenetic background of *Escherichia coli* isolates from patients with cystitis, pyelonephritis, or prostatitis. *J Infect Dis* **191**:46-50.
14. **Johnson, J. R., and A. L. Stell.** 2000. Extended virulence genotypes of *Escherichia coli* strains from patients with urosepsis in relation to phylogeny and host compromise. *J Infect Dis* **181**:261-272.
15. **Justice, S. S., C. Hung, J. A. Theriot, D. A. Fletcher, G. G. Anderson, M. J. Footer, and S. J. Hultgren.** 2004. Differentiation and developmental pathways of uropathogenic *Escherichia coli* in urinary tract pathogenesis. *Proc Natl Acad Sci U S A* **101**:1333-1338.
16. **Malik, A. A., N. Radhakrishnan, K. Reddy, A. D. Smith, and P. C. Singhal.** 2002. Morphine-induced macrophage apoptosis modulates migration of

- macrophages: use of in vitro model of urinary tract infection. *J Endourol* **16**:605-610.
17. **Martinez, J. J., M. A. Mulvey, J. D. Schilling, J. S. Pinkner, and S. J. Hultgren.** 2000. Type 1 pilus-mediated bacterial invasion of bladder epithelial cells. *Embo J* **19**:2803-2812.
 18. **Mulvey, M. A., Y. S. Lopez-Boado, C. L. Wilson, R. Roth, W. C. Parks, J. Heuser, and S. J. Hultgren.** 1998. Induction and evasion of host defenses by type 1-piliated uropathogenic *Escherichia coli*. *Science* **282**:1494-1497.
 19. **Mulvey, M. A., J. D. Schilling, and S. J. Hultgren.** 2001. Establishment of a persistent *Escherichia coli* reservoir during the acute phase of a bladder infection. *Infect Immun* **69**:4572-4579.
 20. **Mysorekar, I. U., and S. J. Hultgren.** 2006. Mechanisms of uropathogenic *Escherichia coli* persistence and eradication from the urinary tract. *Proc Natl Acad Sci U S A* **103**:14170-14175.
 21. **Park, H. K., S. S. Shim, S. Y. Kim, J. H. Park, S. E. Park, H. J. Kim, B. C. Kang, and C. M. Kim.** 2005. Molecular analysis of colonized bacteria in a human newborn infant gut. *J Microbiol* **43**:345-353.
 22. **Roberts, J. A., B. I. Marklund, D. Ilver, D. Haslam, M. B. Kaack, G. Baskin, M. Louis, R. Mollby, J. Winberg, and S. Normark.** 1994. The Gal(alpha 1-4)Gal-specific tip adhesin of *Escherichia coli* P-fimbriae is needed for pyelonephritis to occur in the normal urinary tract. *Proc Natl Acad Sci U S A* **91**:11889-11893.
 23. **Russo, T. A., A. Stapleton, S. Wenderoth, T. M. Hooton, and W. E. Stamm.** 1995. Chromosomal restriction fragment length polymorphism analysis of *Escherichia coli* strains causing recurrent urinary tract infections in young women. *J Infect Dis* **172**:440-445.

24. **Scheenen, W. J., L. R. Makings, L. R. Gross, T. Pozzan, and R. Y. Tsien.** 1996. Photodegradation of indo-1 and its effect on apparent Ca²⁺ concentrations. *Chem Biol* **3**:765-774.
25. **Schilling, J. D., R. G. Lorenz, and S. J. Hultgren.** 2002. Effect of trimethoprim-sulfamethoxazole on recurrent bacteriuria and bacterial persistence in mice infected with uropathogenic *Escherichia coli*. *Infect Immun* **70**:7042-7049.
26. **Slonim, L. N., J. S. Pinkner, C. I. Branden, and S. J. Hultgren.** 1992. Interactive surface in the PapD chaperone cleft is conserved in pilus chaperone superfamily and essential in subunit recognition and assembly. *Embo J* **11**:4747-4756.
27. **Snyder, J. A., B. J. Haugen, E. L. Buckles, C. V. Lockett, D. E. Johnson, M. S. Sonnenberg, R. A. Welch, and H. L. Mobley.** 2004. Transcriptome of uropathogenic *Escherichia coli* during urinary tract infection. *Infect Immun* **72**:6373-6381.

CHAPTER THREE

THE PLASMID PUTI89 FROM UROPATHOGENIC *E. COLI* STRAIN, UTI89, HAS VIRULENCE PROPERTIES IMPORTANT FOR UTI PATHOGENESIS

Manuscript in preparation.

Corinne K. Cusumano¹, Chia S. Hung¹, Scott J. Hultgren^{1*}

¹Department of Molecular Microbiology and Microbial Pathogenesis, Washington
University School of Medicine, St. Louis, Missouri 63110

*Corresponding author: Mailing address: Department of Molecular Microbiology, Box
8230, Washington University School of Medicine, 660 S. Euclid Ave., St. Louis, MO
63110. Phone: (314) 362-6772. Fax: (314) 362-1998. E-mail:
hultgren@borcim.wustl.edu.

Author contributions: CKC and SJH conceived and designed the experiments; CKC
performed the experiments; CKC and SJH analyzed the data; CKC and CSH contributed
reagents/materials/analysis tools; and CKC, CSH and SJH wrote the paper.

Abstract

Urinary tract infections (UTIs) afflict nearly 60% of women within their lifetimes, the majority of which are caused by uropathogenic *Escherichia coli* (UPEC). Studies in mice and humans have revealed that UPEC undergo an unexpectedly complex pathogenesis cycle involving both intracellular and extracellular niches. Despite the commonality of the UPEC pathogenesis cycle, no specific urovirulence profile has been determined likely due to the fluid nature of the UPEC genome as the result of horizontal gene transfer and numerous genes of unknown function. Horizontal gene transfer results in

the uptake of large pieces of DNA termed genomic islands (GIs). If these GIs contain one or more virulence genes they are termed pathogenicity islands (PAIs). PAIs can integrate into the chromosome or remain extrachromosomal as a plasmid. UTI89 has a large extrachromosomal element termed pUTI89. The pUTI89 plasmid has characteristics of both F plasmids and other known virulence plasmids. This study sought to determine if pUTI89 is important for virulence. Both *in vitro* and *in vivo* assays were used to examine the function of pUTI89 using plasmid-cured UTI89. Based on growth, type 1 pilus expression and function and biofilm formation, there was no difference between UTI89 and plasmid-cured UTI89. However, upon inoculation into the mouse model of UTI, there was a significant decrease in bacterial colonization of the pUTI89-cured strain at early timepoints post-infection. This defect was confirmed using bacterial load quantification, gentamicin protection assays, confocal microscopy and IBC quantification. Through directed deletions of specific operons on pUTI89, the *cjr* operon was partially implicated in this observed defect. This work implicates pUTI89 in early aspects of infection.

Introduction

Urinary tract infections (UTIs) represent, by number, the most important bacterial infectious disease in highly industrialized countries (14). Sixty-percent of all women will have at least one UTI within their lifetime (16, 46, 52). This infection results in nearly 7 million physicians office visits and \$3.5 billion dollars annually in the United States alone (15). It is thought that acute UTIs develop when bacteria from the fecal flora colonize the vaginal and periurethral mucosa and are subsequently introduced into the bladder by urethral ascension. Women who present with an initial episode of acute UTI have a 25-44% chance of developing a second and a 3% chance of experiencing three episodes within six months of the initial UTI (14). Recurrence occurs despite appropriate antibiotic

treatment and clearance of the initial infection from the urine. A large percentage of recurrent UTI (rUTI) are caused by the same strain of bacteria as the initial infection. One study followed 58 women and found that 68% of recurrences were caused by the same initial index strain of UPEC as determined by restriction fragment length polymorphism (RFLP) analysis (54). The high frequency of same-strain recurrences supports the notion that a UPEC reservoir may exist in the affected individual.

Uropathogenic *Escherichia coli* (UPEC) is the leading causative agent of UTI, responsible for up to 85% of community-acquired UTI and 25% of nosocomial UTI (51). Using a well-characterized clinical UPEC isolate, UTI89, in a murine cystitis model, it has been demonstrated that the pathogenesis of UTI involves intracellular and extracellular components (27, 28, 38). The bladder surface is covered with a urothelium composed of very large superficial umbrella cells which are coated with uroplakins that expose a terminal mannose moiety (64). Type 1 pili and its adhesin, FimH, are required for attachment and invasion therefore playing a critical role in the infection process (38, 40, 63). The FimH protein has a negatively charged pocket that accommodates a mannose unit, namely those exposed by uroplakins on the bladder surface (23). Once bound a signaling cascade is initiated resulting in bacterial internalization (37, 38). Upon internalization, bacteria rapidly replicate within the umbrella cell forming tightly packed intracellular bacterial communities (IBCs) (1, 27). These IBCs can be seen throughout the murine bladder and have biofilm-like properties. Meanwhile, the host is attempting to eliminate infection by exfoliating the umbrella cells and sending an influx of neutrophils (40). The bacteria combat these defenses by exiting the IBCs and filamenting (41). The filamentous bacteria are resistant to engulfment by neutrophils and can go on to bind other umbrella cells, invade, and form second generation IBCs, perpetuating the infection (27). Additionally, bacteria can invade the transitional epithelium beneath the umbrella cells, establish a quiescent intracellular reservoir (QIR) and remain dormant

until they reemerge and potentially cause a recurrence (42). The IBC/QIR pathway could partially explain the often observed recurrent UTI with isolates identical to the primary infection ones (54). Recent work has shown that this is a common pathway among UPEC isolates (17) and evidence of this pathway also has been observed in humans (53).

Horizontal gene transfer is the movement of genetic material between bacteria independent of cell division. It is essential to generating diversity between bacterial species and, through natural selection, contributes to the evolution of bacterial species (13, 31, 55). In addition to genetic variability, newly acquired DNA can enable adaptation to life in a specialized niche through specific factors. The acquisition of DNA by horizontal gene transfer results in the exchange of large regions of DNA called genomic islands (GIs) between bacteria. GIs can be acquired in several ways; through inheritance of a plasmid that can remain autonomous or recombine into the chromosome, integration of a lysogenic phage into the chromosome, and insertion of a linear DNA fragment into the chromosome usually by transposition or recombination (12, 34, 58). Some GIs are referred to as pathogenicity islands (PAIs) if they contain large genomic DNA regions greater than 20 kb that carry at least one virulence gene, are inserted within or near tRNA genes, contain direct repeats and mobility sequences and can be identified by a differing G+C content relative to the host bacteria (19). Additionally, PAIs often do not represent homogeneous pieces of DNA but instead are mosaic-like structures generated by a multistep process involving genomic acquisition, loss and rearrangement (20). Since UPEC PAIs are among the best understood, UPEC is considered the model system for analysis of the genome structure and composition of PAIs of pathogenic bacteria in general (6). Study of UPEC PAIs has revealed that they encode adherence factors, toxins and iron uptake systems. Interestingly, these same

virulence factors can be plasmid or phage encoded on intestinal *E. coli* isolates whereas in UPEC they are located chromosomally, i.e. alpha-hemolysin. Thus, UPEC PAIs could represent former plasmid-derived sequences. Additionally, UPEC PAIs carry many cryptic genes, open reading frames of unrelated and even unknown functions, pseudogenes and junk DNA sequences. UPEC isolate, UTI89, carries a large extrachromosomal element with many characteristics of UPEC PAIs. This plasmid, pUTI89, has a high proportion of pseudogenes generated by insertion events, open reading frames homologous to proteins of non-plasmid origin and orthologs of enteroinvasive *E. coli* (EIEC) proteins found on a large virulence plasmid (10). These features describe a UPEC PAI that has potentially not yet incorporated into the genome, known as a 'PAI precursor' (32). pUTI89 is approximately 114 kb and, like plasmid F, contains the *tra* operon for conjugative transfer as well as genes associated with plasmid replication and inheritance.

While UPEC manifest disease in the urinary tract, they normally exist within the intestinal tract of humans. Thus UPEC are distinct from the commensal *E. coli* residing in the GI tract in that they possess virulence factors enabling successful transition to and colonization of the urinary tract. To date, the factors required for successful infection in addition to type 1 pili have yet to be fully elucidated (63). While studies have demonstrated that additional adhesin systems, toxins, autotransporters and iron acquisition factors may be important in establishing infection, there is also an abundance of unknown genes labeled as hypothetical or assigned putative functions that may play a role in virulence (26). This study questions whether pUTI89 is important in the virulence of UPEC. Evidence of regions of pUTI89 are present in the majority of clinical isolates tested suggesting maintenance and transmission within the community and importance in some aspect of virulence. Testing of *in vitro* and *in vivo* characteristics reveal that pUTI89 is involved in an early feature of *in vivo* infection, while not altering any of the

tested *in vitro* behavior. A region on pUTI89 encoding the *cjr* operon found in EIEC may be involved in this early defect.

Materials and Methods

Bacterial strains.

E. coli UTI89 is a cystitis-derived isolate of serotype O18:K1:H7 (41). UTI89 was used for all assays within this study. A panel of clinical isolates was used to identify the presence of pUTI89. This panel has been previously described by Garofalo *et al.* (17).

Plasmid purification and PCR to assay for pUTI89.

Bacterial cultures from 18 clinical isolates and UTI89 were incubated overnight at 37°C under shaking conditions. Cells were harvested at 6000 rpm for 10 min and resuspended in 25 mM Tris-HCl (pH 8.0), 50 mM EDTA. After the addition of 0.2 M NaOH, cells were incubated on ice for 10 min followed by the addition of 5 M potassium acetate. After a 5 min incubation, the solution was spun at 9000 rpm for 15 min. Isopropanol was then added to the supernatant and incubated at room temperature for 20 min. The solution was spun for 15 min at 3500 rpm at 4°C. The pellet was air-dried and resuspended in TE buffer. After resuspension, 10 M NH₄OAc was added and incubated on ice for 20 min. The solution was spun, ethanol was added to the supernatant and incubated at -20°C for 20 min. DNA was then precipitated, washed twice with 75% ethanol and resuspended in TE buffer. RNA was eliminated by incubation with RNase A. 5 M NaCl and 30% PEG-6000 were added to the solution and incubated for 30 min on ice. After centrifugation, the precipitate was resuspended in TE buffer and the DNA was extracted using phenol/chloroform. DNA was precipitated with ethanol, washed twice with 75% ethanol and resuspended in TE buffer. The purified plasmid DNA was then used for PCR analysis. Using the sequence of pUTI89, primers

were designed to amplify regions around the plasmid. These 8 primer pairs were named A-H (Table 1). A primer pair amplifying *ompA* was used as a control for genomic contamination. Standard PCR protocols were used. PCR products were run on a 1% agarose gel and bands were detected by ethidium bromide staining. A band migrating the correct distance represented a “+” for that region of pUTI89.

pUTI89 curing.

Using the phage lambda Red recombinase system (11), UP062 and UP063 encoding the stability operon were deleted from UTI89 to make UTI89/pUTI89/ Δ UP062-63, creating a kanamycin-resistant UTI89. This mutant of UTI89 was then cured of pUTI89 by ethidium bromide treatment. Curing was done essentially as described by Bastarrachea and Willetts (4). Briefly, UTI89/pUTI89/ Δ UP062-63 was grown overnight in LB + 50 μ g/ml kanamycin. Approximately 10^2 to 10^4 cells/ml of the overnight culture were inoculated into flasks containing LB + 10 fold dilutions of ethidium bromide beginning with 100 μ g/ml down to 10 μ g/ml and shaken at 37°C for 16 hours. Using the highest concentration of ethidium bromide that sustained growth, the culture was diluted and plated on to LB agar plates and grown overnight at 37°C. Single colonies were picked from the LB agar plate and patched on to LB agar plates containing 50 μ g/ml kanamycin. Colonies sensitive to kanamycin were grown overnight in LB and subjected to plasmid purification and PCR for pUTI89 as described above. Cultures with no positive reactions in the PCR assay were considered to be cured of pUTI89.

Growth curves.

Standard growth curve assays were performed. Bacteria were grown in LB at 37°C shaking overnight. Cultures were diluted 1:1000 into either LB or M9 minimal media +

10 µg/ml niacin and 200 µl was inoculated into a 96 well plate in triplicate. A microplate reader running the SoftmaxPro program was used to read at 37°C, every 20 min for 10 hours with shaking at OD₆₀₀. Data from each read was averaged and graphed to obtain the growth curve.

Immunoblot assay for FimH and FimA.

For immunoblot assays of FimH and FimA expression, bacteria were grown statically in LB at 37°C for 24 hours to obtain optimal type 1 pili expression. Equivalent numbers of cells (OD₆₀₀ = 1.0) from each isolate were suspended in SDS sample buffer, 1 M HCl was added dropwise until a pH indicator (bromophenol blue) turned yellow, and solution was heated at 95°C for 5 min. The samples were then neutralized and analyzed by SDS-polyacrylamide gel electrophoresis followed by immunoblotting with antibodies to either FimH or FimA (raised in rabbits using purified FimH or FimA protein, respectively). Specific FimH or FimA proteins were visualized on nitrocellulose membranes by using the BCIP/NBT liquid substrate system (Sigma) and analyzed for intensity using ImageJ software (<http://rsb.info.nih.gov/ij/>).

Hemagglutination assay.

Bacteria were grown 24h (as described in the immunoblot assay) to induce expression of type 1 pili. Hemagglutination (HA) assays with guinea pig erythrocytes were performed using well-established protocols (22). Briefly, equivalent numbers of cells (OD₆₀₀ = 1.0) from each isolate were suspended in PBS or PBS + 2% mannose and added in 2-fold dilutions to V-bottom 96-well plates (Costar). Guinea pig erythrocytes were cleaned, resuspended in PBS to an OD₆₄₀ = 1.9 and added to the 96-well plate. The plate was incubated at 4°C overnight. The HA titer was scored by the last well with visible agglutination. An HA titer of 1 equals agglutination at a 1:2 dilution whereas an

HA titer of 9 equals agglutination at a 1:512 dilution indicating a high level of type 1 pili function.

Biofilm assay.

Bacteria grown overnight in LB were diluted 1:1000 into LB, M9 minimal media + 10 µg/ml niacin, or YESCA broth and added to 96-well PVC microtiter plates. LB and M9 + 10 µg/ml niacin biofilms were grown at room temperature for 48 hours and YESCA biofilms were grown at 30°C for 48 hours. Plates were rinsed and stained with crystal violet and biofilms were quantified at OD₆₀₀ after solubilization in 33% acetic acid as described (45).

Mouse infections.

All mouse infection studies were approved by the Animal Studies Committee of Washington University. Eight-week-old C3H/HeN (NCI) female mice were anesthetized by inhalation of isoflurane and infected via transurethral catheterization with a 50-µl suspension of $\sim 1 \times 10^7$ CFU of a given isolate. Bacteria for inoculation were grown 24 hours at 37°C statically. At the indicated times post-infection, mice were sacrificed by cervical dislocation under anesthesia, and the bladders were immediately harvested and processed as described below.

Tissue bacterial titer determination.

To enumerate the bacteria present, bladders were aseptically harvested 6, 24, 48 h and 1 and 2 wk post-infection, homogenized in PBS, serially diluted, and plated onto LB agar plates. CFU was enumerated after 16 h of growth at 37°C.

Gentamicin protection assay.

To enumerate the bacteria present in the intracellular versus extracellular compartments, bladders were aseptically harvested at 1 and 6 h post-infection. Bladders were then bisected twice and washed 3 times in 500 μ l PBS each. The wash fractions were pooled, lightly spun at 500 rpm for 5 min to pellet exfoliated bladder cells, serially diluted and plated on LB agar to obtain the luminal fraction. The bladders were treated with 100 μ g/ml gentamicin for 90 min at 37°C. After treatment, the bladders were washed twice with PBS to eliminate residual gentamicin, homogenized in 1 ml PBS, serially diluted and plated on LB agar to obtain the intracellular fraction. CFU was enumerated after 16 h of growth at 37°C.

Confocal scanning laser microscopy.

To visualize bacterial behavior within the bladder, bladders were aseptically harvested at 6 h post-infection. Bladders were bisected and pinned open revealing the luminal surface. The splayed bladders were then incubated for 20 min at room temperature with (i) Alexa Fluor 488-conjugated wheat germ agglutinin (WGA) (1:1000 in PBS; Molecular Probes) to stain the bladder luminal surface and (ii) nucleic acid dye SYTO61 red (1:1000 in PBS; Molecular Probes) to stain bacteria and bladder epithelial cell nuclei. Trolox (10 μ M; Fluka) was added to the splayed bladders to reduce photobleaching (56). Bladders were examined with a Zeiss LSM 510 Meta Laser Scanning inverted confocal microscope using a 63x oil immersion objective. WGA and SYTO61 were excited at 488 and 633 nm, respectively.

Enumeration of IBCs.

To accurately count the number of IBCs, bladders were aseptically harvested at 6 h post-infection, bisected, splayed on silicone plates and fixed in 2% paraformaldehyde. IBCs, readily discernable as punctate violet spots, were quantified by LacZ staining of whole bladders (29).

Results

UTI89 contains a plasmid of unique characteristics.

Many *E. coli* strains possess extra-chromosomal genetic elements carrying genes encoding for DNA transfer apparatus. These elements include the conjugative plasmids F and R100. Some other plasmids carried by pathogenic strains, such as pO157 in EHEC isolates, contain genes encoding for putative virulence factors such as toxins, type III secretion apparatus and adhesive organelles (8, 35). Many studies have demonstrated the involvement of these plasmids in EHEC pathogenesis (5, 30, 59, 60).

UTI89 contains an epichromosomal genetic element of 114,230 nt (10). This plasmid could be divided into two major portions based on their homology with other *E. coli* plasmids. One half of the plasmid contains genes involved in plasmid replication and conjugative DNA transfer similar to those on Plasmid F, an archetypical conjugative plasmid. A large number of ORFs on the other half of pUTI89 show homology (>70% at the amino acid level) to genes present on plasmids from pathogenic *E. coli* plasmids (Figure 1). Three pUTI89 ORFs were identified to be orthologs of EIEC O164 *cjrA*, *cjrB* and *cjrC* genes. In EIEC O164, these genes are found on the large virulence plasmid and encode proteins involved in uptake of colicin Js (57). Expression of these genes appears to be regulated by both iron and temperature. Similar to their orthologs in EIEC O164 plasmid, a putative iron regulation *fur* box was also located upstream of pUTI89 *cjrA* (nt 21010-21028). UTI89 CjrB is homologous to the TonB protein present in many gram-negative bacteria which is thought to be involved in energy transduction between the inner and outer membrane (49). Likewise, UTI89 CjrC shows homology to putative outer membrane siderophore receptors. Similar to the EIEC O164 large virulence plasmid, pUTI89 possesses the *senB* gene, encoding an enterotoxin, downstream of and partially overlapping the *cjrC* gene. The *senB* gene was demonstrated to account for at least 50% enterotoxic activity of another EIEC strain, EI34 (44).

Six pUTI89 ORFs also showed high identity to those located on UTI89 chromosome. Four of these were either transposases or hypothetical proteins of unknown function. Two other ORFs, UP042 and UP043, are homologous to genes predicted to possess transport functions at the membrane. UP042 exhibited 100% amino acid identity to a gene encoding a component of a putative ABC transporter system that is also found in UPECs F11 and UMN026. UP043 was 95% identical at the amino acid level to an outer membrane heme receptor encoded by the UTI89 chromosome. Similar to their counterparts on the plasmid, the two homologs to UP042 and UP043 in UTI89 genome (UTI89_C1129 and UTI89_C1130) were also adjacent to each other on the chromosome. Two transposases adjacent to one another on the plasmid, UP040 and UP041, also had adjacent homologs (UTI89_C2257 and UTI89_C2258) on the chromosome. However, while these two sets of ORFs were located near each other on the plasmid, their homologous sets were actually over 1 megabase apart on the chromosome. It is unclear if these genes were acquired separately or as a result of a gene duplication event.

Several ORFs within pUTI89 are homologous to sequences encoding proteins of non-plasmid origin in the database. These were *scsCD* [*S. typhimurium* LT2]), *nqrC* (sodium-translocating NADH dehydrogenase (ubiquinone) gamma subunit [*V. cholerae*]) and iron transporters (putative membrane protein and putative periplasmic protein [*Y. pestis*]). Acquisition of these genes likely occurred through evolution of the plasmid suggesting that pUTI89 is a hotspot for recombination and genetic exchange. Furthermore, many pseudogenes were present on the plasmid as the result of gene disruption by insertion and deletion (10). The presence of homologs from pathogenic bacteria and the fluid nature of the plasmid genome argue that pUTI89 might play an important role in UTI pathogenesis.

pUTI89 in UPEC Clinical Isolates.

We sought to determine if pUTI89 and/or its genes were common among UPEC isolates since strong selection to maintain the plasmid by human strains implies importance in pathogenesis. We have previously reported on a panel of UPEC clinical isolates that proceed through the IBC pathway, however differ in time, size, and number of IBCs (17). This panel of isolates encompasses all clinical syndromes of UTI to obtain a representative pool of strains from women with UTI. Extrachromosomal DNA was purified from 18 clinical isolates and PCR amplification of 8 regions on pUTI89 was used to assess its presence in the clinical isolates (Table 2). Of the 18 isolates, 4 (22%) had all 8 regions of pUTI89 suggesting the presence of the entire plasmid and 6 (33%) had no evidence of pUTI89. Of the 12 isolates that had evidence of pUTI89 (67%), 100% of them had the region containing UP100 and UP101, both hypothetical proteins. This would suggest that these proteins are an important characteristic of pUTI89 since it is most commonly maintained in human UPEC isolates. Furthermore, the prevalence of pUTI89 regions within this panel of clinical isolates (67%) suggests its involvement in pathogenesis within the urinary tract. Due to small amounts of genomic contamination in the plasmid preparation it is possible that the regions identified within the clinical isolates exist on the chromosome of the isolate rather than as an extrachromosomal element. However, that these regions are still maintained in the population is evidence of their importance.

Deletion of pUTI89.

Due to the unique characteristics of pUTI89, further study was required to elucidate its function. We sought to eliminate pUTI89 from UTI89 and assess the behavior of the bacteria without the plasmid *in vitro* and *in vivo*. Currently there are multiple ways to eliminate a plasmid from its host. Traditional ways of curing involve intercalating dyes, DNA gyrase inhibitors, Rifampicin, and SDS. More advanced ways

use transposon-based elimination (25) and SacB curing (24). Unfortunately pUTI89 did not respond to any of the above methods and was not successfully eliminated from UTI89. A new approach was taken based on the genes present on the plasmid. pUTI89 contains the stability (*stb*) locus which is involved in stable inheritance of the plasmid. It is thought to be involved in the partition of plasmid molecules to daughter cells during cell division, which is essential for stable plasmid inheritance. Mutations that inactivate *stb* function result in plasmid instability, so that plasmid-free cells are segregated at a rate consistent with random distribution of plasmid copies at cell division (39). We took advantage of the requirement of these genes for stability to cure pUTI89. First, the stability locus was deleted using the λ red recombinase system (11).

UTI89/pUTI89 Δ stbA/stbB was then subjected to curing by an intercalating dye, ethidium bromide. At a concentration of 90 μ g/mL ethidium bromide, the plasmid was eliminated from UTI89; this was confirmed by selective plating and PCR (Figure 2). Thus, it required both gene manipulation and a traditional curing method to delete pUTI89 from UTI89.

In vitro affect of pUTI89.

Once pUTI89 was successfully eliminated from UTI89, we analyzed its effects on UTI89 *in vitro*. In addition to the *tra* operon, there are several putative outer membrane proteins that may alter the proteinaceous make up of the bacterial membrane and a putative regulator that could have an effect on genes expressed under different environmental conditions. Additionally there are many hypothetical proteins that could have an effect on growth rate, protein expression and biofilm formation. Upon testing growth in both rich media (LB) and minimal media (M9 + 10 μ g/mL niacin), both UTI89 and Δ pUTI89 grew equally well, suggesting that, under these conditions, the plasmid is

not essential for bacterial growth (Figure 3A). Type 1 pili are an essential virulence factor to UTI89 *in vivo* (63), thus it was very important to identify if expression of the *fim* operon was altered by removal of pUTI89. An immunoblot using anti-FimH and anti-FimA antisera showed no difference in expression levels of either protein in UTI89 versus Δ pUTI89 bacteria (Figure 3B). Since expression does not necessarily confirm function, the pili were tested for their ability to agglutinate guinea pig red blood cells. Hemagglutination (HA) titers were analyzed in the presence and absence of mannose to confirm that agglutination was type 1 specific. Both strains had equal mannose-resistant and mannose-sensitive HA titers suggesting that pUTI89 is not involved in type 1 pili expression and function (Figure 3D). Previous work has shown that UTI89 within the bladder forms biofilm-like intracellular bacterial communities (IBCs) (1). Thus, the ability of UTI89 and Δ pUTI89 to form biofilms *in vitro* was evaluated as an indicator of potential behavior *in vivo*. Furthermore, F plasmids have been shown to promote biofilm formation in a K-12 genetic background (18). In both rich media (LB) and minimal media (M9 + 10 μ g/mL niacin), Δ pUTI89 behaved identical to wild-type UTI89 (Figure 3C). Additionally, it was recently discovered that different media conditions require different adhesive fibers for robust biofilm formation, so a second measure of biofilm formation was assayed to look for curli-dependent biofilms (Cegelski *et al*, submitted). These biofilms are grown in YESCA media at 30°C. Both strains had equivalent curli-dependent biofilm formation (Figure 3C). Taken together, these data suggest that UTI89 and Δ pUTI89 are virtually indistinguishable in these aspects of comparative analysis *in vitro*.

In vivo mouse infection.

Although UTI89 and Δ pUTI89 behaved identical *in vitro*, the loss of pUTI89 could have affected the virulence of UPEC in a way that was not measurable by the *in vitro* tests. The *in vivo* pathogenesis was subsequently assessed in the UTI mouse model. In this infection model, UTI89 as well as multiple clinical isolates proceed through an IBC pathway (1, 17, 27). C3H/HeN mice were inoculated with 10^7 of either UTI89 or Δ pUTI89 and bacterial burden was evaluated at different points during infection. At 6 hours post-infection the bacterial load of Δ pUTI89-infected bladders was significantly lower ($p < 0.0001$) than UTI89-infected bladders (Figure 4A). To confirm this observation and minimize the possibility that a secondary mutation contributed to the attenuation, additional clones of Δ pUTI89 constructed independently also showed a significant defect in titers at 6 hours post-infection (Figure 4B). Nevertheless by 24 hours, Δ pUTI89 titers were comparable to UTI89 and remained that way through the entirety of the time course. These data suggest that genes on pUTI89 may be involved in the early stages of infection but does not affect the overall outcome of infection.

In vivo survival.

Due to the significant defect during early infection of the Δ pUTI89 strain despite equivalent *in vitro* type 1 pili expression, we assessed the bacteria's ability to bind to and invade the urothelium *in vivo*. Bladders from 1 and 6 hour infected C3H/HeN mice were removed and both the intracellular and luminal populations were enumerated. At both 1 and 6 hours post-infection there were significant decreases in both binding and invasion of Δ pUTI89 relative to UTI89 (Figure 5). These results suggest pUTI89 is potentially enhancing invasion, enhancing extracellular survival or aiding in immune evasion. In order to confirm the phenotype observed in the gentamicin protection assay, we sought to visually demonstrate a diminished invasion or reduced extracellular colonization by

confocal microscopy. At 6 hours post-infection, UTI89- or Δ pUTI89-infected bladders were removed, splayed and stained. Although both strains form IBCs successfully (Figure 6), the Δ pUTI89-infected bladder had little to no observable extracellular bacteria and IBCs were less numerous than its wild-type-infected counterpart. In addition, UTI89-infected bladders had numerous extracellular bacteria, many in filamentous morphology. In an effort to more accurately enumerate IBCs, we performed LacZ staining on UTI89- and Δ pUTI89-infected bladders. This quantification revealed a significant defect in the number of IBCs observed between the two isolates (Figure 6). These data are consistent with the results from the gentamicin protection assay and identifies pUTI89 as a potential mediator in invasion, extracellular survival or host evasion at the early stage of infection.

Identification of virulence factors on pUTI89.

Deletion of pUTI89 alters UTI89's behavior *in vivo*. In an attempt to decipher which region of pUTI89 is responsible for this observed phenotype, we eliminated small regions of the plasmid and examined their effects in the mouse UTI model. Table 3 specifies the gene, size and predicted function of the regions chosen for deletion. Each of the constructed deletions was individually inoculated into the mouse and bacterial load was evaluated at 6 hours post-infection. Of the 7 deletions made, 2 had a significant decrease on bacterial load relative to UTI89 at 6 hours post-infection (Figure 7). These mutants were Δ UP028-30 and Δ UP062-63. Δ UP062-63 has a 1.4 kb region deleted encoding for the *stbA* and *stbB* genes of the stability operon. These genes are involved in maintenance of the plasmid. The reduction in bacterial titers upon deletion of *stbA/B* confirms the results observed with the Δ pUTI89 mutant (Figure 3); when pUTI89 is not successfully maintained *in vivo* the bacterial infection is reduced. Δ UP028-30 has

a 4.7 kb region deleted encoding for *cjrB*, *cjrC* and *senB*. The *cjr* operon (for colicin Js receptor) encodes for proteins involved in colicin Js uptake as described above (57). The operon contains 3 proteins, however it was shown that only CjrB and CjrC are essential for colicin Js sensitivity. This deletion, however, did not cause as much of a decrease in bacterial titers as does the loss of pUTI89 which suggests that other genes on pUTI89 may also be important during UTI pathogenesis. With these deletion mutants, we have identified at least two regions on pUTI89 that are important for virulence. This work shows that pUTI89 is used to acquire important virulence factors for the early stage of infection. Further work will be required to understand the role of these operons in early infection. Studies are currently underway to examine the expression patterns of the *cjr* and *sen* loci, and their impact on UTI pathogenesis.

Discussion

Virulence in *Enterobacteriaceae* is associated with the acquisition of large plasmids that confer distinguishing phenotypic pathogenic traits. These virulence plasmids are generally low copy number, approximately 60 to 200-kb in size and similar to F plasmid or R100 plasmid (62). Virulence plasmids of other pathogenic *E. coli*, enteropathogenic *E. coli* (EPEC), enterotoxigenic *E. coli* (ETEC) and enteroaggregative *E. coli* (EAEC) are large F-like plasmids that encode different fimbrial adhesins that give characteristic modes of colonization of intestinal epithelia (43). UPEC isolate, UTI89, carries a large F-like plasmid, pUTI89. We attempted to find a role for pUTI89 as a virulence plasmid in the setting of urinary tract infections. The model used to identify virulence focused heavily on the IBC pathway within the mouse, looking at interaction with bladder epithelia and intracellular and extracellular survival.

Our studies of the *in vitro* effects of pUTI89 on UTI89 showed equivalent behavior in every aspect tested. However, many of the genes on pUTI89 encode

hypothetical proteins that could be critical in establishing *in vivo* infection. A similar phenomenon was seen with a *Chlamydia trachomatis* plasmid where there was no observable phenotype *in vitro*, however upon *in vivo* infection in the absence of the plasmid there was a significantly lower ID₅₀ and lack of glycogen accumulation (9). The defect was partially attributed to plasmid-dependent regulation of multiple chromosomal genes. Plasmid control of chromosomally encoded genes is not a unique attribute among bacteria. *Yersinia pestis*, EPEC and *Bacillus anthracis* all have plasmid-encoded loci controlling chromosomally encoded genes (3, 7, 48). We observed similar altered regulation of chromosomal genes in the absence of pUTI89, however, the majority of these genes are hypothetical and will require further examination (data not shown), nonetheless suggesting that pUTI89 functions in *trans* to regulate the transcription of multiple chromosomal genes. Genes on the chromosome were both positively and negatively regulated. Thus, it is likely that there are multiple transcriptional regulators on pUTI89. However, it is also possible that one regulator may function as both a repressor and an activator, as has been reported for some transcriptional regulators (47). Approximately 76 plasmid genes were differentially expressed in the absence of pUTI89 implying their expression in wild type UTI89. It is clear that all of these genes are not transcriptional regulators and may participate in *in vivo* infection.

We have demonstrated that pUTI89 is involved in the early aspect of UPEC pathogenesis, such as binding, invasion or survival. The reduction of luminal population at 6 hours post-infection as revealed by gentamicin protection assay and confocal microscopy (Figures 5-6) suggest the involvement of pUTI89 in extracellular survival during UPEC infection. There may be more to pUTI89 than just extracellular survival since upon quantification of IBCs there was a significant reduction in the number observed at 6 hours post-infection. Interestingly, while there is a reduction in IBC number there is still chronic-active infection at 2 weeks. This would suggest that while

there are less IBCs the threshold of IBC formation has still been reached to enable UTI89 to establish a foothold within the bladder and carry out long term infections.

Selective deletions of operons on pUTI89 revealed that the *cjr* operon may be playing a role in infection. CjrC is homologous to a putative outer member siderophore receptor and a *fur* box is located upstream of this operon suggesting it is regulated by iron. Iron is an essential cofactor of many enzymes and bacteria require iron concentrations at around 10^{-7} to 10^{-5} M to achieve optimal growth. The level of free iron is estimated to be very low in the environment and biological fluids (10^{-18} M) (2). Only bacteria that have strategies to acquire iron sequestered by the host can survive in specific niches and consequently cause infections. Thus, iron acquisition for the survival of UPEC within the urinary tract is extremely important (50, 61, 65). A recent study evaluating the genomic composition specific to UPEC identified that UPEC contain 3-5 iron acquisition systems whereas fecal/commensal isolates contain 2-3 iron-related operons suggesting that the redundancy in these systems may provide a competitive advantage to UPEC within the urinary tract (33). A more recent study comparing siderophore production between urinary and rectal isolates within individual patients revealed that while all strains produced enterobactin, strong preferential expression of yersiniabactin and salmochelin were observed among urinary strains (21). Reigstad *et al.* showed that in the absence of *chuA* there is a significant decrease in IBC size but not an elimination of IBCs (50). This result suggests that the redundancy of the iron acquisition systems allows alternate systems to compensate for the lack of *chuA* highlighting the importance of iron sequestration and transport within the urinary tract. This is why deletion of one system will not completely eliminate infection capabilities as seen with the deletion of the *cjr* operon. Work is currently underway to complement and characterize this operon to understand its role in the early stage of infection. Perhaps it is expressed early in infection whereas other iron acquisition systems are expressed

later, potentially explaining the delayed growth *in vivo* in the absence of the Cjr proteins until more systems are turned on.

Strong selection for UTI89 to maintain pUTI89 provides a compelling argument for its importance in pathogenesis. Large plasmids impose a significant metabolic burden on the bacteria and, in the absence of selection, may be lost from the host in spite of plasmid maintenance systems that are assumed to prevent loss (62). pUTI89 has two prominent features, the presence of the *tra* operon involved in DNA transfer and the presence of virulence genes found on other pathogenic plasmids, in other organisms. Plasmid transfer via conjugation is an important mechanism for DNA exchange or dissemination and accelerates the evolution of bacterial pathotypes (19). The presence of the *tra* operon allows pUTI89 to be maintained and disseminated to other UPEC and *Enterobacteriaceae*. In addition, the large virulence plasmid serves as a genetic hot spot where extrachromosomal DNA can be freely acquired without disrupting essential genes. It is likely that free exchange of DNA between the symbiotic gut bacteria resulted in the diverse genomes seen in UPEC isolates. The presence of the *cjr* operon on pUTI89 as well as on a virulence plasmid in EIEC supports the stated hypothesis. The plasmid, pUTI89, serves as a genetic hotspot where virulence genes are acquired and lost without selection in the gut. Only upon invasion and colonization of the bladder are genes, which increase fitness, selected for. In the example of the *cjr* operon the fitness of the UTI89 was increased and thus selected for. This is supported by nearly 50% of isolates tested showing presence of this operon. This percentage is surprisingly high due to the redundancy in iron acquisition operons.

The presence of pUTI89-like plasmids in UPEC strains could serve multiple roles, allowing for efficient incorporation of foreign DNA without disruption of essential genes. Plasmid stability genes ensure newly acquired genes are replicated without the strong selective pressure of a bladder environment, while a functional *tra* operon allows

for conjugation and dissemination of these genes to other UPEC and *Enterobacteriaceae*. All of these activities provide UPEC with a broad arsenal of proteins, some of which are necessary for colonization of the bladder. Due to the lack of constant selective pressure, UPEC strains, early in evolution, devised multiple strategies for colonization of the bladder, resulting in the diverse genomes of UPEC strains seen today. This process more than likely occurred slowly with virulence plasmids necessary for bladder survival being lost in the gut, and virulence genes incorporated in the genome resulting in genomic instability. The acquisition of a large virulence plasmid with maintenance and stability machinery solved both of these problems. Incorporation of extrachromosomal DNA did not disrupt essential cellular pathways and a stable plasmid allowed genes, which increased fitness in the bladder to be passed on in the bladder or gut. This constant evolution has allowed UPEC to acquire multiple and redundant mechanisms to adapt and thrive in the urinary tract environment explaining why despite the well-studied nature of UPEC, especially in regards to virulence factors and colonization strategies, no single feature accurately defines an isolate as UPEC. The difficulty of this was evident in a study that determined that half of all UPEC isolates contain none or only one of the urovirulence determinants to date (36). Instead, UPEC contains a mosaic genome that is the result of genomic acquisition, loss and rearrangement.

It remains unclear as to when, evolutionarily, pUTI89 was acquired, and to what extent it helped shape the landscape of the UTI89 genome by acting as a midway point for virulence genes incorporation into the genome. We discovered that the presence of pUTI89 increases the ability of UTI89 to invade and colonize the bladder. Further investigations will examine how less virulent strains without pUTI89 are influenced by its addition. Examining a gain of function in less virulent strains could help elucidate at what stage(s) pUTI89 virulence genes function. Additionally, characterizing plasmids and

genes from different UPEC will facilitate our understanding of the mechanism of virulence and the evolution of UPEC, and the design of efficacious strategies to fight UTI.

Acknowledgements

This study was funded by NIH/NIDDKD grant DK 64540 ORWH and the Infectious Diseases/Basic Microbial Pathogenesis Mechanisms Training Grant.

Tables and Figures

Table 1. Primers for plasmid PCR

Gene	Primer sequence (5'-3')	Primer name	Size of product (bp)	Primer coordinates¹
<i>scsD</i>	CATACGCTGGACGGGGAAAC	A-forward	143	+4384
	GACGCTCTCCCCTCCGACT	A-reverse		-4527
<i>senB</i>	GCAGATTCGCGTTTTGAGCA	B-forward	302	+25705
	CGGATCTTCAACGGGATGG	B-reverse		-26006
<i>guaA</i>	CCCGTAGTGGGGGTGTTGAG	C-forward	375	+49081
	GCCCCTGCCACCTACCTTCT	C-reverse		-49456
transposase	GCTTCGGGAACGCTGTAACG	D-forward	414	+60645
	AGAAGGCTGCGGTGCTGAAG	D-reverse		-61059
<i>ycfA</i>	CGCCTGGTGGTGAAGGAAAG	E-forward	236	+64115
	GACCACCTCCCGCAGAACAC	E-reverse		-64351
<i>UP100/UP101</i>	TGGGGGCTGAAAACCAGAGA	F-forward	531	+75326
	ACCGAAGGCACGAACTGCAT	F-reverse		-75857
<i>traU</i>	TTCCTTCTGCCGGTCATGT	G-forward	111	+89649
	CCAGCGAGAGCGGGAAAATA	G-reverse		-89760
<i>traI</i>	GCGATGCGGTCAAGTGTCTG	H-forward	190	+106531
	GGACAGCCGTTTCATCTGCT	H-reverse		-106721

¹GenBank accession no. - NC_007941

Table 2. Evidence of pUTI89 in a panel of clinical isolates.

Strain	<i>scsD</i>	<i>senB</i>	<i>guaA</i>	transposase	<i>ycfA</i>	<i>UP100/UP101</i>	<i>traU</i>	<i>traI</i>	IBCs present (hrs PI)
	A	B	C	D	E	F	G	H	
ASB1	-	-	-	-	-	-	-	-	6,24
ASB2	+	+	+	+	+	+	+	+	6,24
ASB3	+	+	+	+	+	+	+	+	6,24
ASB4	+	+	+	+	+	+	+	+	6
ASB5	-	-	-	-	-	-	-	-	24(rare)
acute1	-	-	-	-	+	+	+	-	12(rare)
acute2	-	-	-	-	-	-	-	-	6 (rare)
acute3	-	-	-	-	-	-	-	-	3(rare)
acute4	-	-	-	-	-	-	-	-	-
rUTI1	-	-	-	-	-	-	-	-	-
rUTI2	-	-	-	-	+	+	-	-	6
rUTI3	-	+	-	-	+	+	-	-	6(few)
rUTI4	+	+	+	+	+	+	+	+	24
rUTI5	-	+	-	-	+	+	+	+	3
pyelo1	-	-	+	-	+	+	-	-	6
pyelo2	+	+	-	+	-	+	-	-	6
pyelo3	-	-	-	+	+	+	+	+	-
pyelo4	-	-	-	-	+	+	+	-	6
UTI89	+	+	+	+	+	+	+	+	3,6,24
% prevalence	31.6	47.4	31.6	36.8	63.2	68.4	47.4	36.8	

scsD secreted copper-sensitivity suppressor D
senB enterotoxin TieB protein
guaA hypothetical protein
transposase transposase for insertion sequence element IS21
ycfA hypothetical protein
UP100/101 hypothetical proteins
traU F pilus assembly protein
traI DNA helicase I

Table 3: Directed knock-outs on pUTI89.

Gene Annotation	Size	Gene Name	Function
UP007-UP014	8.4 kb	<i>scsC/D</i>	secreted copper-sensitivity suppressor, <i>Yersinia</i> export
UP015-UP017	1.6 kb		ABC transporter, ATP-binding protein, putative thioredoxin-family protein
UP028-UP030	4.7 kb	<i>cjrB/C, senB</i>	colicin Js sensitivity protein and OM receptor, enterotoxin
UP042-UP046	6.8 kb		hemin receptor, serine-threonine protein kinase
UP062-UP063	1.4 kb	<i>stbA/B</i>	stable plasmid inheritance proteins
UP095	0.4 kb	<i>psiB</i>	regulator of SOS induction
UP145	0.2 kb	<i>hmo</i>	putative regulator

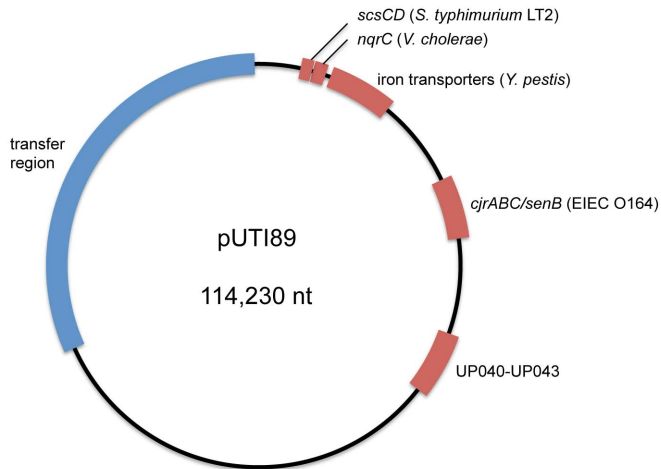


Figure 1: pUTI89 diagram. pUTI89 can be divided into two major portions. One half contains genes involved in conjugative DNA transfer (in blue) and the other half contains genes present on plasmids from pathogenic *E. coli* and other pathogenic bacteria, as well as genes encoded chromosomally in other bacteria (in red). Indicated next to each region is the gene name, organism it is also found in and/or operon function.

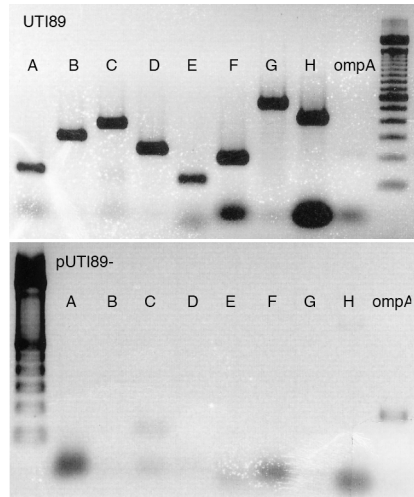


Figure 2: Confirmation of pUTI89 curing by PCR. pUTI89 was cured from UTI89 by ethidium bromide treatment. Plasmid purification followed by PCR with primer pairs A-H was used to identify plasmid-less strains. UTI89 with intact pUTI89 (top panel) reveals a banding pattern as observed with very little genomic contamination as evidenced by the ompA band. PCR of the plasmid-cured strain (bottom panel) revealed no positive PCR reaction confirming the elimination of pUTI89.

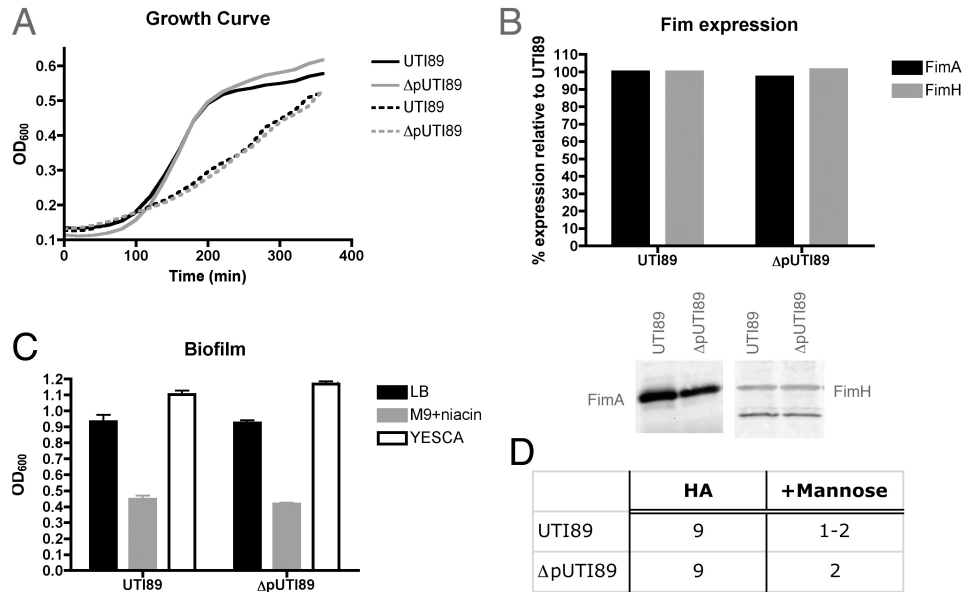


Figure 3: *In vitro* characteristics of pUTI89. Plasmid-cured UTI89 behaved identically to UTI89. (A) Growth of UTI89 and DpUTI89 were equivalent in LB broth (solid line) and M9 + 10 μ g/ml niacin broth (dashed line). (B) Type 1 expression based on FimH and FimA immunoblots was equivalent in both strains. Densitometry analysis quantified the bands observed. (C) Biofilm formation under type 1-dependent and curli-dependent conditions were indistinguishable in UTI89 versus Δ pUTI89. (D) Both UTI89 and Δ pUTI89 exhibited equal mannose-sensitive HA titers, indicating equal expression levels and functionality of type 1 pili.

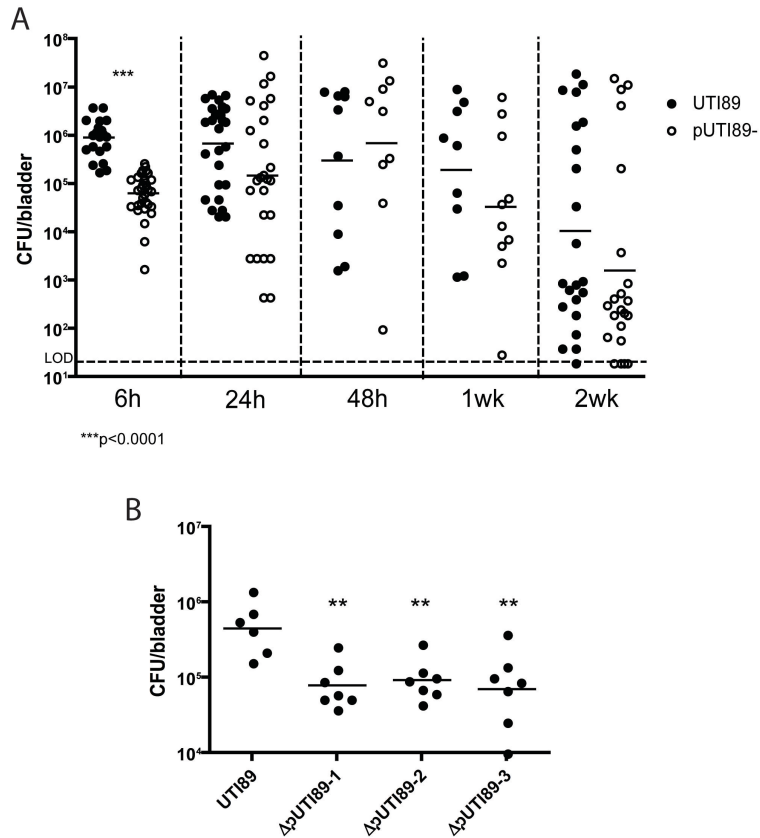


Figure 4: *In vivo* timecourse of UTI89 and Δ pUTI89. (A) Δ pUTI89 tested in our mouse model of UTI revealed a significant decrease in bladder colonization at 6 h post-infection compared to wild type UTI89 ($p < 0.0001$ by Mann Whitney). However by 24 h post-infection and beyond, colonization was equivalent in both strains. (B) Additional clones of Δ pUTI89 confirmed that the defect was due to the loss of pUTI89 and not additional mutations within the genome.

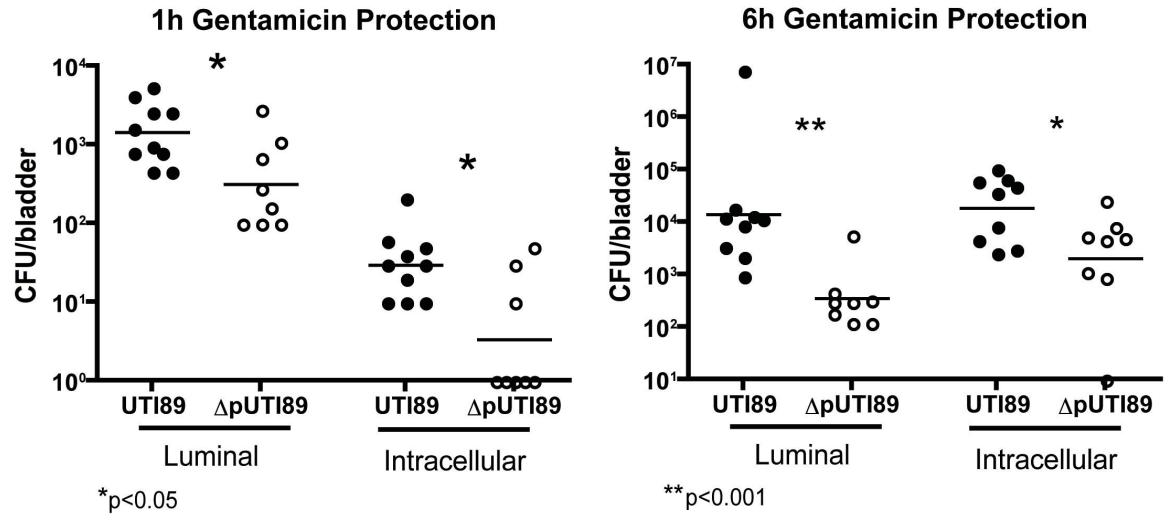


Figure 5: Colonization and invasion of UTI89 versus ΔpUTI89. One and 6 h gentamicin protection assays revealed a significant decrease in both the extracellular (luminal) and intracellular population for ΔpUTI89. A more significant decrease in luminal colonization with ΔpUTI89 was observed at 6 h post-infection (p<0.001).

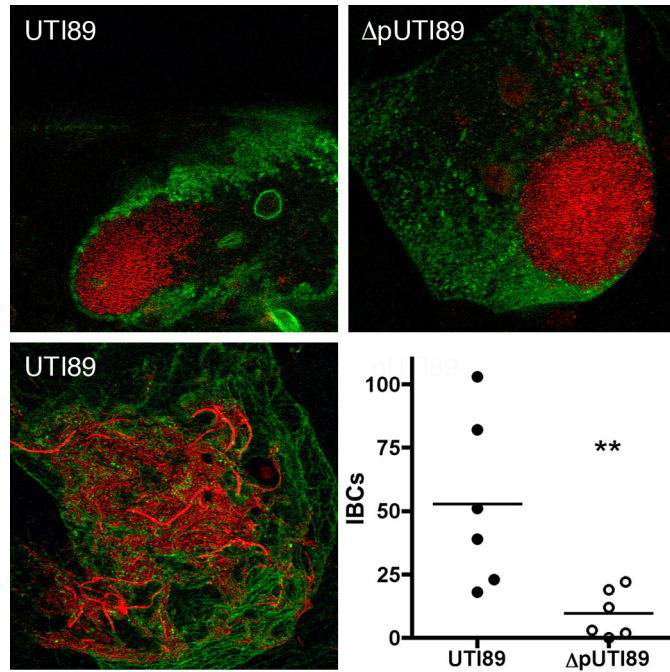


Figure 6: Confocal microscopy and LacZ staining for IBCs. Mice were infected with UTI89 or $\Delta pUTI89$ and bladder were harvest at 6 h post-infection, splayed and stained with WGA (green) and SYTO61 (red). Confocal microscopy revealed IBC formation in bladder infected with either isolate. However, extensive filamentation was only observed in wild-type UTI89. IBCs were quantitated by LacZ staining revealing a significant defect in the number of IBCs observed in $\Delta pUTI89$ -infected bladders.

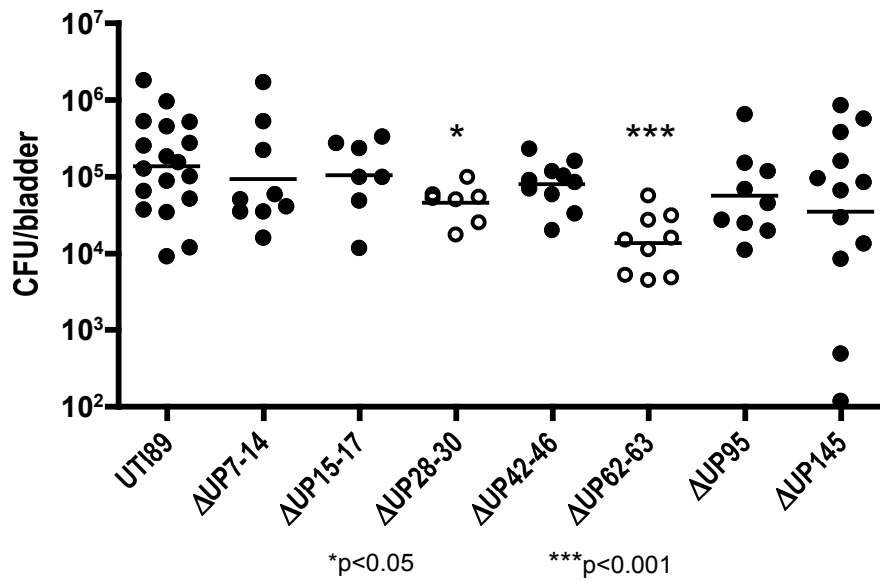


Figure 7: Identification of virulence factors on pUTI89. Regions on pUTI89 were deleted using the lamda red recombinase system. Deletions encompassing UP028-30 and UP062-63 (open circles) resulted in a significant reduction in bacterial load at 6 h post-infection. UP062-63 encodes the stability operon and UP028-30 encodes the *cjr* operon.

References

1. **Anderson, G. G., J. J. Palermo, J. D. Schilling, R. Roth, J. Heuser, and S. J. Hultgren.** 2003. Intracellular bacterial biofilm-like pods in urinary tract infections. *Science* **301**:105-107.
2. **Andrews, S. C., A. K. Robinson, and F. Rodriguez-Quinones.** 2003. Bacterial iron homeostasis. *FEMS Microbiol Rev* **27**:215-237.
3. **Bai, G., E. Smith, A. Golubov, J. Pata, and K. A. McDonough.** 2007. Differential gene regulation in *Yersinia pestis* versus *Yersinia pseudotuberculosis*: effects of hypoxia and potential role of a plasmid regulator. *Adv Exp Med Biol* **603**:131-144.
4. **Bastarrachea, F., and N. S. Willetts.** 1968. The elimination by acridine orange of F30 from recombination-deficient strains of *Escherichia coli* K12. *Genetics* **59**:153-166.
5. **Bauer, M. E., and R. A. Welch.** 1996. Characterization of an RTX toxin from enterohemorrhagic *Escherichia coli* O157:H7. *Infect Immun* **64**:167-175.
6. **Blum, G., M. Ott, A. Lischewski, A. Ritter, H. Imrich, H. Tschape, and J. Hacker.** 1994. Excision of large DNA regions termed pathogenicity islands from tRNA-specific loci in the chromosome of an *Escherichia coli* wild-type pathogen. *Infect Immun* **62**:606-614.
7. **Bourgogne, A., M. Drysdale, S. G. Hilsenbeck, S. N. Peterson, and T. M. Koehler.** 2003. Global effects of virulence gene regulators in a *Bacillus anthracis* strain with both virulence plasmids. *Infect Immun* **71**:2736-2743.
8. **Burland, V., Y. Shao, N. T. Perna, G. Plunkett, H. J. Sofia, and F. R. Blattner.** 1998. The complete DNA sequence and analysis of the large virulence plasmid of *Escherichia coli* O157:H7. *Nucleic Acids Res* **26**:4196-4204.

9. **Carlson, J. H., W. M. Whitmire, D. D. Crane, L. Wicke, K. Virtaneva, D. E. Sturdevant, J. J. Kupko, 3rd, S. F. Porcella, N. Martinez-Orengo, R. A. Heinzen, L. Kari, and H. D. Caldwell.** 2008. The *Chlamydia trachomatis* plasmid is a transcriptional regulator of chromosomal genes and a virulence factor. *Infect Immun* **76**:2273-2283.
10. **Chen, S. L., C. S. Hung, J. Xu, C. S. Reigstad, V. Magrini, A. Sabo, D. Blasiar, T. Bieri, R. R. Meyer, P. Ozersky, J. R. Armstrong, R. S. Fulton, J. P. Latreille, J. Spieth, T. M. Hooton, E. R. Mardis, S. J. Hultgren, and J. I. Gordon.** 2006. Identification of genes subject to positive selection in uropathogenic strains of *Escherichia coli*: a comparative genomics approach. *Proc Natl Acad Sci U S A* **103**:5977-5982.
11. **Datsenko, K. A., and B. L. Wanner.** 2000. One-step inactivation of chromosomal genes in *Escherichia coli* K-12 using PCR products. *Proc Natl Acad Sci U S A* **97**:6640-6645.
12. **Davison, J.** 1999. Genetic exchange between bacteria in the environment. *Plasmid* **42**:73-91.
13. **Dobrindt, U., F. Agerer, K. Michaelis, A. Janka, C. Buchrieser, M. Samuelson, C. Svanborg, G. Gottschalk, H. Karch, and J. Hacker.** 2003. Analysis of genome plasticity in pathogenic and commensal *Escherichia coli* isolates by use of DNA arrays. *J Bacteriol* **185**:1831-1840.
14. **Foxman, B.** 2003. Epidemiology of urinary tract infections: incidence, morbidity, and economic costs. *Dis Mon* **49**:53-70.
15. **Foxman, B.** 2002. Epidemiology of urinary tract infections: incidence, morbidity, and economic costs. *Am J Med* **113 Suppl 1A**:5S-13S.

16. **Foxman, B., R. Barlow, H. D'Arcy, B. Gillespie, and J. D. Sobel.** 2000. Urinary tract infection: self-reported incidence and associated costs. *Ann Epidemiol* **10**:509-515.
17. **Garofalo, C. K., T. M. Hooton, S. M. Martin, W. E. Stamm, J. J. Palermo, J. I. Gordon, and S. J. Hultgren.** 2007. *Escherichia coli* from urine of female patients with urinary tract infections is competent for intracellular bacterial community formation. *Infect Immun* **75**:52-60.
18. **Ghigo, J. M.** 2001. Natural conjugative plasmids induce bacterial biofilm development. *Nature* **412**:442-445.
19. **Hacker, J., G. Blum-Oehler, I. Muhldorfer, and H. Tschape.** 1997. Pathogenicity islands of virulent bacteria: structure, function and impact on microbial evolution. *Mol Microbiol* **23**:1089-1097.
20. **Hacker, J., and J. B. Kaper.** 2000. Pathogenicity islands and the evolution of microbes. *Annu Rev Microbiol* **54**:641-679.
21. **Henderson, J. P., J. R. Crowley, J. S. Pinkner, J. N. Walker, P. Tsukayama, W. E. Stamm, T. M. Hooton, and S. J. Hultgren.** 2009. Quantitative metabolomics reveals an epigenetic blueprint for iron acquisition in uropathogenic *Escherichia coli*. *PLoS Pathog* **5**:e1000305.
22. **Hultgren, S. J., J. L. Duncan, A. J. Schaeffer, and S. K. Amundsen.** 1990. Mannose-sensitive haemagglutination in the absence of piliation in *Escherichia coli*. *Mol Microbiol* **4**:1311-1318.
23. **Hung, C. S., J. Bouckaert, D. Hung, J. Pinkner, C. Widberg, A. DeFusco, C. G. Auguste, R. Strouse, S. Langermann, G. Waksman, and S. J. Hultgren.** 2002. Structural basis of tropism of *Escherichia coli* to the bladder during urinary tract infection. *Mol Microbiol* **44**:903-915.

24. **Hynes, M. F., J. Quandt, M. P. O'Connell, and A. Puhler.** 1989. Direct selection for curing and deletion of Rhizobium plasmids using transposons carrying the Bacillus subtilis sacB gene. *Gene* **78**:111-120.
25. **Imre, A., F. Olasz, J. Kiss, and B. Nagy.** 2006. A novel transposon-based method for elimination of large bacterial plasmids. *Plasmid* **55**:235-241.
26. **Johnson, J. R.** 1991. Virulence factors in Escherichia coli urinary tract infection. *Clin Microbiol Rev* **4**:80-128.
27. **Justice, S. S., C. Hung, J. A. Theriot, D. A. Fletcher, G. G. Anderson, M. J. Footer, and S. J. Hultgren.** 2004. Differentiation and developmental pathways of uropathogenic Escherichia coli in urinary tract pathogenesis. *Proc Natl Acad Sci U S A* **101**:1333-1338.
28. **Justice, S. S., D. A. Hunstad, P. C. Seed, and S. J. Hultgren.** 2006. Filamentation by Escherichia coli subverts innate defenses during urinary tract infection. *Proc Natl Acad Sci U S A* **103**:19884-19889.
29. **Justice, S. S., S. R. Lauer, S. J. Hultgren, and D. A. Hunstad.** 2006. Maturation of intracellular Escherichia coli communities requires SurA. *Infect Immun* **74**:4793-4800.
30. **Lathem, W. W., T. E. Grys, S. E. Witowski, A. G. Torres, J. B. Kaper, P. I. Tarr, and R. A. Welch.** 2002. StcE, a metalloprotease secreted by Escherichia coli O157:H7, specifically cleaves C1 esterase inhibitor. *Mol Microbiol* **45**:277-288.
31. **Lawrence, J. G.** 1999. Gene transfer, speciation, and the evolution of bacterial genomes. *Curr Opin Microbiol* **2**:519-523.
32. **Lee, C. A.** 1996. Pathogenicity islands and the evolution of bacterial pathogens. *Infect Agents Dis* **5**:1-7.

33. **Lloyd, A. L., D. A. Rasko, and H. L. Mobley.** 2007. Defining genomic islands and uropathogen-specific genes in uropathogenic *Escherichia coli*. *J Bacteriol* **189**:3532-3546.
34. **Maiden, M. C.** 1998. Horizontal genetic exchange, evolution, and spread of antibiotic resistance in bacteria. *Clin Infect Dis* **27 Suppl 1**:S12-20.
35. **Makino, K., K. Ishii, T. Yasunaga, M. Hattori, K. Yokoyama, C. H. Yutsudo, Y. Kubota, Y. Yamaichi, T. Iida, K. Yamamoto, T. Honda, C. G. Han, E. Ohtsubo, M. Kasamatsu, T. Hayashi, S. Kuhara, and H. Shinagawa.** 1998. Complete nucleotide sequences of 93-kb and 3.3-kb plasmids of an enterohemorrhagic *Escherichia coli* O157:H7 derived from Sakai outbreak. *DNA Res* **5**:1-9.
36. **Marrs, C. F., L. Zhang, P. Tallman, S. D. Manning, P. Somsel, P. Raz, R. Colodner, M. E. Jantunen, A. Siitonen, H. Saxen, and B. Foxman.** 2002. Variations in 10 putative uropathogen virulence genes among urinary, faecal and peri-urethral *Escherichia coli*. *J Med Microbiol* **51**:138-142.
37. **Martinez, J. J., and S. J. Hultgren.** 2002. Requirement of Rho-family GTPases in the invasion of Type 1-piliated uropathogenic *Escherichia coli*. *Cell Microbiol* **4**:19-28.
38. **Martinez, J. J., M. A. Mulvey, J. D. Schilling, J. S. Pinkner, and S. J. Hultgren.** 2000. Type 1 pilus-mediated bacterial invasion of bladder epithelial cells. *EMBO J* **19**:2803-2812.
39. **Miki, T., A. M. Easton, and R. H. Rownd.** 1980. Cloning of replication, incompatibility, and stability functions of R plasmid NR1. *J Bacteriol* **141**:87-99.
40. **Mulvey, M. A., Y. S. Lopez-Boado, C. L. Wilson, R. Roth, W. C. Parks, J. Heuser, and S. J. Hultgren.** 1998. Induction and evasion of host defenses by type 1-piliated uropathogenic *Escherichia coli*. *Science* **282**:1494-1497.

41. **Mulvey, M. A., J. D. Schilling, and S. J. Hultgren.** 2001. Establishment of a persistent *Escherichia coli* reservoir during the acute phase of a bladder infection. *Infect Immun* **69**:4572-4579.
42. **Mysorekar, I. U., and S. J. Hultgren.** 2006. Mechanisms of uropathogenic *Escherichia coli* persistence and eradication from the urinary tract. *Proc Natl Acad Sci U S A* **103**:14170-14175.
43. **Nataro, J. P., and J. B. Kaper.** 1998. Diarrheagenic *Escherichia coli*. *Clin Microbiol Rev* **11**:142-201.
44. **Nataro, J. P., J. Seriwatana, A. Fasano, D. R. Maneval, L. D. Guers, F. Noriega, F. Dubovsky, M. M. Levine, and J. G. Morris, Jr.** 1995. Identification and cloning of a novel plasmid-encoded enterotoxin of enteroinvasive *Escherichia coli* and *Shigella* strains. *Infect Immun* **63**:4721-4728.
45. **O'Toole, G. A., and R. Kolter.** 1998. Initiation of biofilm formation in *Pseudomonas fluorescens* WCS365 proceeds via multiple, convergent signalling pathways: a genetic analysis. *Mol Microbiol* **28**:449-461.
46. **Patton, J. P., D. B. Nash, and E. Abrutyn.** 1991. Urinary tract infection: economic considerations. *Med Clin North Am* **75**:495-513.
47. **Perez-Martin, J., F. Rojo, and V. de Lorenzo.** 1994. Promoters responsive to DNA bending: a common theme in prokaryotic gene expression. *Microbiol Rev* **58**:268-290.
48. **Porter, M. E., P. Mitchell, A. J. Roe, A. Free, D. G. Smith, and D. L. Gally.** 2004. Direct and indirect transcriptional activation of virulence genes by an AraC-like protein, PerA from enteropathogenic *Escherichia coli*. *Mol Microbiol* **54**:1117-1133.
49. **Postle, K.** 1993. TonB protein and energy transduction between membranes. *J Bioenerg Biomembr* **25**:591-601.

50. **Reigstad, C. S., S. J. Hultgren, and J. I. Gordon.** 2007. Functional genomic studies of uropathogenic *Escherichia coli* and host urothelial cells when intracellular bacterial communities are assembled. *J Biol Chem* **282**:21259-21267.
51. **Ronald, A. R., L. E. Nicolle, E. Stamm, J. Krieger, J. Warren, A. Schaeffer, K. G. Naber, T. M. Hooton, J. Johnson, S. Chambers, and V. Andriole.** 2001. Urinary tract infection in adults: research priorities and strategies. *Int J Antimicrob Agents* **17**:343-348.
52. **Ronald, A. R., and A. L. Pattullo.** 1991. The natural history of urinary infection in adults. *Med Clin North Am* **75**:299-312.
53. **Rosen, D. A., T. M. Hooton, W. E. Stamm, P. A. Humphrey, and S. J. Hultgren.** 2007. Detection of intracellular bacterial communities in human urinary tract infection. *PLoS Med* **4**:e329.
54. **Russo, T. A., A. Stapleton, S. Wenderoth, T. M. Hooton, and W. E. Stamm.** 1995. Chromosomal restriction fragment length polymorphism analysis of *Escherichia coli* strains causing recurrent urinary tract infections in young women. *J Infect Dis* **172**:440-445.
55. **Saunders, N. J., D. W. Hood, and E. R. Moxon.** 1999. Bacterial evolution: bacteria play pass the gene. *Curr Biol* **9**:R180-183.
56. **Scheenen, W. J., L. R. Makings, L. R. Gross, T. Pozzan, and R. Y. Tsien.** 1996. Photodegradation of indo-1 and its effect on apparent Ca^{2+} concentrations. *Chem Biol* **3**:765-774.
57. **Smajs, D., and G. M. Weinstock.** 2001. The iron- and temperature-regulated *cjrBC* genes of *Shigella* and enteroinvasive *Escherichia coli* strains code for colicin Js uptake. *J Bacteriol* **183**:3958-3966.

58. **Sowers, K. R., and H. J. Schreier.** 1999. Gene transfer systems for the Archaea. *Trends Microbiol* **7**:212-219.
59. **Stevens, M. P., A. J. Roe, I. Vlisidou, P. M. van Diemen, R. M. La Ragione, A. Best, M. J. Woodward, D. L. Gally, and T. S. Wallis.** 2004. Mutation of *tox*B and a truncated version of the *efa-1* gene in *Escherichia coli* O157:H7 influences the expression and secretion of locus of enterocyte effacement-encoded proteins but not intestinal colonization in calves or sheep. *Infect Immun* **72**:5402-5411.
60. **Tatsuno, I., M. Horie, H. Abe, T. Miki, K. Makino, H. Shinagawa, H. Taguchi, S. Kamiya, T. Hayashi, and C. Sasakawa.** 2001. *tox*B gene on pO157 of enterohemorrhagic *Escherichia coli* O157:H7 is required for full epithelial cell adherence phenotype. *Infect Immun* **69**:6660-6669.
61. **Torres, A. G., P. Redford, R. A. Welch, and S. M. Payne.** 2001. TonB-dependent systems of uropathogenic *Escherichia coli*: aerobactin and heme transport and TonB are required for virulence in the mouse. *Infect Immun* **69**:6179-6185.
62. **Venkatesan, M. M., Burland, V.** 2004. Genome-Scale Analysis of Virulence Plasmids: the Contribution of Plasmid-Borne Virulence Genes to Enterobacterial Pathogenesis, p. 395-411. *In* B. E. Funnell, Phillips, G. J. (ed.), *Plasmid Biology*. ASM Press, Washington, D.C.
63. **Wright, K. J., P. C. Seed, and S. J. Hultgren.** 2007. Development of intracellular bacterial communities of uropathogenic *Escherichia coli* depends on type 1 pili. *Cell Microbiol* **9**:2230-2241.
64. **Wu, X. R., T. T. Sun, and J. J. Medina.** 1996. In vitro binding of type 1-fimbriated *Escherichia coli* to uroplakins Ia and Ib: relation to urinary tract infections. *Proc Natl Acad Sci U S A* **93**:9630-9635.

65. **Zhao, L., S. Gao, H. Huan, X. Xu, X. Zhu, W. Yang, Q. Gao, and X. Liu.** 2009. Comparison of virulence factors and expression of specific genes between uropathogenic *Escherichia coli* and avian pathogenic *E. coli* in a murine urinary tract infection model and a chicken challenge model. *Microbiology*.

CHAPTER FOUR

INTERVENING WITH URINARY TRACT INFECTIONS USING ANTI-ADHESIVES BASED ON THE CRYSTAL STRUCTURE OF THE FIMH – OLIGOMANNOSE-3 COMPLEX

Modified from: Wellens *et al.* (2008) *PLoS ONE*.

Adinda Wellens^{1,2#}, Corinne Garofalo^{3#}, Hien Nguyen^{1,2}, Nani Van Gerven⁴, Rikard Slättegård⁵, Jean-Pierre Hernalsteens⁴, Lode Wyns^{1,2}, Stefan Oscarson⁶, Henri De Greve^{1,2}, Scott Hultgren³ and Julie Bouckaert^{1,2*}

First authors with equal contribution

* To whom correspondence should be addressed. E-mail: bouckaej@vub.ac.be

¹ Department of Molecular and Cellular Interactions, VIB, Brussels, Belgium

² Ultrastructure, Vrije Universiteit Brussel, Pleinlaan 2, 1050 Brussels, Belgium

³ Department of Molecular Microbiology, Box 8230, Washington University School of Medicine, 660 S. Euclid Avenue, St. Louis, MO 63110, USA

⁴ Viral Genetics, Vrije Universiteit Brussel, Pleinlaan 2, 1050 Brussels, Belgium

⁵ Department of Organic Chemistry, Arrhenius Laboratory, Stockholm University, SE-10691 Stockholm, Sweden

⁶ Centre for Synthesis and Chemical Biology, University College Dublin, Belfield, Dublin 4, Ireland

Author contributions: S.H., J.B., A.W., C.G. and H.D. conceived and designed the experiments; J.B., A.W., C.G., H.N., N.V. and J.H. performed the experiments; S.H., J.B., A.W., C.G., H.N. and N.V. analyzed the data; S.H., J.B., R.S., J.H., L.W., S.O. and

H.D. contributed reagents/materials/analysis tools; and S.H., J.B., A.W. and C.G. wrote the paper.

Abstract

Background. *Escherichia coli* strains adhere to the normally sterile human uroepithelium using type 1 pili, that are long, hairy surface organelles exposing a mannose-binding FimH adhesin at the tip. A small percentage of adhered bacteria can successfully invade bladder cells, presumably via pathways mediated by the high-mannosylated uroplakin-Ia and $\alpha 3\beta 1$ integrins found throughout the uroepithelium. Invaded bacteria replicate and mature into dense, biofilm-like inclusions in preparation of fluxing and of infection of neighboring cells, being the major cause of the troublesome recurrent urinary tract infections.

Methodology/Principal Findings. We demonstrate that α -D-mannose based inhibitors of FimH not only block bacterial adhesion on uroepithelial cells but also antagonize invasion and biofilm formation. Heptyl α -D-mannose prevents binding of type 1-piliated *E. coli* to the human bladder cell line 5637 and reduces both adhesion and invasion of the UTI89 cystitis isolate instilled in mouse bladder via catheterization. Heptyl α -D-mannose also specifically inhibited biofilm formation at micromolar concentrations. The structural basis of the great inhibitory potential of alkyl and aryl α -D-mannosides was elucidated in the crystal structure of the FimH receptor-binding domain in complex with oligomannose-3. FimH interacts with $\text{Man}\alpha 1,3\text{Man}\beta 1,4\text{GlcNAc}\beta 1,4\text{GlcNAc}$ in an extended binding site. The interactions along the $\alpha 1,3$ glycosidic bond and the first $\beta 1,4$ linkage to the chitobiose unit are conserved with those of FimH with butyl α -D-mannose. The strong stacking of the central mannose with the aromatic ring of Tyr48 is congruent

with the high affinity found for synthetic inhibitors in which this mannose is substituted for by an aromatic group.

Conclusions/Significance. The potential of ligand-based design of antagonists of urinary tract infections is ruled by the structural mimicry of natural epitopes and extends into blocking of bacterial invasion, intracellular growth and capacity to fluxing and of recurrence of the infection.

Introduction

Pili and fimbriae on the bacterial cell are virulence factors that mediate adhesion of pathogenic bacteria to host cell receptors [1]. Urinary tract infections (UTIs) in humans are frequently caused by uropathogenic *Escherichia coli* (UPEC) expressing type 1 pili. The FimH adhesin at the tip of type 1 pili recognizes terminal mannose units of uroplakin Ia (UPIa), a membrane glycoprotein that is abundantly expressed on superficial epithelial umbrella cells of the urinary tract [2]. Bacterial attachment stimulates the innate host immune system in a Toll-like receptor 4 - dependent manner [3]. This induces the secretion of cytokines by the urothelial cells and recruitment of neutrophils to the mucosal surfaces for the elimination of the bacteria [4]. A subpopulation of UPEC escapes this eradication mechanism of the host by invading into the large superficial epithelial cells in a type 1 pili-dependent mechanism [5,6]. However, hosts with a robust and timely innate immune response manage to get rid of this bacterial intracellular nesting by exfoliation of the large, superficial umbrella cells and discharge of these infected cells with the urine [7,8].

Bacteria within the cytosol of umbrella cells replicate and within hours develop into tightly packed, biofilm-like intracellular bacterial communities (IBCs) [9]. Upon maturation of the IBCs, the bacteria disperse from the IBCs and re-emerge in the

bladder lumen in long, filamentous shapes that helps them to evade neutrophil phagocytosis [10,11]. They can then reinvade neighbouring epithelial cells to re-establish infection. As such, even after the acute infection is resolved, bacteria can remain within the bladder for many days to weeks, regardless of standard antibiotic treatments, and can be implicated in recurrent urinary tract infection (rUTI) [12–14]. Most UPEC isolates from women with acute or rUTIs, asymptomatic bacteriuria and pyelonephritis replicate in IBCs in C3H/HeN mice, although IBCs from isolates associated with acute UTIs remained significantly smaller [15]. UPEC that are unable to express type 1 pili are dramatically attenuated in their virulence, refrain from intracellular aggregation and maturation into an IBC and therefore fail to flux back out of the cells [16].

A different, intracellular path of the bacteria is commenced through the endocytosis in the fusiform or discoidal vesicles of superficial umbrella cells [17]. The bacteria make use of the vesicle trafficking in the umbrella cells to escape elimination during voiding. Endocytosis in the umbrella cells is coupled to exocytosis of secretory lysosomes [18]. Exocytosis helps to enlarge the apical membrane during bladder filling under hydrostatic pressure. High intracellular cAMP and calcium levels enhance exocytosis of the UPECs back into the lumen of the bladder [17]. It is unclear whether the bacteria are fit enough following their stay in the umbrella cell lysosomes to start another invasive cycle [19]. The uroepithelial cell layer underlying the umbrella cells can also be subject to invading bacteria, possibly upon the incomplete elimination of type 1 piliated *E. coli* during exfoliation of the superficial, highly differentiated umbrella cells [8]. In those immature cells, the bacteria do not reside in the cytosol but rather are sequestered in late endosomes or lysosomes where they remain in a non-replicating state [20]. Those quiescent intracellular reservoirs (QIRs) persist for months even in the

face of antibiotics and the host defense, that mainly attack growing bacteria [8,12,13]. Only upon differentiation of the immature host cells and rearrangement of the cytoskeleton that tends to inhibit the intracellular replication, the QIRs resolve to develop intracellular inclusions similar to experimental IBCs [20]. Host cytokeratin intermediate filaments are closely associated with and probably help with biofilm formation within these pod-shaped inclusions [20].

The attachment of adhesins on the bacterial cell surface to definite carbohydrates on the host tissue surface is considered to be an initial and critical step in pathogenesis. Antibodies that specifically block the binding of FimH to its natural receptor also prevent infection [21]. Revealing the interaction between FimH and its structural receptor would allow the design of carbohydrate-based anti-adhesives [22]. The preference of the fimbrial adhesin for structures found in mannosylated *N*-linked glycan chains on eukaryotic cell glycoproteins suggested that these structures would serve as the receptors for type 1-piliated *E. coli* strains [23,24]. The group of Sharon described in the early eighties the strong inhibitory potency of $\text{Man}\alpha 1,3\text{Man}\beta 1,4\text{GlcNAc}$ on the agglutination of red blood cells and yeast cells and suggested that this trisaccharide would best fit the FimH binding pocket [25]. More recently, equilibrium dissociation constants (K_d) derived from surface plasmon resonance (SPR) solution affinity measurements or from the displacement of tritiated mannose from the receptor-binding domain (RBD) of FimH, consistently approved the strong preference of FimH for oligomannosides exposing $\text{Man}\alpha 1,3\text{Man}$ at the non-reducing end of the D1 arm of high-mannose glycans [26]. Mannotriose and mannopentaose do not exhibit a significantly higher affinity than their linear moiety $\text{Man}\alpha 1,3\text{Man}$ ($K_d \sim 200$ nM). Conversely, oligomannose-3 and oligomannose-5, carrying the $\beta 1,4$ -linked chitobiose as an anchor

to an asparagine in the Asn-X-Ser/Thr motif of N-linked glycoproteins, have another 10-fold increase in affinity for the FimH RBD ($K_d \sim 20$ nM) over $\text{Man}\alpha 1,3\text{Man}$ [26].

Regardless of the well-characterized fine-specificity of FimH, FimH variant strains have also been categorized into those with a high affinity for D-mannose, predominantly represented by UPECs, *versus* fecal, commensal *E. coli* strains that only displayed an intermediate affinity for mannotriose ($\text{Man}\alpha 1,6(\text{Man}\alpha 1,3)\text{Man}$) [27]. These different bacterial binding characteristics under static binding conditions had been attributed to variation in the FimH RBD. Nonetheless, the isolated RBDs of all FimH variants, except for the enterohaemorrhagic isolates carrying the Asn135Lys mutation in their pocket, do not differ in their affinities for high-mannose glycans [26,28]. Isolated RBDs or fimbrial tip adhesin that are out of the context of their own fimbriae have recently been suggested to always occur in a high-affinity conformation [29]. On the other hand, when present within their endogenous pilus, the adhesin can undergo a transition to the high-affinity conformation under shear force enhanced adhesion, and it is this phenomenon where amino acid variation in FimH can give rise to ten-fold differences in bacterial adhesion. Shear enhanced bacterial adhesion was most pronounced to layers coated with the weakly binding mannose than to a surface coated with the more specific mannotriose and involved a minimum of shear for the fecal FimH variant *E. coli* F18 strain [30]. However, no such shear threshold was observed for type 1-piliated *E. coli* binding to mannotriose or for a P-piliated pyelonephritis strain binding to $\text{Gal}\alpha 1,4\text{Gal}$ [31]. Thus changes in the receptor structure, that affect the fine-specificity of FimH, can more dramatically than FimH variation impact on the colonization behaviour of type 1-piliated bacteria under flow conditions. In this context, the relevance of a shear threshold observed for single-exposed mannose is feeble given that mannose, recognized by FimH at the termini of naturally occurring glycans, is almost invariably involved in a glycosidic linkage.

FimH has been reported to bind to several glycosylation-dependent receptors in the urinary tract, among which are uroplakin Ia (UPIa) [2], Tamm-Horsfall glycoprotein (THP) [32] and very recently $\beta 1$ and $\alpha 3$ integrins [33]. Many pathogens gain entry into target host cells by binding integrins either directly or indirectly via the recognition of extracellular matrix proteins. UPIa is an integral membrane protein of the large superficial epithelial cells of the bladder located as a FimH receptor on the six inner domains of the uroepithelial plaque particle [34]. It belongs to the superfamily of tetraspanins [35] that are often found to complex with $\beta 1$ integrin receptors [36]. Mouse UPIa4 presents high-mannose glycans on Asn169 with a heterogeneity ranging from $\text{Man}_6\text{GlcNAc}_2$ to $\text{Man}_9\text{GlcNAc}_2$ [37]. The same high-mannose type glycans decorate $\beta 1$ and $\alpha 3$ integrins [38]. None of these structures expose $\text{Man}\alpha 1,3\text{Man}\beta 1,4\text{GlcNAc}$, terminally at the non-reducing end of the glycan branch. Perhaps this is not so striking, as glycoproteins bearing $\text{Man}_5\text{GlcNAc}_2$ glycans are degraded preferentially [39]. The only isomer of oligomannose-6 encountered so far on uroplakins covers $\text{Man}\alpha 1,3\text{Man}\beta 1,4\text{GlcNAc}$ with an extra $\alpha 1,2$ -linked D-mannose [37], thus masking the epitope with high affinity for FimH [40]. THP is secreted in the urine as a natural inhibitor of type 1-mediated bacterial adhesion through its high-mannosylated Asn251 residue [41].

UTIs are one of the most prevalent infections for humans. Almost half of all women will experience at least one UTI in their lifetime. More problematic is the evolution of acute UTIs into chronic infections, with recurrence of the symptoms two or more times within months of a primary infection [42]. Modifications in the glycosylation of FimH receptor proteins on eukaryotic cells may alter the host sensitivity to UTI causing strains. For example, diabetic patients and elderly women show increased bladder cell binding by FimH [43] and this is further correlated with an increased frequency of

asymptomatic bacteriuria [44]. Free $\text{Man}\alpha 1,3\text{Man}\beta 1,4\text{GlcNAc}$ oligosaccharide can be isolated in abnormally high amounts from urine of patients with mannosidosis [45]. For mannosidosis patients the abundance of this high-affinity FimH epitope in the urine may act as a natural inhibitor for urinary tract infections, although a decreased risk of UTIs in patients with α -mannosidase deficiency has not been described. The high frequency of recurrent infections and the increasing antibiotic resistances of UPECs [46] highlight the need for alternative treatments using carbohydrate-derived molecules as potential anti-adhesives. Their non-bactericidal effect makes the selection of strains resistant to such agents much more unlikely than those resistant to antibiotics [22].

Biochemical and docking studies predicted that the enhanced binding of $\text{Man}\alpha 1,3\text{Man}\beta 1,4\text{GlcNAc}$ is accomplished by interactions of the central mannose and GlcNAc in the tyrosine gate extending from the FimH mannose-binding pocket [26,47]. To gain insight into the selectivity of FimH for this trisaccharide epitope, we co-crystallized FimH with the trisaccharide-presenting oligomannose-3 and investigated the importance of the glycosidic linkage of $\text{Man}\alpha 1,3\text{Man}$ with *N*-acetyl glucosamine (GlcNAc) of the chitobiose unit of *N*-linked glycans. The FimH RBD shows high affinities for alkyl α -D-mannosides, with affinities up to a K_d of 5 nM for heptyl α -D-mannose (HM) [47]. We set out to explore the inhibitory capacity of HM for lower UTIs caused by type 1-piliated UPECs in mice. We find that alkyl α -D-mannosides and other synthetic inhibitors of FimH confirm binding properties of the high-mannose epitope. The alkyl chain of butyl α -D-mannose, bound to FimH in two previously determined co-crystal structures, follows the trail of the $\alpha 1,3$ linkage to the central mannose and the first $\beta 1,4$ glycosidic linkage to the chitobiose. The potential of ligand-based design of antagonists of UTIs appears to be ruled by structural mimicry of specific spots on mannosylated receptors. This anti-

adhesive ability extends into blocking of bacterial invasion, intracellular growth and capacity to fluxing and recurrence of the infection.

Materials and methods

Sugar compounds

Oligomannose-3 was custom-synthesized at the Zelinsky Institute of Organic Chemistry (Russia). Methyl α -D-mannose and D-mannose were purchased from Sigma-Aldrich. Man α 1,3Man β OMe (S. Oscarson, to be communicated) and HM [47] have been synthesized. Affinity measurements using surface plasmon resonance (SPR) were performed as described [26]. Briefly, the equilibrium dissociation constants of mannose derivatives for FimH were determined using competition in solution for FimH binding of the sugars with an immobilized Fab fragment from the monoclonal antibody 1C10.

Purification of FimH

The receptor-binding domain (RBD) of the FimH protein (residues 1 till 158 of UPEC J96) was expressed from plasmid pMMB91 transformed into *E. coli* C43 (DE3) cells. C43 (DE3) (pMMB91) *E. coli* cells were grown in minimal medium containing 40 μ g/ml of all the amino acids, 0.4% glucose, 2 μ g/ml biotin, 2 μ g/ml thiamine, 2 mM MgCl₂ and 25 μ g/ml kanamycin at 37°C. At OD_{600nm} = 0,6 the bacteria cells were induced with 1mM IPTG. After overnight incubation at 37°C, cells were collected and the periplasmic content was extracted. The receptor-binding domain of FimH was purified by dialysing it 4h at 4°C against 20 mM Na formate pH 4 and loading it on a Mono S HR column (Pharmacia Biotech). The protein was eluted with 20 mM Na formate, 1M NaCl pH 4. Fractions containing the FimH receptor-binding domain were pooled and dialyzed overnight at 4°C against 20 mM Hepes pH 8 and 150 mM NaCl, before crystallization.

Co-crystallization of the FimH RBD with oligomannose-3

Crystallization conditions were screened at the high-throughput crystallization facility of the EMBL in Hamburg. Crystals grew at 292K, using the vapor diffusion method with sitting drops composed of 300 nL FimH-oligomannose-3 solution FimH at 13.6 mg/ml mixed with 2 mM oligomannose-3 in a 2:1 molar ratio and 300 nL precipitant (Figure S1), equilibrated against a 100 μ l reservoir of 1.0 M lithium sulfate, 0.1 M Tris-HCl at pH 8.5, 0.01 M nickel (II) chloride. To optimize these conditions, hanging drops were set up consisting of 1 μ l FimH at 13.6 mg/ml mixed with 2 mM oligomannose-3 in a 2:1 molar ratio and 1 μ l of the precipitant solution, equilibrated against 500 μ l of the same precipitant complemented with 3% glycerol. Glycerol has a beneficial effect on crystallization by preventing showering of the protein prior to nucleation, allowing a more controlled crystal nucleation and growth process.

Structure determination and refinement

X-ray data have been collected to 2 Å resolution at the European Molecular Biology Laboratory (EMBL) beam line X12 at the Deutsches Elektronen Synchrotron (DESY, Hamburg, Germany). The crystal was flash cooled to 100K in the precipitant solution complemented with 30% isopropanol. All data were processed with DENZO and SCALEPACK from the *HKL* suite [62]. TRUNCATE from the CCP4 suite was used to calculate structure-factor amplitudes from the intensities. The structure has been solved by molecular replacement with MolRep [63] using the structure of the receptor-binding domain of FimH as the search model (PDB entry code 1UWF) [47]. The model was refined using rigid body refinement and the maximum likelihood function of CNS version 1.1 [64] and Refmac 5.2.0019 [65], with 5% of the data retained for cross-validation purposes. The initial molecular replacement solution was submitted to simulated annealing refinement. Successive positional and individual temperature factor

refinements were alternated with manual model adjustment using TURBO-FRODO [66] and COOT [67] graphics.

Structure analysis

A Ramachandran plot was drawn using Molprobit [68]. Baverage from the CCP4 suite [69] defined the average B-factors of the main chain atoms of the protein and of the water molecules. The packing contacts were analyzed using the CCP4 program CONTACT [69], using an intermolecular cut-off distance of 4 Å. Potential hydrogen bonds in the FimH-oligomannose-3 complex were identified using HBPLUS [70]. Subsequently, the predicted interactions were carefully checked with Coot [67]. Pictures have been generated using Pymol version 0.99.

Bacterial binding in vitro to a human urothelial cell line

The *E. coli* strains AAEC185(pUT2002)(pMMB66) and AAEC185(pUT2002) have been used in bladder cell binding experiments. AAEC185 *E. coli* cells are *fim*-null mutants [72]. The pUT2002 plasmid carries the complete *fim* gene cluster with the deletion of *fimH*, resulting in FimH-deficient type 1 pili [72]. The *fimH* gene of J96 *E. coli* is located on the pMMB66 plasmid [53]. Strains AAEC185(pUT2002) and AAEC185(pUT2002)(pMMB66) were grown statically in 100 ml LB for 48 hours at 37°C to induce pili production. The bacterial cells were harvested under sterile condition by centrifugation at 3500 rpm for 20 min (Megafuse 1.0R, Heraeus instruments) and washed two times in phosphate buffered saline (PBS). The expression of type 1 pili was always checked using haemagglutination [26] prior to the infection of the bladder cells. Human bladder epithelial cell line 5637 (American Type Culture Collection HTB-9) was seeded in 12-well plates and cultured in Roswell Park Memorial Institute (RPMI) 1640 medium, supplemented with 10% fetal calf serum (FCS). The cells were maintained 2-4

days at 37°C in a humidified atmosphere containing 5% CO₂ for confluent growth. The plate was washed 5 times with PBS complemented with 0.5 mM MgCl₂ and 1 mM CaCl₂ directly before use. Each well was incubated with 0.5 ml of 10⁶ to 10⁷ colony forming units (cfu) per ml in PBS. The plates were slowly shaken for 15 minutes to allow binding of the bacteria to the tissue cells. Five washes were performed with PBS to remove unbound bacteria. Bladder cells were lysed by adding 0.4 ml trypsin/EDTA for 10-15 minutes. Finally, the lysis was stopped by the addition of 10% FCS, when all cells were released from the plate. The input colony forming units (cfu) and the output cfu in each well were determined by 10-fold serial dilutions (1, 10⁻², 10⁻³, 10⁻⁴, 10⁻⁵) in PBS and spotting 20 µl drops on LB-agar with the appropriate antibiotics. Inhibition of bladder cell binding was performed simultaneously as binding on the same 12-well plate, but with the bacterial inoculum pre-incubated with different concentrations of mannose or HM.

In vivo bladder binding

All studies using mice were approved by the Animal Studies Committee of Washington University. Eight-week-old female C3H/HeN mice (NCI) were anesthetized and inoculated with a 50 µl suspension of ~10⁷ UTI89 (in PBS or sugar solution) via transurethral catheterization [12]. Prior to inoculation, the inoculum was incubated for 20 min at 37°C with one of the following: 1 M methyl α-D-mannose, 0.5 mM heptyl α-D-mannose, 5 mM heptyl α-D-mannose. Six hours after inoculation, animals were euthanized, and their bladders harvested and homogenized in 1 mL of 0.025% Triton X-100/PBS. Bacterial titers were determined by plating serial dilutions of the homogenates on LB agar plates. Duplicate experiments of 5 mice each were performed.

Gentamicin protection assay

UTI89 was grown overnight in LB and resuspended in PBS to an inoculum of $\sim 10^7$ cfu in 50 μ l. The inoculum was then incubated for 20 min at 37°C with 5 mM methyl α -D-mannose, 0.5 mM heptyl α -D-mannose, 5 mM heptyl α -D-mannose, or PBS. After incubation, 6-7 week old C3H/HeN mice were inoculated via transurethral catheterization [12]. An *ex vivo* gentamicin protection assay was performed as previously described [11]. Briefly, at 1 hour post-infection, the mice were sacrificed and bladders were dissected aseptically. Each bladder was washed 3 times with sterile PBS. The washes were collected and plated to obtain the luminal fraction of bacteria. The bladders were then treated with 100 μ g/ml gentamicin for 90 min at 37°C. After treatment, the supernatant was removed and titered to ensure efficient killing of extracellular bacteria. The bladders were washed twice more to remove residual gentamicin and homogenized in 1 mL 0.025% triton X-100/PBS and bacterial counts were determined by plating serial dilutions on LB agar plates.

Biofilm assay

UTI89 was grown overnight in LB broth at 37°C with shaking and diluted 1:1000 in LB or LB with varying amounts of methyl α -D-mannose or heptyl α -D-mannose. 96-well round bottom polyvinyl chloride plates (Falcon) were sterilized in tissue culture hood under UV irradiation for at least 30 minutes. 100 μ l of the solutions were then added to the sterile PVC plate, 6 wells per variable. LB without bacteria was added to 6 wells as a blank. The plate was incubated for 48 hours at room temperature, washed 3 times in PBS and allowed to dry. 125 μ l of 1% crystal violet solution was added to each well for 10 minutes. After staining, the plates were washed again in PBS 3 times and allowed to dry. The crystal violet was solubilized with 150 μ l of 33% acetic acid, 100 μ l was transferred to a flat bottom plate and absorbance was read at 600 nm.

Protein Data Bank accession number

The coordinates and the structure factors have been submitted to the Protein Data Bank with accession codes 2vco and r2vcosf respectively.

Results

The chitobiose anchor to Asn-glycosylated FimH receptors is important for specificity

Previous epitope mapping on high-mannose glycan receptors revealed the highest affinity of the FimH RBD for oligomannose-3 and oligomannose-5 [26]. Both these oligomannosides expose $\text{Man}\alpha 1,3\text{Man}\beta 1,4\text{GlcNAc}$ at the non-reducing end of the D1 branch and have an increased affinity for FimH over mannotriose and mannopentaose that lack the chitobiose unit (Figure 1). The increased affinity was thought to be due partially to the β -anomeric linkage to the chitobiose $\text{GlcNAc}\beta 1,4\text{GlcNAc}$. The binding constants of the FimH RBD from the J96 cystitis strain for $\text{Man}\alpha 1,3\text{Man}\beta \text{OME}$ and for the anomeric mixture of $\text{Man}\alpha 1,3\text{Man}$ have been determined using SPR, to investigate the contribution of the glycosidic linkage. This resulted in affinities of $K_d = 112 \text{ nM}$ and 281 nM respectively, showing that FimH selects out the β -anomeric configuration on Man3. It also indicated that the presence of the β -linkage alone is not sufficient to explain the more significant increase in affinity between on the one hand mannotriose or mannopentaose, and on the other hand oligomannose-3 and oligomannose-5 [26]. Thus the chitobiose unit that bridges the mannosides to the asparagine in the Asn-X-Ser/Thr motif of the glycoprotein receptor contributes more significantly to the interaction with FimH.

Crystal structure of the FimH receptor-binding domain in complex with oligomannose-3

Oligomannose-3 has been crystallized in complex with the FimH RBD. This oligosaccharide exposes the substructure $\text{Man}\alpha 1,3\text{Man}\beta 1,4\text{GlcNAc}$ terminally on its D1 branch (Figure 1). Therefore it is ideally suited to reveal the structural basis of its high-affinity interaction with FimH. Initial crystals have been grown by equilibration through vapor diffusion and the crystallization condition was optimized through the addition of 3% glycerol (Figure S1).

The solution of the molecular replacement contains two FimH RBDs per asymmetric unit in the $P3_121$ space group (Figure 2, Table S1). Upon the first atomic refinement a clearly interpretable electron density for $\text{Man}\alpha 1,3\text{Man}\beta 1,4\text{GlcNAc}$ was visible, equally well in both RBDs. Refinement against the crystallographic data with a 2.1 Å high-resolution cut-off led to good protein geometry and oligosaccharide conformation determination. The root mean square deviation between the two RBDs is 0.56 Å for all main chain atoms. The torsion angles of the $\text{Man}\beta 1,4\text{GlcNAc}$ and $\text{Man}\alpha 1,3\text{Man}$ glycosidic bonds in oligomannose-3 resemble within a few degrees to those observed in the crystal structure of the $\text{Man}\alpha 1,3\text{Man}\beta 1,4\text{GlcNAc}$ trisaccharide [48]. Although the ψ torsion angle of $\text{Man}\alpha 1,3\text{Man}$ deviates from the average minimum energy modelled for these glycans for all distinct conformers of glycosidic linkages found in either *N*- or *O*-linked glycans [49], it falls well within the range of allowed minimum energy conformations for ϕ and ψ glycosidic torsion angles [50].

Oligomannose-3 conforms into a relatively planar structure that inserts almost like a sheet into the tyrosine gate (Figures 2 and 3A), with an angle at both ends. The same extensive hydrogen bonding, hydrophobic contacts and van der Waals interactions are achieved by binding of oligomannose-3 in both FimH RBDs of the crystal structure (Figure 2). The solvent accessible surface area buried through the binding of oligomannose-3 leads to a reduction of solvent accessible surface area of $312.1 \pm 1.3 \text{ \AA}^2$

for oligomannose-3 and $462.2 \pm 6.6 \text{ \AA}^2$ for FimH both, using the CCP4 program NACCESS. Between the two crystallographically-independent FimH RBDs $537.5 \pm 6.75 \text{ \AA}^2$ is excluded from the solvent. This agrees well with the average areas excluded from the solvent by pairwise interactions ($388.1 \pm 3 \text{ \AA}^2$ between FimH and oligomannose-3 and 534 \AA^2 between the two FimH RBDs) calculated by MSDpisa version v1.14 [51].

The non-reducing end Man4 anchors into the mannose-binding pocket, whereas the reducing end GlcNAc1 folds over Thr51. Very specific interactions with the tyrosine gate occur in the mannose-binding pocket itself and all along $\text{Man}\alpha 1,3\text{Man}\beta 1,4\text{GlcNAc}$ via the $\alpha 1,3$ and the first $\beta 1,4$ glycosidic linkages. FimH is not directly recognizing the second non-reducing end mannose, Man4' (Figure 3). Man4' and GlcNAc1, the two saccharides that exit from the receptor-binding site, display a larger flexibility in an extensively hydrated environment, resulting in less-well defined electron density and higher temperature factors. Crystal packing contacts with Phe142 and Ile13 of a symmetry-related RBD with Man4' bound to the second RBD (forest-green molecule in Figure 2) stabilize some of these waters, whereas Man4' bound to the first RBD is fully solvent exposed.

For the first time in a FimH structure [47,52,53], a nickel ion was observed, interlinked with the mannose binding pocket by Asp47 (Figure 2). The nickel ion is ligated in an octahedral setting by the carboxylate group of Asp47, the imidazole group of His45 and four water molecules. Also unseen before in any FimH structure are two sulphate ions in a highly charged interface in the crystal packing (Figure 2).

The non-reducing end Man4 of oligomannose-3 (Figure 1) is attracted to the deep, monomannose-binding polar pocket (Figure 3A, red) through a hydrophobic tyrosine gate (Figure 3A, blue) to make previously well-defined interactions [47,53]. Eleven hydrogen bonds are formed between the Man4 and the FimH residues Phe1, Asn46,

Asp47, Asp54, Gln133, Asn135 and Asp140 (Figure 4). A water molecule interacting with O2 of Man4 is a strongly conserved feature in the mannose binding pocket. The apolar B-face of Man4 provides interaction with Ile13 and Phe142, and its C5-C6 bond interacts with Ile52. Residues Tyr48, Ile52 and Tyr137 of the tyrosine gate are involved in several aromatic/hydrophobic and van der Waals contacts with oligomannose-3, thus stabilizing the glycan-lectin complex (Figures 3 and 4). Man3 hooks over the side chain of Ile52 while stacking its apolar B-face onto the Tyr48 aromatic side chain (Figures 3A-C). A close apolar contact is achieved between C5 of GlcNAc2 and Tyr137. The C6-O6 bond of GlcNAc2 fares well in a hydrophobic environment created by Tyr48 and Ile52 (Figure 4). This could help to orient the strong (2.7 Å) hydrogen bond of the O6 hydroxyl on GlcNAc2 directly towards the hydroxyl of the Thr51 side chain (Figure 3D). This latter threonine interacts hydrophobically with the C7-C8 bond of the acetyl group of the reducing end GlcNAc1. GlcNAc1 intramolecular hydrogen bonds with GlcNAc2 and its *N*-acetyl group makes a van der Waals contact with the methyl group of the Thr51 side chain (Figure 3D). It can be seen that glycosidic linkage of GlcNAc1 via O1 to a glycoprotein would pull FimH very close to its receptor upon binding (Figure 3D).

Parallels between the binding of oligomannose-3 and alkyl α -D-mannosides with FimH

Butyl α -D-mannose is a high-affinity ligand for FimH ($K_d = 150$ nM) that was found serendipitously in two previous FimH crystal structures [47]. We compared the interaction interfaces between FimH and oligomannose-3 with those between FimH and butyl α -D-mannose. Superposing the mannose of the butyl α -D-mannosides onto Man4 of oligomannose-3 and application of the transformation matrix to the whole molecules showed that the butyl chain follows the hydrophobic trail through the tyrosine gate by the Man α 1,3Man and Man β 1,4GlcNAc linkages (Figure 5A). In contrast to the stable

position of the mannose bound in the monosaccharide-binding pocket, the temperature factors of the ligand atoms gradually increase beyond the α 1,3 position, both for oligomannose-3 and for butyl α -D-mannose.

The side of oligomannose-3 that is not embraced by the tyrosine gate displays hydration of the exocyclic glycosidic oxygens (Figures 4 and 5A) that is maintained between oligomannose-3 and butyl α -D-mannose. The hydration on the α -anomeric oxygen of the mannose bound into the polar pocket is conserved, as well as its hydrogen bonding network with Asn138 and Asp140 (Figure 5B) that are residues in the loop connecting β -strands F and G (Figure 3). Also a water molecule hydrogen bonding to the exocyclic glycosidic oxygen linking Man3 to GlcNAc2 is maintained (Figures 5 and 6B). It appears that synthetic inhibitors strive for the best mimic of the interactions of FimH with its natural receptor. Previous solution affinity measurements indicated that heptyl α -D-mannose is the best-binding alkyl α -D-mannoside ($K_d = 5$ nM) [47]. A simulation in which the butyl chain of butyl α -D-mannose was elongated to a heptyl allowed a conformation in which the elongated tail follows GlcNAc2 further along C4-C5-C6, expecting to form the important interactions with Thr51, Ile52 and Tyr48. The anti-adhesive proficiency with heptyl α -D-mannose was subsequently tested both on the human bladder cell line 5637 and in C3H/HeN mice.

Mannose and heptyl α -D-mannose inhibit in vitro adhesion of type 1-piliated E. coli

Type 1 pili-expressing AAEC185(pUT2002)(pMMB66) *E. coli* cells at 10^6 cfu/ml were supplemented with a ten-fold dilution series of D-mannose (Man) or heptyl α -D-mannose (HM) and incubated for adhesion on bladder cell line 5637. Increasing concentrations of Man or HM caused a significant reduction to complete inhibition of bacterial bladder cell binding (Figure 6). Adhesion could be completely inhibited by the

addition of 100 mM Man to the bacterial inoculum, or by a 100-fold lower concentration of HM. No inhibition was obtained with 100 μ M Man, whereas 1 μ M of HM still had some inhibitory effect. Similar data have been obtained with an inoculum of 10^7 cfu/ml. These results suggest that HM is more efficient at reducing FimH-mediated bacterial adherence, in accordance with its higher affinity for FimH.

Heptyl α -D-mannose reduces bacterial levels in a murine cystitis model

Extensive research has shown that type 1 pili and their adhesin, FimH, are essential for binding and invasion in the murine cystitis model [6,33,53]. It was hypothesized that blocking of the FimH binding pocket by preferential binding to a soluble mannose residue would reduce the binding to uroplakins on the epithelial cell surface of the bladder. This loss of binding would result in less invasion and ultimately a reduced infection. To test this hypothesis, bacteria were incubated in the presence of a derivative of mannose prior to inoculation into mouse bladders. Introductory to this experiment, the intrinsic toxicity of HM was assessed in Female BALB/c mice. HM was administered at 50 mM concentration through a catheter (50 μ l), intranasal (20 μ l) and intravenously (150 μ l) to three mice each, but no acute toxicity has been observed. At 6 hours post-infection, the bacteria present within the bladder were enumerated. Wild-type UTI89 incubated with PBS alone had a mean level of infection of $\sim 3 \times 10^5$ cfu/mL (Figure 7). Incubation of UTI89 with 0.5 mM of HM showed no significant decrease in infection. However, at a concentration of 5 mM HM, there was a significant decrease in infection at 6 hours post-infection ($p \leq 0.0001$). Methyl α -D-mannose (MM) gave no decrease in bacterial numbers at the same concentration. A significant decrease in bacterial burden was only observed when increasing the concentration of MM to 1M (data not shown), a 200 fold higher concentration than the one sufficient for HM. The tighter binding of HM to FimH, as compared to MM, could explain this difference. These results suggest that by

inhibiting the ability of FimH to bind to mannosylated uroplakins, the bacterial infection can be prevented.

Heptyl α -D-mannose reduces intracellular bacterial levels

Since there is a reduction in the amount of bacteria present in the bladder at 6 hours post-infection with HM incubation (Figure 7), we wanted to assess the amount of bacteria that went intracellular. Mice were infected with UTI89 in PBS or in a MM or HM solution. At 1 hour post-infection, the luminal and intracellular bacterial loads were assessed. There was a significant decrease in the number of luminal bacteria bound to the uroepithelium when treated with 5 mM and 0.5 mM HM ($p \leq 0.01$) (Figure 8). This same decrease was not seen when using 5 mM MM. Relative to untreated UTI89, UTI89 incubated with 5 mM HM had a significant decrease in intracellular population ($p \leq 0.01$). There was no significant decrease in invaded bacteria treated with 5 mM MM or 0.5 mM HM. These data indicate that HM is interfering not only with type 1 pili-mediated bacterial binding but also with type 1 pili-dependent invasion of UPEC.

Heptyl α -D-mannose inhibits biofilm formation in vitro

The development and maturation of IBCs into communities with biofilm-like properties has been shown recently to depend on type 1 pili [16]. We speculated that blocking the FimH binding pocket on type 1 pili would inhibit biofilm formation by inhibiting the adhesive properties of the pili. Bacterial biofilms were grown in the presence of varying concentrations of either HM or MM to elucidate their biofilm inhibiting properties (Figure 9). Biofilm of UTI89 *E. coli* was significantly reduced ($p < 0.01$) only at the highest concentration of MM, 1 mM. However, in the presence of HM, there was a significant decrease in biofilm formation at 10 μ M ($p < 0.001$) and both 1 mM and 100 μ M concentrations ($p < 0.0001$). This suggests that blocking of the type 1 pili

FimH adhesion with HM inhibits biofilm formation. Interestingly, at the lowest concentration of HM (1 μ M) there was a significant increase in biofilm formation ($p < 0.001$). A low concentration of a weak inhibitor appears to allow the bacteria to organize into a better matrix through their type 1 pili [54].

Discussion

Adhesion, invasion and the formation of intracellular biofilms

UPEC express type 1 pili which bind to mannosylated residues on the surface of epithelial bladder cells. Once bound, some bacteria can invade the cells and rapidly replicate into intracellular bacterial communities, named IBCs, which mature into tightly packed biofilm-like societies [15,16]. As the infection proceeds, the bacteria filament and flux out of the cells [7,11]. They can then reinvade neighbouring cells to re-establish infection [14]. Inhibition of UPEC binding to bladder cells will potentially inhibit invasion and limit the bacteria's ability to build up formidable numbers within the bladder. A competitive sugar could potentially disrupt the IBC pathway.

Blocking bacterial invasion could reduce the infection and decrease recurrences. It had been demonstrated already from very early on by Sharon's group that mannose can inhibit FimH-mediated bacterial adhesion [55]. We looked into the ability of heptyl α -D-mannose (HM) to reduce infection, because HM has an optimized alkyl length for interaction with FimH [47]. Inhibition by soluble mannose (Man) or methyl α -D-mannose (MM) or HM of bacterial adhesion to the bladder cell line *in vitro* or upon transurethral catheterization into the mouse bladder indicates that the bacteria cannot switch between HM and the mannosylated uroplakins. Once HM is bound to FimH on the type 1 pili, the bacteria are irreversibly inhibited in their binding to the bladder surface and the infection is reduced. However, the weak inhibitor MM has a relatively high efficiency in the

bladder binding assay that is not in direct correlation with its affinity compared to HM. The affinity of MM for FimH is 500-times less than this of HM, but a concentration of MM a 100-fold higher than the inhibitory concentration of HM is sufficient. The explanation may be in the fact that the *in vitro* adhesion assay is being performed under shaking conditions. Nilsson studied the inhibitory effect of MM on binding of type 1-piliated *E. coli* to mannosylated surfaces under different shear stress conditions. During rolling, FimH molecules transiently bind and detach from surface receptors, allowing a weak soluble inhibitor such as MM to eventually bind to all FimH molecules, thereby preventing further adhesion [54,56]. In contrast, stationary adhesion is mediated by long-lived adhesin-receptor bonds that prevent inhibitor binding during the time course of the experiments (~10 min). HM forms such high-affinity interactions with FimH, also under still conditions. The data on the inhibition by MM or HM of adhesion in the C3H/HeN mice indeed pledge that, for a free small-molecule ligand to be an efficient FimH anti-adhesive even under conditions of fluid flow, such as in the bladder, it must bind significantly tighter to FimH than the binding of FimH to the receptor molecules on the bladder cells, in order to overcome the shear-enhanced affinity. HM corresponds to these requirements, having an affinity for FimH higher than any known natural mannosylated receptor. In this context it is interesting to note that whereas human uroplakin UP1a and integrins only carry mannose receptors with intermediate affinity for FimH, the abundantly secreted urinary glycoprotein human THP displays 8% of the high-affinity oligomannose-5 receptors and 75% of oligomannose-6 exposing $\text{Man}\alpha 1,3\text{Man}$ on the D2 branch (Figure 1) [57].

IBCs are biofilm-like groups of bacteria that form upon adhesion, invasion and replication. Biofilm development requires tight interactions between individual cells in the community. Biofilm formation and maturation in UPEC IBCs is type 1-pili dependent [16] and the homotypic interactions between *E. coli* by means of type 1 pili are glycan

dependent [58]. Therefore, the ability to disrupt biofilm formation using MM or HM was evaluated. A significant decrease in biofilm formation was observed with as little as 10 mM HM, a 100-fold lower concentration than was needed with MM. The only other data that exist on the inhibition of biofilm formation by a glycan are the inhibition of Gram-positive and Gram-negative biofilms by a secreted group II capsule polysaccharide [59]. The concentration-dependent inhibition of biofilm formation by mannose glycans indicates that the FimH adhesin is involved in biofilm formation [58]. Another very interesting observation is the significant increase in biofilm with very low concentrations of MM (Figure 9). The presence of low concentrations of a soluble inhibitor such as MM during a longer period of time (hours) under conditions of low shear can sometimes help the bacteria to spread further and thus colonize larger surfaces [54]. The absence of shear and the presence of MM loosen the interactions between the adhering bacteria and the surface, allowing them to (re-)organize the biofilm. The extent to which the factors that are important for biofilm formation on abiotic surfaces (our assay) are also applicable for biofilm formation on biotic surfaces (e.g. in IBCs) needs to be further studied. However the observation of bacterial biofilm formation on abiotic surfaces is highly relevant in view of the use of medical implants such as urinary catheters. The glycan-based inhibition of UPEC biofilms is interesting in view of the thought that glycoproteins abundantly secreted in the urine, such as THP, could coat the catheter walls and serve as a glue for type 1-piliated *E. coli* to initiate biofilm growth.

The IBCs, or the non-replicating bacteria in quiescent intracellular reservoirs (QIRs), form a repository that can seed a recurrent infection [12]. It was investigated whether the inhibition of binding and biofilm formation *in vitro* could also reduce this intracellular population during UTIs in a mouse model and thus the likelihood of a recurrence. In the presence of 5 mM HM a significant reduction in bacterial numbers in the bladders occurred. Two-hundred times more MM was needed to obtain the same

effect. The results on inhibition with high concentrations of mannose were less consistent, perhaps because FimH can still switch between the mannose on the uroplakins and the mannose in the solution. If this switch happens in time, the bacteria are not urinated out. The adhesin is more tightly bound to HM, thus the bacteria are urinated out before being able to bind to the uroplakins. The tighter binding of the heptyl sugar is potentially reducing the number of UPEC able to bind and invade the bladder cells, and establish a robust infection. To confirm this, an *ex vivo* gentamicin protection assay was performed. This allows enumeration of both the extracellularly bound and intracellular bacteria. There was a significant reduction in both bound and invaded bacteria in the presence of 5 mM HM. In summary, HM is interfering not only with binding but also with invasion of UPEC. A 5 mM concentration of HM is needed for full inhibition of bacterial adhesion *in vivo* (Figures 7 and 8), *versus* a 1 mM concentration *in vitro* (Figure 6). In the mouse model, there is likely some loss of the sugar due to voiding or possibly degradation in the bladder. It is also not clear how the number and nature of mannose receptors in the mouse bladder relate to those on the human bladder cell line 5637. Moreover in the mouse the innate immune responses has an influence on bacterial adhesion and invasion.

What is clear is that the UTI89 cystitis strain binds HM, which deters binding to the bladder cells, limiting invasion, and reducing the level of infection. These data confirm that invasion in bladder cells is type 1-dependent [6], as was demonstrated by the non-invasive character of FimH mannose-binding pocket mutants [53]. Several possible invasion pathways for UPECs have been described. Direct binding of FimH to $\alpha 3$ and $\beta 1$ integrins has been very recently observed and has been shown to depend upon the glycosylation of the integrins, because treatment of $\alpha 3/\beta 1$ integrins with PNGaseF or EndoHf abolished all binding [33]. Bacterial invasion through glycan-

mediated interactions of FimH with integrins could also happen indirectly via cellular receptors of differentiated bladder cells, such as CD151, CD46 and UPIa [36].

Structure, specificity and drug design

The type 1 pilus fimbrial adhesin FimH was co-crystallized with oligomannose-3 to study in detail the interactions with this most specific and natural glycan receptor for FimH. As expected, the tyrosine gate plays a dominant role in the strength and specificity of these interactions. A remarkable feature when analysing the PHI/PSI-chology of the FimH RBD main chain are the tyrosine residues of the tyrosine gate. Both Tyr48 and Tyr137 and even Ile13 are on the borderline for allowed main chain conformations of the Ramachandran plot [60]. The higher affinity of mannopentaose over mannotriose is not reflected in the oligomannose-5 versus oligomannose-3 affinities [26]. The lack of an increased affinity of oligomannose-5 over oligomannose-3 indicates that the choice of FimH is in both cases directed straightforwardly towards the $\text{Man}\alpha_{1,3}\text{Man}\beta_{1,4}\text{GlcNAc}\beta_{1,4}\text{GlcNAc}$ epitope at the non-reducing end of the D1 arm in both oligosaccharides (Figure 1). Further substitution on the $\alpha_{1,6}$ linked mannose (Man4') would at least not hinder binding of oligomannose-5 via the same epitope, as Man4' does not interact with FimH and extends into the solvent.

The similarity of interactions found in the crystal structures of FimH with oligomannose-3 and butyl α -D-mannose is remarkably high. The butyl chain follows the hydrophobic trail through the tyrosine gate along the $\alpha_{1,3}$ and the first $\beta_{1,4}$ glycosidic linkage to GlcNAc2 (Figure 5A). The same trail is conservedly hydrated near the presumable $\alpha_{1,3}$ and the first $\beta_{1,4}$ exocyclic glycosidic linkages (Figure 5B). Finally and as expected, the extensive hydrogen network around the non-reducing mannose residue in the mannose-binding pocket of FimH is fully conserved [45].

Considerable interest exists in the molecular basis for FimH-mediated adhesion, being fed by long-standing observations that blocking the FimH-receptor interaction prevents bacterial infection [21,55]. Structural insight in the basis for specificity into the extended binding site of FimH was lacking until now, seriously hampering and invalidating structure-based design of anti-adhesive molecules using organic chemistry. Due to the great need for anti-adhesives to treat and prevent UTIs, the search was nevertheless continued. Dendrimers of mannose-based inhibitors were most often unable to act multivalently on *E. coli*, however the monovalent moiety of the best inhibitors among those dendrimers contain structures whose interactions can closely mimic those of oligomannose-3, such as glycocluster 4 in the recent study by Touaibia [61]. In these inhibitors, the α -anomeric oxygen of the non-reducing mannose is linked to a phenyl ring, containing an ethyn group in the para position and finalizing in a hydroxyl or ether function. A cocrystal structure for such a complex is unfortunately unknown, however it can be easily imagined that the mannose would anchor in the FimH polar pocket, the α -linkage to the phenyl group would resemble the $\text{Man}\alpha 1,3\text{Man}$ linkage, and the phenyl group would ideally stack with the aromatic side chain of Tyr48. The phenyl to ethyn coupling would strengthen the van der Waals contacts that the $\text{Man}\beta 1,4\text{GlcNAc}$ glycosidic linkage makes with Tyr137 (Figure 4). The triple-bond character of the ethyn could replace the stacking between the C4-C5 bond of GlcNAc2 and the aromatic ring of Tyr137 (Figure 4). Finally, the methoxy or methanol carbon atom would mimic the interaction of C6 of GlcNAc2 with Tyr48 and Ile52, and the terminal hydroxyl or ether oxygen may form a hydrogen bond with Thr51 (Figures 3D and 4).

In conclusion, subnanomolar inhibitors precisely mimic the kind of interactions FimH makes with oligomannose-3, and do so in an enhanced fashion dependent on the chemical nature of the synthetic moieties engineered to replace all but the mannose that enters the monosaccharide binding pocket. The knowledge of all specific

interactions between FimH and its natural high-mannose receptor and the possibility to relate the specificity- and affinity determining spots on the ligand with the efficiency of synthetic inhibitors can greatly enhance structure-based drug design against lower UTIs.

Acknowledgments

We thank K. Decanniere and L. Buts for critical discussions and Chia-Sui Hung and Sheryl Justice for the initial set-up of the mouse experiments.

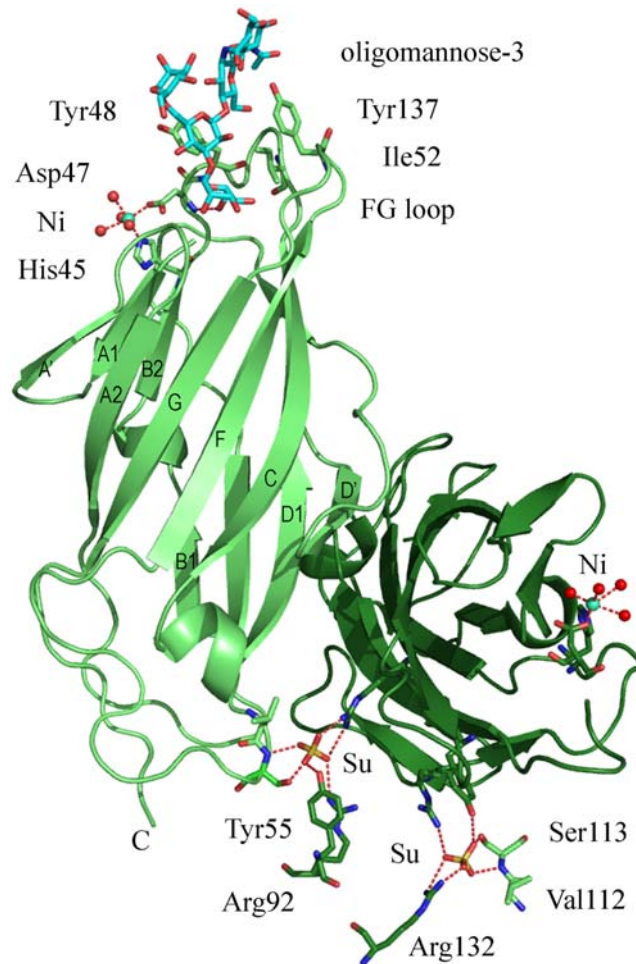


Figure 2. Crystal structure of FimH in complex with oligomannose-3. The two FimH RBDs related by non-crystallographic symmetry (green and forest-green, Ig-fold labeling) both bind oligomannose-3 (only one is shown in blue cyan), interconnected via Asp47 to a nickel ion (green cyan). His45 and Asp47 and four waters ligate the nickel ion in an octahedral configuration. Sulphate ions (yellow with red oxygens) stabilize a highly charged crystal packing interface by bridging Val112 and Ser113 with Arg132 from the two crystallographically independent RBDs with Arg92 and Tyr55 from a symmetry-related RBD.

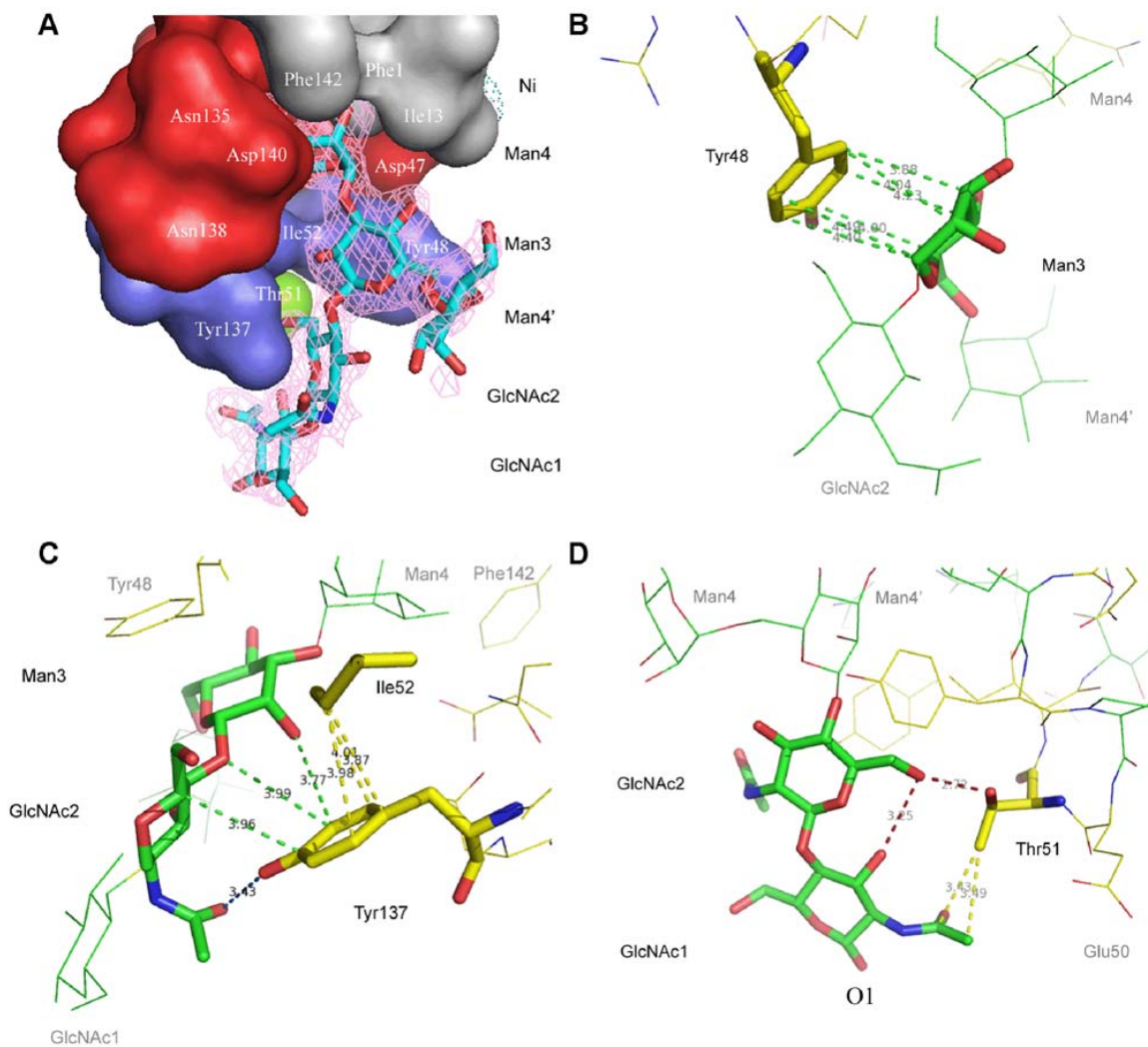


Figure 3. Panel of FimH lectin domain interactions along the oligomannose-3 chain. **A**, Electron density map, contoured at $1 \text{ e}/\text{\AA}^3$, for oligomannose-3 in the FimH receptor-binding site. The surface of the binding site is subdivided into its hydrophobic support platform (grey, residues Phe142, Phe1 and Ile13), its polar pocket (red, residues Asn46, Asp47, Asp54, Gln133, Asn135, Asn138 and Asp140), the tyrosine gate (blue, residues Tyr137, Ile52 and Tyr48) and residue Thr51 (green). **B**, Aromatic-to-saccharide stacking (green dashed lines) of the Tyr48 side chain onto the B-face of Man3. **C**, van der Waals support of the β 1,4 linkage (yellow dashed lines) and an hydrophobic contact of C5 of GlcNAc2 by Tyr137 (green dashed lines). **D**, Thr51 tops of the site by

hydrophilic (red), hydrophobic and van der Waals (yellow) interactions with the chitobiose. The anomeric O1 of GlcNAc1 would be exchanged for by the nitrogen of the amide of asparagine on a receptor glycoprotein for FimH.

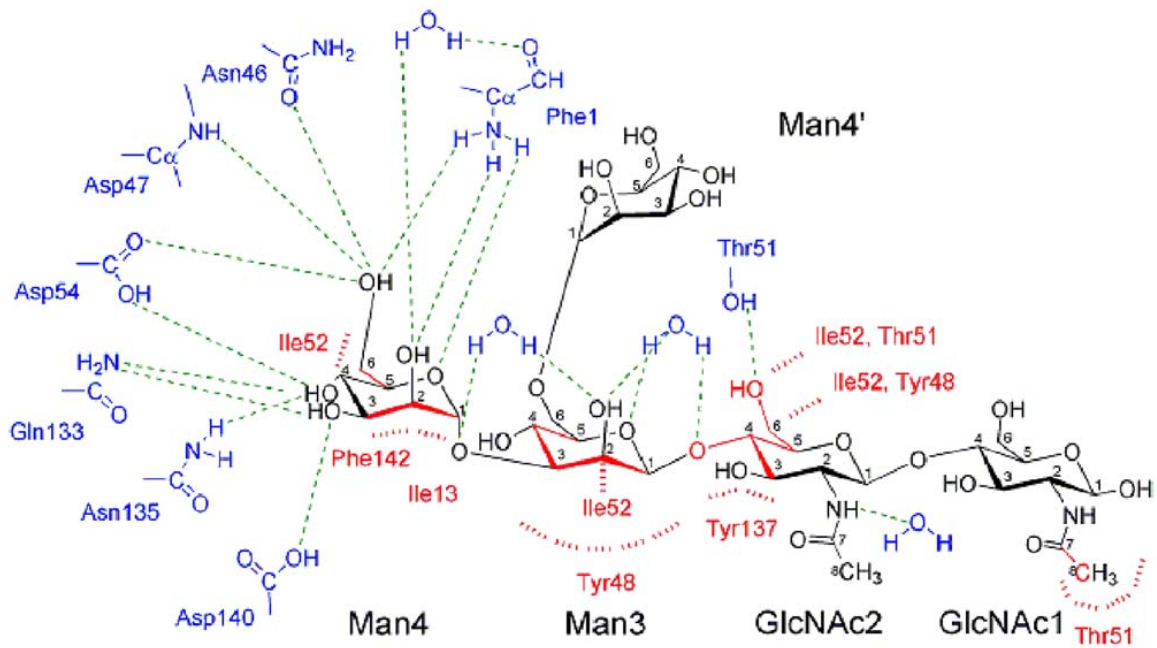


Figure 4. Scheme of the interactions in the extended FimH receptor-binding pocket. A network of hydrogen bonds (green dashed lines) surrounds Man4. Further along oligomannose-3, only water molecules make hydrogen bonds along one side of oligomannose-3 except for the Thr51 side chain. The residues of the tyrosine gate, Tyr48, Ile52 and Tyr137, interact via aromatic stackings, hydrophobic and van der Waals contacts (all marked in red) mainly with Man3 and GlcNAc2.

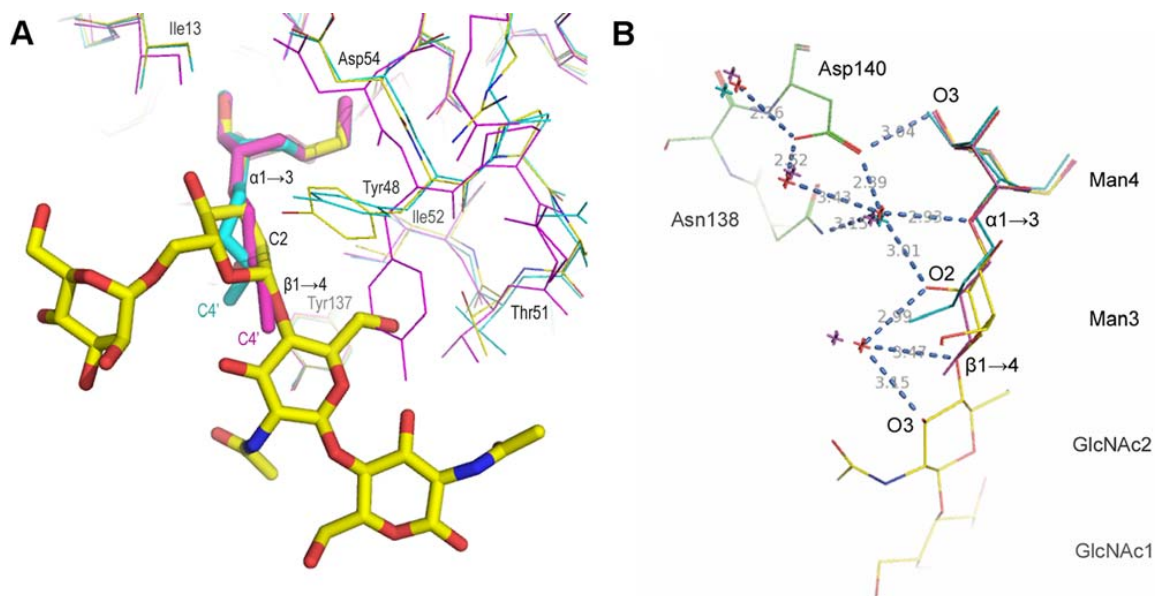


Figure 5. Specificity spots for interaction with FimH. **A**, Superposing the FimH RBDs with the oligomannose-3 ligand (yellow, PDB entry 2vco, 2.1 Å resolution), with butyl α -D-mannose (magenta, 1uwf, 1.7 Å resolution) and with butyl α -D-mannose (cyan, 1tr7, 2.1 Å resolution). Tyr48 in the 1uwf structure (magenta) adopts a different side chain conformation, for the reason to avoid clashes in the crystal packing. The butyl tail takes on a conformation that matches the C3-C2-C1 greasy trace of the central Man3 almost precisely. **B**, Water positions in the crystal structures of the FimH RBD (green) in complex with the oligomannose-3 ligand (yellow, waters in red and hydrogen bonds in blue dashed lines) match those of the FimH RBDs of the butyl α -D-mannose-liganded structures (waters in magenta for 1uwf, waters in cyan for 1tr7).

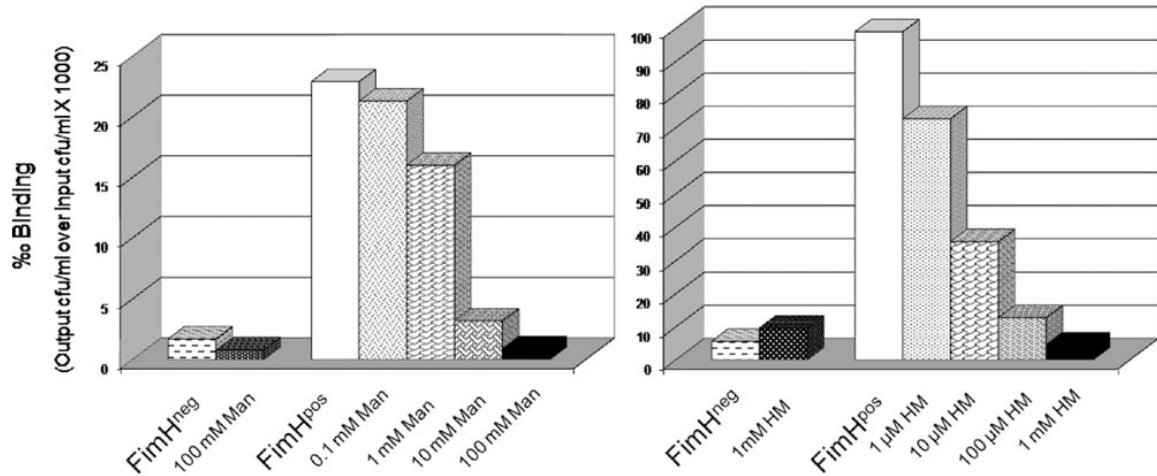


Figure 6. Inhibition of bacterial adhesion to 5637 bladder cells by mannose or heptyl α -D-mannose. Type 1 pili-expressing *E. coli* were incubated at 10^6 cfu/ml (FimH^{pos}) with the bladder cells, or had been mixed with a ten-fold dilution series of Man or HM prior to incubation, to compare inhibition of bacterial binding by the two sugars. An isogenic *fimH*-negative strain served as a negative control (FimH^{neg}).

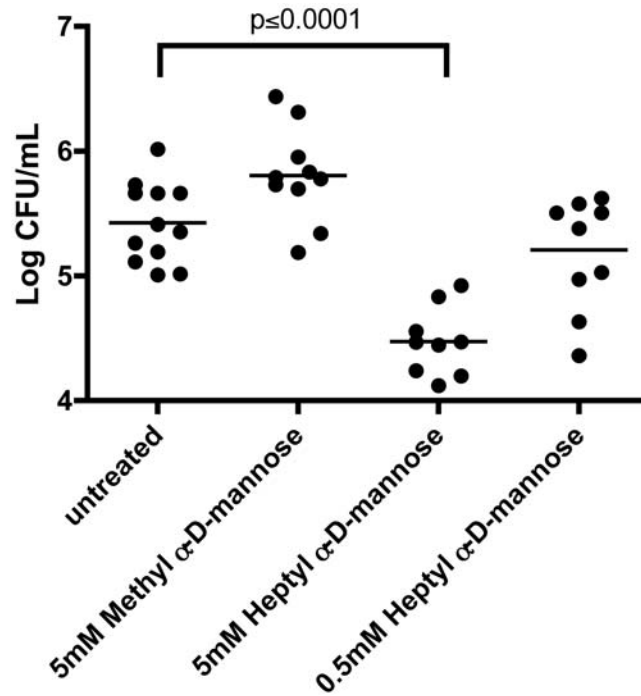


Figure 7. Bacterial load in the mouse bladder 6 hours post-infection. Mice were inoculated with UTI89, either untreated or treated with MM or HM. At 6 hours post-infection there was a significant decrease in the amount of bacteria treated with 5 mM HM in the bladder ($p \leq 0.0001$ by Mann Whitney test). This same decrease was not observed with bacteria treated with 5 mM MM. Bacteria treated with 0.5 mM HM were not significantly reduced relative to the untreated infection.

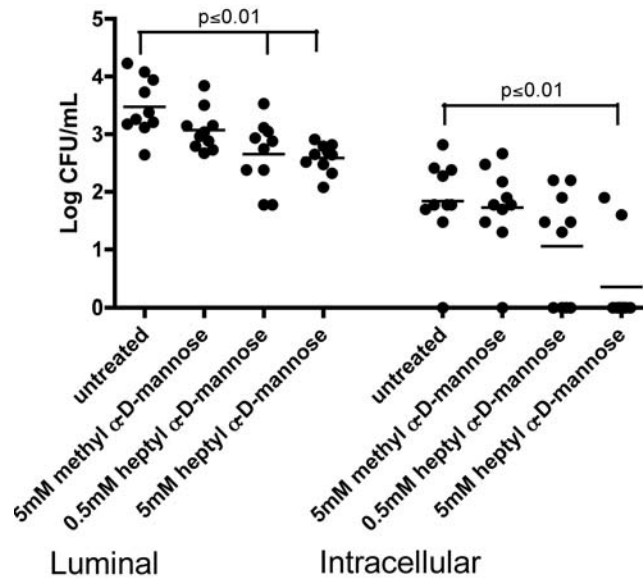


Figure 8. Gentamicin protection assay to determine luminal versus intracellular bacterial population. Mice were inoculated with UTI89 either untreated or treated with MM HM. At 1 hour post-infection, bladders were harvested and processed. Luminal bacteria were obtained from washes of the bladder. The remaining extracellular bacteria were killed with gentamicin and invaded, intracellular bacteria were counted.

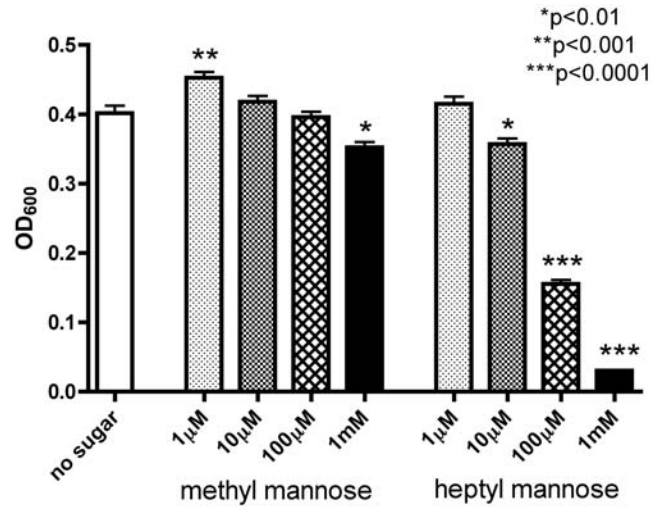


Figure 9. Biofilm formation in the presence of methyl or heptyl α -D-mannose.

Standard biofilm assays showed a great reduction of UTI89 biofilm formation in the presence of 100 μ M and 1 mM HM ($p < 0.0001$) and a significant increase ($p < 0.01$) in the presence of 1 mM MM.

Supporting Information

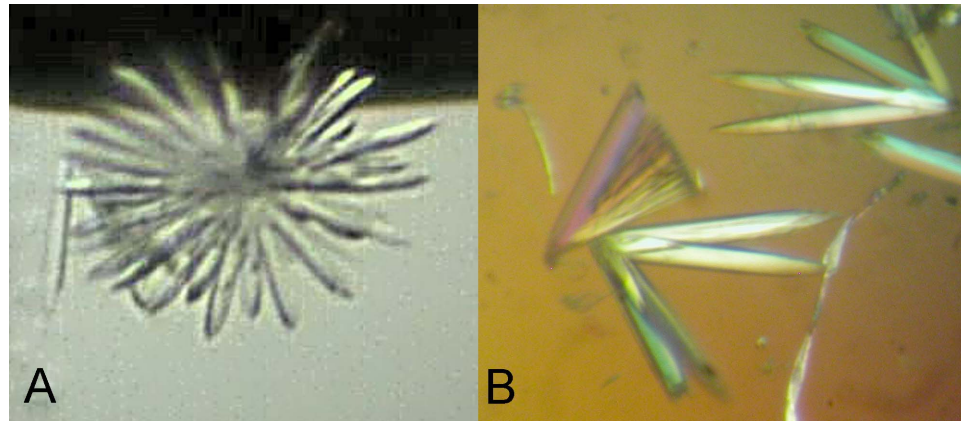


Figure S1. Crystals of the FimH receptor-binding domain in complex with oligomannose-3. The crystals were grown by the vapour diffusion method in 1.0 M Li_2SO_4 , 0.1 M Tris pH 8.5, 0.01 M NiCl_2 , **A**, in sitting drop, diffracting to 2.6 Å resolution, and **B**, in hanging drop, optimized by the addition of 3% glycerol to the precipitant and diffracting to a maximum resolution of 2.0 Å.

Table S1. Data collection and processing, refinement statistics and model quality

Space group	P3 ₁ 21
Unit cell dimensions (Å)	a = b = 90.562 c = 79.480
Molecules per asymmetric unit	2
Solvent content (%)	55.6
Resolution range (Å)	78.33 – 2.1
Reflections (total/unique)	142,687 / 22,429
Completeness (%) ^a	99.8 (100.0)
R _{merge} ^{a,b}	0.099 (0.42)
<I/σ(I)> ^{a,b}	16.0 (5.8)
R _{free}	0.241 (0.310)
R _{cryst}	0.184 (0.228)
R _{all}	0.187
Ramachandran	
% of residues in favored regions	97.12
allowed regions	100.00
Rmsd bond lengths (Å)	0.010
Rmsd bond angles (°)	1.178
Average B-factors main chain	24.4
Average B-factors water	36.1

^a Values in parentheses indicate statistics for the highest resolution shell (2.14 - 2.1 Å). ^b

$R_{\text{merge}} = \sum_{\mathbf{h}} \sum_i |I_{\mathbf{h},i} - \langle I_{\mathbf{h}} \rangle| / \sum_{\mathbf{h}} \sum_i \langle I_{\mathbf{h}} \rangle$, where $I_{\mathbf{h},i}$ is the i th observation of reflection \mathbf{h} and $\langle I_{\mathbf{h}} \rangle$ is the weighted average intensity for all observations i of reflection \mathbf{h} .

References

1. De Greve H, Wyns L, Bouckaert J (2007) Combining sites of bacterial fimbriae. *Curr Opin Struct Biol* 17: 506-512.
2. Zhou G, Mo WJ, Sebbel P, Min G, Neubert TA, et al. (2001) Uroplakin Ia is the urothelial receptor for uropathogenic *Escherichia coli*: evidence from in vitro FimH binding. *J Cell Sci* 114: 4095-4103.
3. Schilling JD, Martin SM, Hung CS, Lorenz RG, Hultgren SJ (2003) Toll-like receptor 4 on stromal and hematopoietic cells mediates innate resistance to uropathogenic *Escherichia coli*. *Proc Natl Acad Sci USA* 100: 4203-4208.
4. Svanborg C, Bergsten G, Fischer H, Godaly G, Gustafsson M, et al. (2006) Uropathogenic *Escherichia coli* as a model of host-parasite interaction. *Curr Opin Microbiol* 9: 33-39.
5. Mulvey MA, Lopez-Boado YS, Wilson CL, Roth R, Parks WC, et al. (1998) Induction and evasion of host defenses by type 1-piliated uropathogenic *Escherichia coli*. *Science* 282: 1494-1497.
6. Martinez JJ, Mulvey MA, Schilling JD, Pinkner JS, Hultgren SJ (2000) Type 1 pilus-mediated bacterial invasion of bladder epithelial cells. *EMBO J* 19: 2803-2812.
7. Mulvey MA, Schilling JD, Martinez JJ, Hultgren SJ (2000) Bad bugs and beleaguered bladders: Interplay between uropathogenic *Escherichia coli* and innate host defenses. *Proc Natl Acad Sci U S A* 97: 8829-8835.

8. Mysorekar IU, Hultgren SJ (2006) Mechanisms of uropathogenic *Escherichia coli* persistence and eradication from the urinary tract. Proc Natl Acad Sci U S A 103: 14170-14175.
9. Anderson GG, Palermo JJ, Schilling JD, Roth R, Heuser J, et al. (2003) Intracellular bacterial biofilm-like pods in urinary tract infections. Science 301: 105-107.
10. Justice SS, Lauer SR, Hultgren SJ, Hunstad DA (2006) Maturation of intracellular *Escherichia coli* communities requires SurA. Infect Immun 74: 4793-4800.
11. Justice SS, Hunstad DA, Seed PC, Hultgren SJ (2006) Filamentation by *Escherichia coli* subverts innate defenses during urinary tract infection. Proc Natl Acad Sci U S A 103: 19884-19889.
12. Mulvey MA, Schilling JD, Hultgren SJ (2001) Establishment of a persistent *Escherichia coli* reservoir during the acute phase of a bladder infection. Infect Immun 69: 4572-4579.
13. Schilling JD, Hultgren SJ (2002) Recent advances into the pathogenesis of recurrent urinary tract infections: the bladder as a reservoir for uropathogenic *Escherichia coli*. Internatl J Antimicrob Ag 19: 457-460.
14. Justice SS, Hung C, Theriot JA, Fletcher DA, Anderson GG, et al. (2004) Differentiation and developmental pathways of uropathogenic *Escherichia coli* in urinary tract pathogenesis. Proc Natl Acad Sci U S A 101: 1333-1338.
15. Garofalo CK, Hooton TM, Martin SM, Stamm WE, Palermo JJ, et al. (2007) *Escherichia coli* from urine of female patients with urinary tract infections

- is competent for intracellular bacterial community formation. *Infect Immun* 75: 52-60.
16. Wright KJ, Seed PC, Hultgren SJ (2007) Development of intracellular bacterial communities of uropathogenic *Escherichia coli* depends on type 1 pili. *Cell Microbiol* 9: 2230-2241.
 17. Bishop BL, Duncan MJ, Song J, Li G, Zaas D, et al. (2007) Cyclic AMP-regulated exocytosis of *Escherichia coli* from infected bladder epithelial cells. *Nat Med* 13: 625-630.
 18. Apodaca G (2004) The uroepithelium: not just a passive barrier. *Traffic* 5: 117-128.
 19. Eto DS, Mulvey MA (2007) Flushing bacteria out of the bladder. *Nat Med* 13: 531-532.
 20. Eto DS, Sundsbak JL, Mulvey MA (2006) Actin-gated intracellular growth and resurgence of uropathogenic *Escherichia coli*. *Cell Microbiol* 8: 704-717.
 21. Langermann S, Mollby R, Burlein JE, Palaszynski SR, Auguste CG, et al. (2000) Vaccination with FimH adhesin protects cynomolgus monkeys from colonization and infection by uropathogenic *Escherichia coli*. *J Infect Dis* 181: 774-8.
 22. Sharon N (2006) Carbohydrates as future anti-adhesion drugs for infectious diseases. *Biochim Biophys Acta* 1760: 527-537.

23. Firon N, Ofek I, Sharon N (1983) Carbohydrate specificity of the surface lectins of *Escherichia coli*, *Klebsiella pneumoniae* and *Salmonella typhimurium*. Carbohydr Res 120: 235-249.
24. Neeser JR, Koellreutter B, Wuersch P (1986) Oligomannoside-type glycopeptides inhibiting adhesion of *Escherichia coli* strains mediated by type 1 pili: preparation of potent inhibitors from plant glycoproteins. Infect Immun 52: 428-36.
25. Sharon N (1987) Bacterial Lectins, cell-cell recognition and infectious disease. FEBS Lett 217: 145-157.
26. Bouckaert J, Mackenzie J, de Paz JL, Chipwaza B, Choudhury D, et al. (2006) The affinity of the FimH fimbrial adhesin is receptor-driven and quasi-independent of *Escherichia coli* pathotypes. Mol Microbiol 61: 1556-1568.
27. Sokurenko EV, Chesnokova V, Doyle RJ, Hasty DL (1997) Diversity of the *Escherichia coli* type 1 fimbrial lectin. Differential binding to mannosides and uroepithelial cells. J Biol Chem 272: 17880-17886.
28. Duncan MJ, Mann EL, Cohen MS, Ofek I, Sharon N, et al. (2005) The distinct binding specificities exhibited by enterobacterial type 1 fimbriae are determined by their fimbrial shafts. J Biol Chem 280: 37707-37716.
29. Aprikian P, Tchesnokova V, Kidd B, Yakovenko O, Yarov-Yarovoy V, et al. (2007) Interdomain interaction in the FimH adhesin of *Escherichia coli* regulates the affinity to mannose. J Biol Chem 282: 23437-23446.

30. Thomas WE, Trintchina E, Forero M, Vogel V, Sokurenko EV (2002) Bacterial adhesion to target cells enhanced by shear force. *Cell* 109: 913-923.
31. Nilsson LM, Thomas WE, Trintchina E, Vogel V, Sokurenko EV (2006) Catch bond-mediated adhesion without a shear threshold - Trimannose versus monomannose interactions with the FimH adhesin of *Escherichia coli*. *J Biol Chem* 281: 16656-16663.
32. Pak J, Pu Y, Zhang ZT, Hasty DL, Wu XR (2001) Tamm-Horsfall protein binds to type 1 fimbriated *Escherichia coli* and prevents *Escherichia coli* from binding to uroplakin Ia and Ib receptors. *J Biol Chem* 276: 9924-30.
33. Eto DS, Jones TA, Sundsbak JL, Mulvey MA (2007) Integrin-mediated host cell invasion by type 1-piliated uropathogenic *Escherichia coli*. *PLoS Pathog* 3: e100.
34. Min G, Stolz M, Zhou G, Liang F, Sebbel P, et al. (2002) Localization of uroplakin Ia, the urothelial receptor for bacterial adhesin FimH, on the six inner domains of the 16 nm urothelial plaque particle. *J Mol Biol* 317: 697-706.
35. Liang FX, Riedel I, Deng FM, Zhou G, Xu C, et al. (2001) Organization of uroplakin subunits: transmembrane topology, pair formation and plaque composition. *Biochem J* 355: 13-18.
36. Berditchevski F, Odintsova E (2007) Tetraspanins as regulators of protein trafficking. *Traffic* 8: 89-96.

37. Xie B, Zhou G, Chan SY, Shapiro E, Kong XP, et al. (2006) Distinct glycan structures of uroplakins Ia and Ib: Structural basis for the selective binding of FimH adhesin to uroplakin Ia. *J Biol Chem* 281: 14644-14653.
38. Litynska A, Pochec E, Hoja-Lukowicz D, Kremser E, Laidler P, et al. (2002) The structure of the oligosaccharides of alpha3beta1 integrin from human ureter epithelium (HCV29) cell line. *Acta Biochim Pol* 49: 491-500.
39. Foulquier F, Duvet S, Klein A, Mir AM, Chirat F, et al. (2004) Endoplasmic reticulum-associated degradation of glycoproteins bearing Man5GlcNAc2 and Man9GlcNAc2 species in the MI8-5 CHO cell line. *Eur J Biochem* 271: 398-404.
40. Rosenstein IJ, Stoll MS, Mizuochi T, Childs RA, Hounsell EF, et al. (1988) New type of adhesive specificity revealed by oligosaccharide probes in *Escherichia coli* from patients with urinary tract infection. *Lancet* 2: 1327-1330.
41. Serafini-Cessi F, Monti A, Cavallone D (2005) N-Glycans carried by Tamm-Horsfall glycoprotein have a crucial role in the defense against urinary tract diseases. *Glycoconjugate J* 22: 383-394.
42. Foxman B (2003) Epidemiology of urinary tract infections: Incidence, morbidity, and economic costs. *Dis Mon* 49: 53-70.
43. Geerlings SE, Meiland R, van Lith EC, Brouwer EC, Gaastra W, et al. (2002) Adherence of type 1-fimbriated *Escherichia coli* to uroepithelial cells - More in diabetic women than in control subjects. *Diabetes Care* 25: 1405-1409.

44. Geerlings SE, Meiland R, Hoepelman AIM (2002) Pathogenesis of bacteriuria in women with diabetes mellitus. *Internatl J Antimicrob Ag* 19: 539-545.
45. Norden NE, Lundblad A, Svensson S, Ockerman PA, Autio S (1973) Mannose-containing trisaccharide isolated from urines of 3 patients with mannosidosis. *J Biol Chem* 248: 6210-6215.
46. Rijavec M, Erjavec MS, Avgustin JA, Reissbrodt R, Fruth A, et al. (2006) High prevalence of multidrug resistance and random distribution of mobile genetic elements among uropathogenic *Escherichia coli* (UPEC) of the four major phylogenetic groups. *Curr Microbiol* 53: 158-162.
47. Bouckaert J, Berglund J, Schembri M, De Genst E, Cools L, et al. (2005) Receptor binding studies disclose a novel class of high-affinity inhibitors of the *Escherichia coli* FimH adhesin. *Mol Microbiol* 55: 441-455.
48. Warin V, Baert F, Fouret R (1979) The crystal and molecular structure of O- α -d-mannopyranosyl-(1-3)-O- β -d-mannopyranosyl-(1-4)-2-acetamido-2-deoxy- α -d-glucopyranose. *Carbohydrate Res* 76: 11-22.
49. Wormald MR, Petrescu AJ, Pao YL, Glithero A, Elliott T, et al. (2002) Conformational studies of oligosaccharides and glycopeptides: complementarity of NMR, X-ray crystallography, and molecular modelling. *Chem Rev* 102: 371-386.
50. Imberty A, Bourne Y, Cambillau C, Rouge P, Perez S (1993) Oligosaccharide conformation in protein/glycan crystalline complexes, *Adv Biophys Chem* 3: 71-117.

51. Krissinel E, Henrick K (2007) Inference of macromolecular assemblies from crystalline state. *J Mol Biol* 372: 774-797.
52. Choudhury D, Thompson A, Stojanoff V, Langermann S, Pinkner J, et al. (1999) X-ray structure of the FimC-FimH chaperone-adhesin complex from uropathogenic *Escherichia coli*. *Science* 285: 1061-1066.
53. Hung C-S, Bouckaert J, Hung DL, Pinkner J, Winberg C, et al. (2002) Structural basis of tropism of *Escherichia coli* to the bladder during urinary tract infection. *Mol Microbiol* 44: 903-915.
54. Anderson BN, Ding AM, Nilsson LM, Kusuma K, Tchesnokova V, et al. Weak rolling adhesion enhances bacterial surface colonization. *J Bacteriol* 189: 1794-1802.
55. Aronson M, Medalia O, Schori L, Mirelman D, Sharon N, et al. (1979) Prevention of colonization of the urinary-tract by blocking bacterial adherence with methyl-alpha-D-mannopyranoside. *Israel J Med Sci* 15: 88.
56. Nilsson LM, Thornas WE, Sokurenko EV, Vogel V (2006) Elevated shear stress protects *Escherichia coli* cells adhering to surfaces via catch bonds from detachment by soluble inhibitors. *Appl Environ Microbiol* 72: 3005-3010.
57. Cavallone D, Malagolini N, Monti A, Wu XR, Serafini-Cessi F (2004) Variation of high mannose chains of Tamm-Horsfall glycoprotein confers differential binding to type 1-fimbriated *Escherichia coli*. *J Biol Chem* 279: 216-222.
58. Orndorff PE, Devapali A, Palestrant S, Wyse A, Everett ML, et al. (2004) Immunoglobulin-mediated agglutination of and biofilm formation by

Escherichia coli K-12 require the type 1 pilus fiber. Infect Immun 72: 1929-1938.

59. Valle J, Da Re S, Henry N, Fontaine T, Balestrino D, et al. (2006) Broad-spectrum biofilm inhibition by a secreted bacterial polysaccharide. Proc Natl Acad Sci U S A 103: 12558-12563.
60. Kleywegt GJ, Jones TA (1996) Phi/psi-chology: Ramachandran revisited. Structure 4: 1395-1400.
61. Touaibia M, Wellens A, Shiao TC, Wang Q, Sirois S, et al. (2007) Mannosylated G(0) dendrimers with nanomolar affinities to *Escherichia coli* FimH. ChemMedChem 2: 1190-1201.
62. Otwinowski Z, Minor W (1997) Processing of X-ray diffraction data collected in oscillation mode. Methods Enzymol 276: 307-326.
63. Vagin A, Teplyakov A (1997) MOLREP: An automated program for molecular replacement. J Appl Crystallogr 1022-1025.
64. Brunger AT, Adams PD, Clore GM, DeLano WL, Gros P, et al. (1998) Crystallography & NMR system: A new software suite for macromolecular structure determination. Acta Crystallogr D Biol Crystallogr 54: 905-921.
65. Murshudov GN, Vagin AA, Dodson EJ (1997) Refinement of macromolecular structures by the maximum-likelihood method. Acta Crystallogr D Biol Crystallogr 53: 240-255.
66. Cambillau C (1992) TURBO-FRODO: Molecular Graphics Program for Silicon Graphics. IRIS 4D Series, version Bio-Graphics, Marseille, France.

67. Emsley P, Cowtan K (2004) Coot: model-building tools for molecular graphics. *Acta Crystallogr D Biol Crystallogr* 60: 2126-2132.
68. Lovell SC, Davis IW, Arendall WB, de Bakker PI, Word JM, Prisant MG, Richardson JS, Richardson DC (2003) Structure validation by Calpha geometry: phi, psi and Cbeta deviation. *Proteins* 50: 437-450.
69. Dodson EJ, Winn M, Ralph A (1997) Collaborative computational project, number 4: Providing programs for protein crystallography. *Methods Enzymol* 277: 620-633.
70. McDonald IK, Thornton JM (1994) Satisfying hydrogen bonding potential in proteins. *J Mol Biol* 238: 777-793.
71. Blomfield IC, McClain MS, Eisenstein BI (1991) Type 1 fimbriae mutants of *Escherichia coli* K12: characterization of recognized afimbriate strains and construction of new fim deletion mutants. *Mol Microbiol* 5: 1439-45.
72. Minion FC, Abraham SN, Beachey EH, Goguen JD (1989) The genetic determinant of adhesive function in type 1 fimbriae of *Escherichia coli* is distinct from the gene encoding the fimbrial subunit. *J Bacteriol* 165: 1033-36.

CHAPTER FIVE

FUTURE DIRECTIONS AND CONCLUDING REMARKS

Conservation of the IBC pathogenic pathway among UPEC

A study of uropathogenic *Escherichia coli* (UPEC) clinical isolates from different clinical syndromes revealed that the intracellular bacterial community (IBC) pathway is a common pathway of UPEC (18). Additionally, analysis of human urine specimens suggests an association between IBCs, filamentous bacteria and acute uncomplicated cystitis in young women (42). The ramifications of this work result in a vastly improved understanding of urinary tract infections (UTIs) which will ultimately lead to better therapeutic options and less treatment failures. Clinically UTIs are thought to be due to simple extracellular colonization of the urothelium by UPEC, however intracellular bacteria have been found in the human bladder following UTI (15). The notion of an intracellular niche in human UTI should change the way physicians treat the disease. Episodes of cystitis caused by UPEC in humans likely involve an IBC pathogenic pathway similar to that observed in mice. The ability to utilize an intracellular bladder niche in both murine and human infection may represent an imperative virulence determinant. Intracellular bacteria are largely protected from host innate immunity. While in the intracellular niche, bacteria are not subject to the shear forces of urine flow and are not subject to phagocytosis by host neutrophils or macrophages allowing bacteria to build up in numbers despite potent innate defenses. Additionally, the formation of intracellular biofilms may allow bacteria to withstand many antimicrobial therapies, as is the case for bacteria in extracellular biofilms (14). IBC formation may also explain how the relatively few bacteria introduced into the bladder with sexual intercourse (9, 10, 24) are able to survive and replicate to numbers high enough to elicit symptoms in the host. The introduction of low numbers of bacteria into the bladder is

likely a relatively common occurrence but controlled by the host immune system and the ability of urothelial cells to expel invaded UPEC (7). It may be that only in the event of invasion, escape to the cytosol and IBC formation can bacteria replicate and persist to sufficiently initiate symptomatic cystitis. In line with this theory, acute UTI isolates formed significantly smaller and fewer IBCs within the mouse urinary tract indicative of a less robust infection. In general, ASB, rUTI and pyelonephritis strains are associated with longer-term persistence in the human, and, in the murine bladder, IBC size and number were significantly greater in these isolates suggesting that IBCs relate to persistence. Since IBC formation is a rare event among acute isolates perhaps they are not meeting the threshold of IBCs to establish a persistent infection. Further investigation is required to decipher what acute isolates lack preventing robust and numerous IBCs. Recent studies indicate that complicated signal transduction pathways are initiated in response to bacterial binding to eliminate colonization. Bacteria must overcome expulsion in response to increased cyclic AMP (7) and must disrupt F-actin and escape the vacuole to achieve access to the cytoplasm for IBC formation (16). Perhaps acute isolates lack the necessary factors to overcome these host factors and enter their desired niche.

Evaluation of the immune response elicited by the host in the presence of acute isolates versus UTI89 could indicate essential differences in immune evasion strategies among acute isolates. It was shown that UTI89 actually dampens the IL-6 response from the host relative to K-12 *E. coli* strains (27). Perhaps acute isolates are unsuccessful at preventing the robust production of IL-6 by the host and are thus eliminated more quickly from the host, reducing the amount that are able to invade and form IBCs. Another way to evaluate the reduction in IBC size and number in the acute isolates would be to transform these strains with a fosmid library of UTI89 and screen for IBC numbers and size. Those mutants with enhanced IBC number or size would

potentially identify virulence factors involved in IBC formation. Previously this work was laborious due to the absence of a tissue culture model, however, it was recently discovered that treating human urothelial cells with filipin facilitates the development of IBC-like structures enabling a more feasible screen of mutant bacteria (6). Knowledge as to why acute isolates are less persistent in regards to immune response and IBC formation could identify new therapeutic targets to prevent persistent infection observed with ASB, rUTI and pyelonephritis isolates.

The IBC pathogenic pathway is conserved among UPEC and in human UTI. The extent of this conservation and the prevalence of this pathway in patients with cystitis remains obscure, however, the commonality of IBCs among UPEC and in humans is a remarkable discovery. This finding changes the historical paradigm that UTI is an extracellular infection and validates the already established murine cystitis model. UTI pathogenesis is clearly more complex than once considered and these newly elucidated steps in the infectious process raise several novel questions and may provide additional therapeutic targets for this common disease.

Evaluation of the Co-infection phenotype

Of the 18 clinical isolates tested for IBC formation, IBCs were not observed in three isolates and they were thus deemed outliers. An *ex vivo* gentamicin protection assay revealed that the three isolates (rUTI1, acute4 and pyelo3) were deficient in invasion. Multiplex virulence factor PCR revealed no association with lack of IBC formation and virulence factors. Likely there is a multitude of virulence factors contributing to IBC formation and perhaps some redundancy in the necessary factors. rUTI1 and pyelo3 did not persist in the murine bladder however were isolated from a persistent infection within the human. It is likely that multiple strains of bacteria are simultaneously introduced into

the urinary tract of women during the early events that lead to a UTI. The diagnosis of UTIs rarely delineates whether multiple strains of *E. coli* are present. Thus, these strains could have “piggy-backed” with a more invasive IBC-forming strain that went undetected. In an effort to emulate what may have happened with the three outlying strains, each clinical isolate was inoculated with equal amounts of UTI89. Upon co-inoculation, each strain demonstrated altered behavior from their single infection phenotype. These results demonstrate the complexities of co-infection and might explain the occurrence of different clinical syndromes manifested by the same organism (25) or the differing behavior in single versus mixed infections.

While unable to form IBCs alone, rUTI1 formed IBCs in the presence of UTI89, acute4 formed IBCs mixed with UTI89, and pyelo3 was still unable to form IBCs in the presence of UTI89. Instead, co-inoculation of UTI89 and pyelo3 resulted in massive filamentation of both isolates. Since filamentation occurs in response to an inflammatory response (28), further study is required to assess whether pyelo3 is triggering a more robust innate response that leads to the massive filamentation observed. Evaluation of the immune response elicited by single infection bladders versus co-infection bladders could shed some light on the reason for the filamentation phenotype. First, tissue titers revealed that upon individual inoculation of UTI89 and pyelo3, UTI89 had higher titers in the bladder at 6 h, 24 h and 2 weeks post-infection, however kidney titers were equivalent at all time points post-infection (Figure 1). Upon co-infection, bacterial load in the bladder resembled a UTI89 single infection suggesting that UTI89 is the dominant bacteria driving the infection. Next, the immune response in the single infection tissues versus the co-infection tissues was evaluated to determine if the immune response mimics the tissue titer observations. While bacterial load differences were only observed in the bladder, evaluation of 12 cytokines revealed no significant difference in immune response when single infection of UTI89 and pyelo3 and co-infection were evaluated.

However, significant differences were observed in 9 of 12 cytokines in the kidney. Of the observed differences the majority separated UTI89 single infection from pyelo3 single infection and co-infection. Thus, the immune response of the co-infection more closely mimicked the immune response of the pyelo3 infection. This is interesting since the co-infection mimicked the UTI89 single infection in regards to tissue titers. In general, the immune response in the pyelo3 single infection and the co-infection was much more robust (Figure 2). IL-1 β , IL-6, MCP-1 and MIP-1 β were significantly elevated in pyelo3 infection and co-infection relative to UTI89. All of the above cytokines are secreted by macrophages and result in activation of macrophages and lymphocytes, enhancing the immune response to the pathogen. Although certain cytokines were only significantly elevated in pyelo3 single infection or co-infection, no cytokines were significantly elevated in the UTI89 infection. Thus, the hypothesis that pyelo3 is triggering a more robust innate response that leads to the massive filamentation of both isolates is possible.

We have confirmed that there is a more robust innate response in the presence of pyelo3 however, we have not directly identified that it is this response that is driving the filamentation phenotype. The immune response that leads to massive filamentation could be teased out using a tissue culture model. Addition of various cytokines shown to be upregulated upon infection with pyelo3 could be added to urothelial cells along with bacteria. Filamentation of bacteria could be observed through microscopy and release of IL-6 and IL-8 could be measured through ELISA assay (22). Since, filamentation is a mechanism the bacteria employs to evade neutrophil engulfment and persist in the face of massive immune responses, understanding of this process could identify targets for therapeutics that inhibit bacterial filamentation and reduce the bacteria's chances to perpetuate the infection. It has been shown that the loss of the ability to filament results in reduced persistence within the bladder (29).

Work with the co-infection model has even further changed the paradigm of infection. Not only are UTIs complicated infections involving intracellular and extracellular niches, they are compounded by the high likelihood of inoculating multiple strains of *E. coli* into the bladder at one time. This mechanism of co-inoculation allows multiple strains to persist that perhaps would be eliminated if inoculated by themselves. Thus, targeting multiple mechanisms of virulence throughout the UPEC pathogenic pathway may be necessary to completely eliminate infection and prevent recurrence. Further understanding of how bacteria interact with one another and what virulence factors are important to each step in the UPEC pathogenic pathway will facilitate the development of novel therapeutics that can combat this very common disease.

pUTI89 as a virulence factor

UTI89 contains a 114 kb extrachromosomal element termed pUTI89. pUTI89 is a unique plasmid containing two regions, the *tra* operon and genes found on other virulence plasmids. pUTI89 appears to have many of the characteristics common to pathogenicity islands (PAIs); it occupies a large genomic region, carries genes encoding one or more virulence factors and contains cryptic or functional genes encoding mobility factors such as integrases, transposases, and insertion sequences (20). Yet to be discovered, is whether it is present in the genomes of pathogenic organisms but absent from the genomes of non-pathogenic organisms. To assess the presence of pUTI89 in pathogenic organisms, 18 clinical UPEC isolates were tested for regions of pUTI89 by plasmid purification and PCR. Evaluation revealed that 67% of UPEC clinical isolates had evidence of pUTI89 and 22% appeared to have the entire plasmid based on positive PCR reactions. Due to its maintenance within the population, pUTI89 is likely involved in pathogenesis *in vivo*. However, non-pathogenic organisms such as K-12 *E. coli* were not tested for the presence of pUTI89. Furthermore, it would be interesting to test

pathogenic organisms from different families of *E. coli*, such as enterohemorrhagic *E. coli* (EHEC), enteroinvasive *E. coli* (EIEC), enteroaggregative *E. coli* (EAEC) and avian pathogenic *E. coli* (APEC). Identification of pUTI89 genes in the pathogenic classes of *E. coli* but not K-12 *E. coli* could identify it as an extraintestinal pathogenic *E. coli* (ExPEC) factor for virulence. ExPEC diverge from their commensal cohorts, taking on a more pathogenic nature and the ability to cause serious disease both within the intestinal tract and elsewhere within the host (30, 43). On the contrary, if evidence of pUTI89 is only found in UPEC, then it can be identified as a urovirulence factor. A urovirulence factor implies the presence of genes on pUTI89 in the majority of UPEC isolates potentiating the development of a common target for therapeutics.

The mouse cystitis model was used to determine that pUTI89 contains genes encoding one or more virulence factors. It was shown that pUTI89 enhances survival early in infection, however, normal infection levels were restored within 24 hours of infection. Binding and invasion was reduced in the absence of pUTI89. The *cjr* operon encoding CjrA, CjrB and CjrC was partially implicated in the observed defect. In EIEC, CjrA is an inner membrane protein homologous to PhuW of *Pseudomonas aeruginosa* with unknown function, CjrB is homologous to the TonB protein which is involved in energetic transfer between the inner and outer membranes, and CjrC is homologous to putative outer membrane siderophore receptors (44). Located upstream of the *cjr* operon is a *fur* box implying regulation by iron. Overlapping the *cjrC* gene is the *senB* gene which encodes for an enterotoxin that accounts for 50% of the enterotoxic activity in EIEC strain, EI34 (38). Further work needs to be done to complement this operon and see a restoration of infection. Outer membrane proteins can be difficult to complement since over expression can lead to cell lysis, thus a low copy or inducible plasmid is important for successful complementation. After successful complementation, the expression pattern of the *cjr* operon should be evaluated to determine if and when these

proteins are expressed. It would be useful to see if their expression profile changes during different points of the UPEC pathogenic pathway, for example in intracellular or extracellular survival. Iron acquisition is essential to bacteria residing within the urinary tract (23, 41) thus this operon regulated by the *fur* box is very likely to be expressed in iron limiting conditions such as the urinary tract. Perhaps Cjr proteins are expressed early in infection whereas other iron acquisition systems are expressed later, potentially explaining the delayed growth *in vivo* in the absence of the Cjr proteins until more systems are turned on.

Immune response in the absence of pUTI89

It is clear that the immune response elicited by the host, and the behavior of the bacteria in response to it, go hand in hand. UPEC invade to avoid expulsion from the sheer forces present during urination as well as avoid attack from neutrophils and macrophages (37). When extracellular, UPEC filament to prevent neutrophil engulfment (29). Additionally, UPEC dampen the IL-6 response mounted by the host relative to K-12 *E. coli* (27). There are a multitude of other mechanisms that UPEC use to evade the immune response, thus, due to the necessity of these evasion mechanisms, it is likely that pUTI89 may play a role in immune evasion. However, it is extremely likely that immune evasion mechanisms are redundant, thus may not be recognized in a pUTI89 knock-out strain. Measurement of 12 cytokine levels in the bladder of UTI89-infected and Δ pUTI89-infected bladders at 6 hours post-infection revealed no significant difference in cytokine levels (Figure 3). Thus, either there are no immune evasion mechanisms on pUTI89 or the immune evasion mechanisms are redundant on the chromosome. Deciphering between these two hypotheses will be difficult to do.

Functional tra operon

As mentioned above, pUTI89 essentially has two regions; one region contains genes involved in conjugative DNA transfer and the other region contains genes found on virulence plasmids or in other virulent bacteria. Since the *tra* operon makes up such a large portion of pUTI89, it is important to understand if it is functional. Additionally, conjugative F plasmids promote biofilm formation perhaps through stimulating synthesis of colanic acid and curli (19, 35). The *tra* operon promotes transfer of DNA which can aid in adaptability of bacteria to a certain niche through uptake of genes needed to overcome environmental restrictions for survival and replication (21). Thus, perhaps commensal *E. coli* can become extraintestinal pathogenic *E. coli* (ExPEC) through the uptake of DNA by conjugation implying that the conjugation machinery are important in making virulent bacteria within the gastrointestinal (GI) tract. It is easy to see how these functions would benefit UPEC. Not only do they form biofilm-like structures in the bladder, but they also must survive in a harsh niche within the urinary tract, both extracellularly and intracellularly.

From plasmid purification and PCR methods, 6 of the 18 UPEC clinical isolates had no evidence of pUTI89. In order to confirm functionality of the *tra* operon on pUTI89, pUTI89 was mated into strains containing no evidence of pUTI89. To do this, a kanamycin cassette was inserted on pUTI89 and a spectinomycin cassette was transduced onto the chromosome of the clinical isolates. Three clinical isolates were successfully transduced with the Spec cassette and all three were recipients of pUTI89 upon plate mating. Mating efficiencies ranged from 2×10^{-10} to 3×10^{-4} . The reception of pUTI89 by clinical isolates not only shows the *tra* operon is functional it also shows that pUTI89 is expressed *in vitro*. While this confirms that the *tra* operon is expressed and functional, it does not evaluate its potential role in virulence.

As a surrogate for IBC formation, which resembles intracellular biofilms, biofilm formation was evaluated. Since the nutrients within the intracellular environment are not entirely known, biofilm was grown in minimal and rich media in an effort to mimic the conditions *in vivo*. Growth in minimal or rich media was equivalent in the clinical isolate relative to its pUTI89-containing counterpart as was biofilm formation (Figure 4). Since lack of pUTI89 does not affect biofilm formation in UTI89, it is not surprising that addition of pUTI89 to clinical isolates does not enhance biofilm formation. However, lack of pUTI89 does affect colonization at 6 hours post-infection, which begs the question, does addition of pUTI89 to clinical isolates enhance colonization at 6 hours post-infection? C3H/HeN female mice were infected with each clinical isolate and its pUTI89-plus counterpart and bacterial load was determined at 6 h, 24 h and 2 wk post-infection. There was no significant difference in bacterial load in the bladder at 6 hours post-infection in the clinical isolates versus its pUTI89-plus counterpart, only acute3 + pUTI89 was close to being significant relative to acute3 (Figure 5). Additionally, there was no difference in bacterial titers of the clinical isolates with and without pUTI89 at 24 hours or 2 weeks post-infection as was seen with UTI89 in the presence and absence of pUTI89. There does not seem to be a gain of function effect on the clinical isolates with pUTI89. However, it is extremely possible that some of the genes on pUTI89 are present on the chromosome of the clinical isolates since PCR for pUTI89 only tested for 8 small regions. Since these genes are already present within the genome of the clinical isolate, adding a second copy from pUTI89 does not, therefore, enhance infection. Since the *cjr* operon has been implicated in virulence in UTI89, one can now test each clinical isolate for the presence of that specific operon. In fact, nearly 50% of the clinical isolates tested positive for the *senB* gene found in the *cjr* operon, implying its role in virulence. Future investigation is needed to evaluate IBC formation, filament formation and binding and

invasion in clinical isolates conjugated with pUTI89 to determine if pUTI89 is important in other UPEC isolates.

pUTI89 has an effect on chromosomal genes

Yersinia pestis, enteropathogenic *E. coli* (EPEC), *Bacillus anthracis* and *Chlamydia trachomatis* all were shown to have chromosomally encoded genes that are regulated by plasmid-encoded loci (5, 8, 11, 40). We sought to determine whether chromosomally encoded genes were affected by the loss of pUTI89. Microarray and 2D gel analysis were used to identify if the altered regulation is at the transcriptional and/or translational level. For microarray analysis, we chose to examine bacteria from cultures grown for inoculation into the murine cystitis model, as we are unable to isolate enough bacterial RNA from infected bladders. All results presented were obtained from three independent culture replicates (biological) consisting of three replicates (experimental) of UTI89 and Δ pUTI89. Principal-component analysis demonstrated a high degree of replicate grouping. Only those genes that were significantly different were graphed. 76 plasmid genes showed greater than two-fold transcript differential (Figure 6). Interestingly, *repB*, *rsvB*, *stbA* and *stbB* were all extremely down in Δ pUTI89 versus UTI89 suggesting that they are on during growth in wild-type bacteria. Considering these genes are involved in plasmid replication and stability it implies the plasmid is expressed *in vitro*. Furthermore, *UP060*, *UP061*, *UP097* and *UP141* were all extremely down suggesting that they are highly expressed in wild-type *in vitro*. These genes are hypothetical and will require further investigation to determine their function. Of all the genes on the chromosome, only 24 were significantly different in the absence of pUTI89 (Figure 7) and 14 showed greater than two-fold transcript differential. Seven genes were extremely downregulated in the absence of pUTI89: *yccB*, *UC1727*, *ydiA*, *ydjA*, *c2508*, *ygeA*, *ygfA* and *yhfA* (Table 1). Again all of these are hypothetical and will require

further examination. The caveat of this work is that RNA was isolated from cultures grown *in vitro*, while the Δ pUTI89 phenotype was only observed *in vivo*. These data suggest that pUTI89 functions in *trans* to regulate the transcription of multiple chromosomal genes. Their role in pathogenesis is the study of future work.

This work has demonstrated that pUTI89 increases the ability of UTI89 to invade and colonize the bladder. Additionally, it aids in understanding why UPEC genomes are mosaic. Perhaps these F-like plasmids are shaping UPEC isolates by facilitating frequent genomic acquisition, loss and rearrangement. pUTI89-like plasmids could explain why there is not a list of definitive virulence factors that define an isolate as UPEC (33). A greater understanding and characterization of these types of plasmids from different UPEC could facilitate the understanding of their mechanism of virulence and their evolution, and the design of efficacious strategies to fight UTI.

Type 1 pili as a virulence factor

Type 1 pili are essential cystitis virulence determinants (4, 34, 37, 48). FimH, located at the tip of type 1 pili, is the essential adhesive domain for binding to mannose on uroplakins on the surface of bladder epithelial (urothelial) cells. In the absence of type 1 pili or FimH bacteria are non-invasive, unable to persist in the bladder and are eliminated by the host. Thus, while there are many other virulence factors involved in infection such as capsule, siderophores, flagella and certain toxins, type 1 pili are absolutely required to initiate infection. After infection is initiated by type 1 pili, factors downstream perpetuate and maintain the infection within the host.

Sequencing of over 300 *fimH* genes from UPEC has revealed that the mannose binding pocket is invariant (12). However, amino acids outside the binding pocket vary and four residues, 27, 62, 66 and 163, are positively selected in UPEC FimH (Figure 8). Their role in infection is yet undiscovered, but suggests that there is more to FimH than

just its ability to bind mannose. Alignment of the FimH sequences from the panel of 18 clinical isolates previously studied identified the residues differing from UTI89 FimH (Table 2). Since the panel of clinical isolates has been characterized in the mouse, we used them to determine the role of these positively selected amino acids and, specifically, their role in IBC formation. We hoped to identify if genetic background plays a role or if FimH is the determinant virulence factor for IBC formation. Based on the confocal microscopy results from Garofalo *et al.* (18), those isolates that did poor *in vivo* were used for IBC quantification by LacZ staining (Figure 9). Five of the 7 isolates that were poor IBC-formers had a valine at position 27 instead of an alanine as in UTI89 FimH. Thus, it seems that this residue may be important to IBC formation and/or colonization of the bladder. We hypothesized that UTI89 FimH in place of clinical isolate FimH will result in enhanced IBC formation and colonization. The isolates that were poor IBC formers or did not form IBCs were manipulated to contain the FimH of UTI89 in place of their FimH on the chromosome, thus under the same regulation. Thus far, one isolate, acute4, was manipulated to contain UTI89 FimH. IBC quantification revealed that IBCs were not observed in either acute4 or acute4 + UTI89 FimH (Figure 10A) suggesting genetic background does play a role in IBC formation. However, bacterial titers revealed that while there was no difference at 6 hours post-infection, there was a significant difference at 24 hours post-infection, with acute4 + UTI89 FimH colonizing nearly 3 logs better than acute4 (Figure 10B). This suggests that FimH is involved in more than IBC formation. Future studies are needed to identify its role in infection outside of mannose binding. It was shown that FimH is a potent inducer of innate antimicrobial responses through direct binding of TLR4 resulting in the production of type 1 interferon (3). It is possible that FimH is modulating the immune system to facilitate successful colonization of the bladder. Evaluating the immune response elicited by the host to acute4 and acute4 + UTI89 FimH could address this question. Or perhaps FimH

makes contact with a secondary receptor outside of its binding pocket to enhance invasion. Since, in acute4, UTI89 FimH still did not result in IBCs, we can take advantage of this to find other factors involved in IBC formation. If acute4 is lacking an essential factor for IBC formation, transformation with UTI89 fosmid library could result in IBC formation. We can then identify the gene(s) involved in IBC formation. If acute4 possesses a factor that is preventing IBC formation, a transposon mutagenesis could identify a region that is inhibitory for IBCs. Furthermore, acute4 was unable to form IBCs so if we put UTI89 FimH into an IBC-competent strain that made IBCs at low numbers such as rUTI3 or acute3 perhaps we can enhance IBC formation. This would suggest that if an isolate has all the capabilities to make an IBC, FimH makes the process much more efficient.

This work has shown that there is more to FimH than mannose binding. Residues outside the pocket are positively selected in UPEC suggesting an important role in infection. Additionally, UTI89 FimH in acute4 increased colonization without IBC formation. Thus, while it is known that type 1 pili are essential for robust UTI, it is not known what additional role type 1 pili plays outside of binding and invasion. While one study showed that type 1 pili are expressed inside the IBCs (47), future work is needed to identify the additional functions of FimH in UTIs. Regardless of the additional function of FimH, it is clear that it is essential for UTI. Thus, therapeutics are needed to eliminate binding of UPEC to the urothelium. They have the potential to eliminate this extremely common disease.

Treatment of UTIs

Urinary tract infections (UTIs) are one of the most common bacterial infections in industrialized countries and impose a significant financial burden based on physician visits and treatment (17). Posing an even greater threat is the high incidence of

recurrence. Nearly 50% of women who get a UTI will get a recurrence. Thus, treatments that can block a UTI or stop frequent recurrences would be extremely beneficial to women and the burden UTIs place on society. Currently, antibiotics are available to treat UTIs, however resistance is rapidly arising. Thus, new strategies must target virulence factors rather than essential growth factors of the bacteria preventing selection that requires the bacteria to either evolve or die. Bacterial colonization begins with adherence to host cells. Disrupting adherence to host cells is an excellent new strategy for anti-virulence therapeutics. The lack of adherence and subsequent colonization will give the host time to eliminate the bacteria prior to establishing a foothold. Strategies to eliminate adhesion involve eliminating pilus function and biogenesis through carbohydrate mimics and chaperone-ushe assembly disruptors. This general strategy is described in Appendix 1. Instead, this section will focus specifically on the inhibition of type 1 pili in UTI.

Mannosides

The first strategy involves inhibiting binding to host cells by blocking the mannose binding pocket on FimH. Based on our extensive elucidation of the UPEC pathogenic cascade, we have identified critical nodes in pathogenesis that mannosides would target and thereby have powerful and potent therapeutic ramifications. The first step in the UPEC pathway involves FimH-mediated colonization of the bladder epithelium via the recognition of mannose receptors. Bacterial invasion into superficial bladder umbrella cells can then ensue. By preventing bacterial attachment, mannosides will also inhibit the subsequent invasion of bacteria into the bladder epithelial cells. Crystallization of FimH has facilitated a precise understanding of how mannose binds to FimH and the interactions that result in high affinity binding (26). We can therefore take advantage of our knowledge of the interactions between mannose and FimH to develop new

therapeutics. Pre-incubation of bacteria with heptyl mannose resulted in significant reduction in bacterial load in the murine bladder (46). These results identify mannose derivatives as a potential therapeutic against UTIs. We can now develop more potent inhibitors based on the success of heptyl mannose.

Mannoside inhibitors were first examined *in vitro*. Two FimH function assays were used to screen mannosides for inhibitory function; (i) hemagglutination of guinea pig red blood cells by type 1 piliated UPEC and (ii) a type 1 dependent biofilm assay. These assays have shown that 23 of 37 currently synthesized and tested compounds are more potent inhibitors of HA titer and biofilm formation than anything commercially available and previously tested, some by as much as 2 logs (Table 3). Future studies will use a more rigorous assay to test the ability of the strongest inhibitory mannoside derivatives to reverse hemagglutination of guinea pig red blood cells and to disrupt preformed type 1 dependent biofilms. The most potent compounds will be subjected to crystallography to better understand their increased activity and to inform further chemical synthesis of even better inhibitory compounds. Further, a fluorescent polarization assay has been developed and miniaturized to monitor the direct binding of a synthesized fluorescently labeled butyl mannose derivative to the FimH receptor as well as competitive displacement by other synthetic mannosides. This fluorescent polarization assay provides a rapid method for monitoring improvements to receptor affinity during the synthetic process, as well as providing K_d binding affinity measurements.

After *in vitro* examination, the most potent mannosides were tested *in vivo*. Utilizing a well-established gentamicin protection assay to determine the lumenally bound fraction versus the intracellular fraction, there was a significant reduction in intracellular bacteria at 1 hour post-infection in the presence of mannosides ZFH177 and ZFH253

(Figure 11), arguing that the mannosides are disrupting specific type 1-mediated binding required for subsequent invasion. It is not clear why a reduction was not observed in the luminal UPEC population. This may be due to contamination from bacteria in the urine or bacteria that are non-specifically associated with the epithelium. In any case, blocking invasion blocks the ability of the bacteria to rapidly expand in numbers. This is due to the ability of the mannosides to block the IBC mechanism. After invasion, UPEC are able to rapidly replicate to form IBCs, thus dramatically expanding in numbers. The ability of mannosides to block IBC formation was evaluated based on LacZ staining of whole mount bladders to enumerate IBCs. Whole bladder titers were also determined by quantifying colony forming units (CFUs) at 6 hours post-infection and later time points. In the presence of mannosides ZFH177 and ZFH253 there was a significant decrease in IBCs observed 6 hours post-infection at concentrations as low as 0.1 mM and almost no IBCs observed at 1 mM mannoside (Figure 12A). A significant decrease was also seen in CFUs at 6 hours post-infection with 1 mM ZFH177 and ZFH253 (Figure 12B). These results strongly argue that the mannosides are able to inhibit first round IBC formation by preventing FimH-mediated binding and invasion into the bladder epithelial cells. The success of these experiments lead us to believe that these compounds will have dramatic potential as potent therapeutics for treating UTI.

Pilicides

The second strategy to inhibit pilus mediated adhesion is to disrupt chaperone/usher pilus assembly using compounds termed pilicides. A pilicide that inhibits the production of type 1 pili has a powerful potential as a non-antibiotic therapeutic and such compounds will become more necessary in the face of antibiotic resistance. Ring-fused 2-pyridones can be found in many biologically active compounds and natural products ranging from the multi-fused natural product Nauclefine and

Camptothecin (a potent anti-cancer drug) to bicyclic systems like the 2-pyridone acid A58365A (an Angiotensin-Converting Enzyme (ACE) inhibitor at nM concentrations) (2, 13, 31) (Figure 13). Thiazolo ring-fused 2-pyridones are highly useful as scaffolds for the development of compounds that inhibit protein-protein interactions in bacteria (1, 39, 45) and we have already produced more than 250 of these compounds with a variety of R group constituents (Figure 13). We have done limited screening on a subset of the available compounds and have identified compounds we call “pilicides” that bind to the chaperone to inhibit its function. Future work continues to screen these compounds to identify ones that hold promise as potential novel antibacterial agents that target bacterial virulence. We have performed limited analysis on a subset of compounds in the library and showed that many of these compounds affected type 1 piliation in HA and biofilm assays. Continued research is need to perform extensive studies on the entire library of compounds, screening for inhibitory activity in type 1 dependent biofilms and HA assays.

We have assessed the ability of the best pilicides, discovered above, to treat or prevent UTI in the murine model. UTI89 is grown in the presence of the pilicide prior to inoculation into the bladders of mice. In the presence of the pilicide FN075, UPEC colonization and invasion in the murine mouse model as measured by bacterial load and IBC formation was severely attenuated thus potentiating the therapeutic potential of pilicides (Figure 14). This experiment confirmed that pilicide FN075 treatment inhibited IBC formation and thus colonization of the murine bladder thus attenuating virulence. Future investigation is required to assess the ability of pilicides to function during infections.

Preliminary studies have revealed that mannosides and pilicides are effective at reducing infection *in vivo*. However, many studies remain to prove their efficacy within a

more clinically relevant setting of UTI. First, studies are needed to evaluate the bioavailability and toxicity of these compounds. It needs to be determined the best method of delivery, oral, IP or IV, to obtain high levels of intact compound in the bladder without detrimental effects to the mouse as measured by weight loss and survival. We have shown that 1 to 0.1 mM of mannoside is needed to inhibit infection, thus, it needs to be determined if it is possible to achieve this level of mannoside within the bladder. However, we have yet to examine synergistic effects of these compounds. Perhaps in the presence of mannoside and pilicide, less compound will be needed to successfully inhibit UTI. One could imagine the mannoside first occupying the FimH mannose binding pocket and preventing initial binding, while the pilicide crosses the membrane and prevents future pilus synthesis, thus allowing the bacteria to be excreted in the urine or phagocytosed by macrophages. Additionally, reduced amounts of antibiotics could be added to further lower the dose required to inhibit bacterial colonization thus reducing the selective pressure for resistance. Once bioavailability and toxicity have been determined, a more clinically relevant situation can be evaluated by treating a pre-existing UTI with compound and see if the infection can be eliminated. Future studies are needed to evaluate the dose, frequency and time of treatments post-infection. Additionally, the prophylactic ability of mannoside could be evaluated to determine if this could be a daily supplement for women who suffer frequent recurrent UTIs.

Clearly there is a lot of work left to do to determine the efficacy of mannosides and pilicides. However, these anti-virulence therapeutics have numerous attractive qualities. There is less selective pressure for the bacteria to evolve resulting in resistance since unlike traditional antibiotics they do not target essential growth factors of the bacteria. Additionally, these therapeutics will leave the commensal bacteria unperturbed. Loss of commensal gut isolates upon treatment with antibiotics usually

results in side effects including diarrhea and secondary opportunistic infections, such as yeast infections. Furthermore, since chaperone/usher systems are numerous to a multitude of Gram-negative pathogens, these strategies can be applied to a multitude of pathogens. Adhesion is the first step in nearly every bacterial infection, thus a ligand-based approach, such as the mannosides, to infection inhibition could translate to an even greater expanse of pathogens encompassing Gram-positives as well. In fact, exogenous sugars have proved efficacious at inhibiting adhesion of *Pseudomonas aeruginosa*, *Staphylococcus* and *Streptococcus in vitro* (32, 36). The development of anti-virulence therapeutics indicates a paradigm shift in the understanding of bacterial pathogens and their interactions with the host and environment. A multitude of virulence factors in addition to adherence are being targeted such as capsule, flagella, siderophores, toxins, type III secretion systems (TTSS) and virulence gene regulation. Vigilance and basic research in the understanding of basic processes associated with bacterial virulence is the only way to continue the development of novel and effective therapeutics.

Concluding remarks

In summary, this thesis work set out to better understand the pathogenesis of UPEC in the urinary tract to facilitate the development of new anti-virulence therapeutics. Prior studies have revealed that UPEC employs a complex developmental process in mice, initiated by the intimate contacts between the pathogen adhesive organelles and the host epithelium, to successfully colonize and persist within the harsh environment of the urinary tract. The IBC pathogenic pathway is critical in the ability of UPEC to cause UTI and interferences at any step in this pathogenic cycle could alter the infection course. This thesis extends our knowledge of the IBC pathogenic pathway in three

important ways. First, this study has demonstrated the commonality of the IBC pathway implying its relevance to UPEC and identifying that targets against this pathway will target a multitude of UPEC isolates. Second, this work identified a virulence plasmid that enhances early events in UTI89 infection and its *tra* operon may contribute to the mosaic nature of the UPEC genome by allowing uptake, deletion and rearrangement of genes throughout the genome. Third, based on the ubiquitous and essential qualities of FimH, this work identified novel anti-virulence therapeutics targeted at adhesion disruption. These findings indicate the importance of thoroughly understanding the mechanisms that underlie this process and how these differ among UPEC. These discoveries alter the current paradigm of bacterial pathogenesis in the urinary tract and could ultimately lead to better treatment modalities for patients suffering UTIs.

Table 1. Chromosomal genes demonstrating a twofold or greater transcript differential via microarray analysis^a

Gene	ORF	Fold change ^b
hypothetical	UTI89_C1048	-458.7
hypothetical	UTI89_C3298	-140.7
hypothetical	UTI89_C1896	-130.8
hypothetical	UTI89_C3859	-69.5
hypothetical yfaQ precursor	UTI89_C2508	-43.3
hypothetical	UTI89_C3244	-23.2
conserved protein YdjA	UTI89_C1960	-14.5
hypothetical	UTI89_C4976	-4.7
hypothetical	UTI89_C1130	-3.0
outer membrane heme/hemoglobin receptor	UTI89_C1129	-2.6
lambdoid prophage Qin tail fiber assembly protein-like protein	UTI89_C0564	-2.4
hypothetical	UTI89_C0954	2.5
bacteriophage ST64T antitermination protein gp23	UTI89_C2663	2.8
hypothetical	UTI89_C1727	6.9

^aGene transcripts passing all statistical and quality tests performed

^bChange in ΔpUTI89 signal compared to UTI89 signal.

Table 2. Alignment of FimH sequences

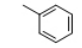
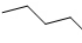
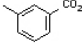
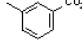
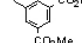
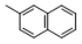
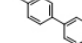
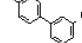
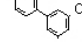
Strain	Position														IBCs present (hrs PI)
	9	27	62	66	70	78	106	117	163	166	195	106	269		
ASB1	T	A	S	G	S	N	A	G	V	R	Y	N	Q	6,24	
ASB2	T	A	S	G	N	N	A	G	V	R	Y	N	Q	6,24	
ASB3	T	A	S	G	N	S	A	G	V	H	Y	N	Q	6,24	
ASB4	T	A	S	G	N	S	T	G	V	R	Y	N	Q	6	
ASB5	T	V	S	G	S	N	A	G	V	R	Y	N	Q	24 (rare)	
acute1	T	V	S	G	N	S	A	G	V	R	Y	N	Q	12 (rare)	
acute2	T	A	S	G	N	S	A	G	V	R	F	N	Q	6 (rare)	
acute3	T	V	S	G	N	S	A	G	V	R	Y	N	Q	3 (rare)	
acute4	T	A	S	S	S	N	A	G	V	R	Y	N	Q	-	
rUTI1	A	A	S	G	N	S	A	R	V	R	F	S	Q	-	
rUTI2	T	A	S	G	N	S	A	G	V	R	Y	N	K	6	
rUTI3	T	V	S	G	N	S	A	G	V	R	Y	N	Q	6 (few)	
rUTI4	T	A	S	G	S	N	A	G	A	R	Y	N	Q	24	
rUTI5	T	A	S	G	S	N	A	G	V	R	Y	N	Q	3	
pyelo1	T	A	S	C	N	S	A	G	V	R	Y	N	K	6	
pyelo2	T	A	S	G	N	S	A	G	V	R	Y	N	Q	6	
pyelo3	T	V	S	G	N	S	A	G	V	R	Y	N	Q	-	
pyelo4	T	A	S	G	S	N	A	G	V	R	Y	N	Q	6	
UTI89	T	A	A	G	S	N	A	G	V	R	Y	N	Q	3,6,24	

Highlighted residues differ from UTI89 residues

Only residues that differ from UTI89 are shown

Bolded residues were identified as positively selected for in UPEC

Table 3. Structure Activity Relationship

Compound	R	HA Titer (μM)	Biofilm IC ₅₀ [calculated] (approximated) μM
Phenyl- α -D-mannoside		30	(~100)
1ZFH84		125	(~500)
1ZFH101		6	[15.0]
1ZFH216		60	
1ZFH177		1.5	[1.9]
1ZFH185		6	
1ZFH279		8	
1ZFH253		1	[0.5]
1ZFH296		0.25	[0.3]

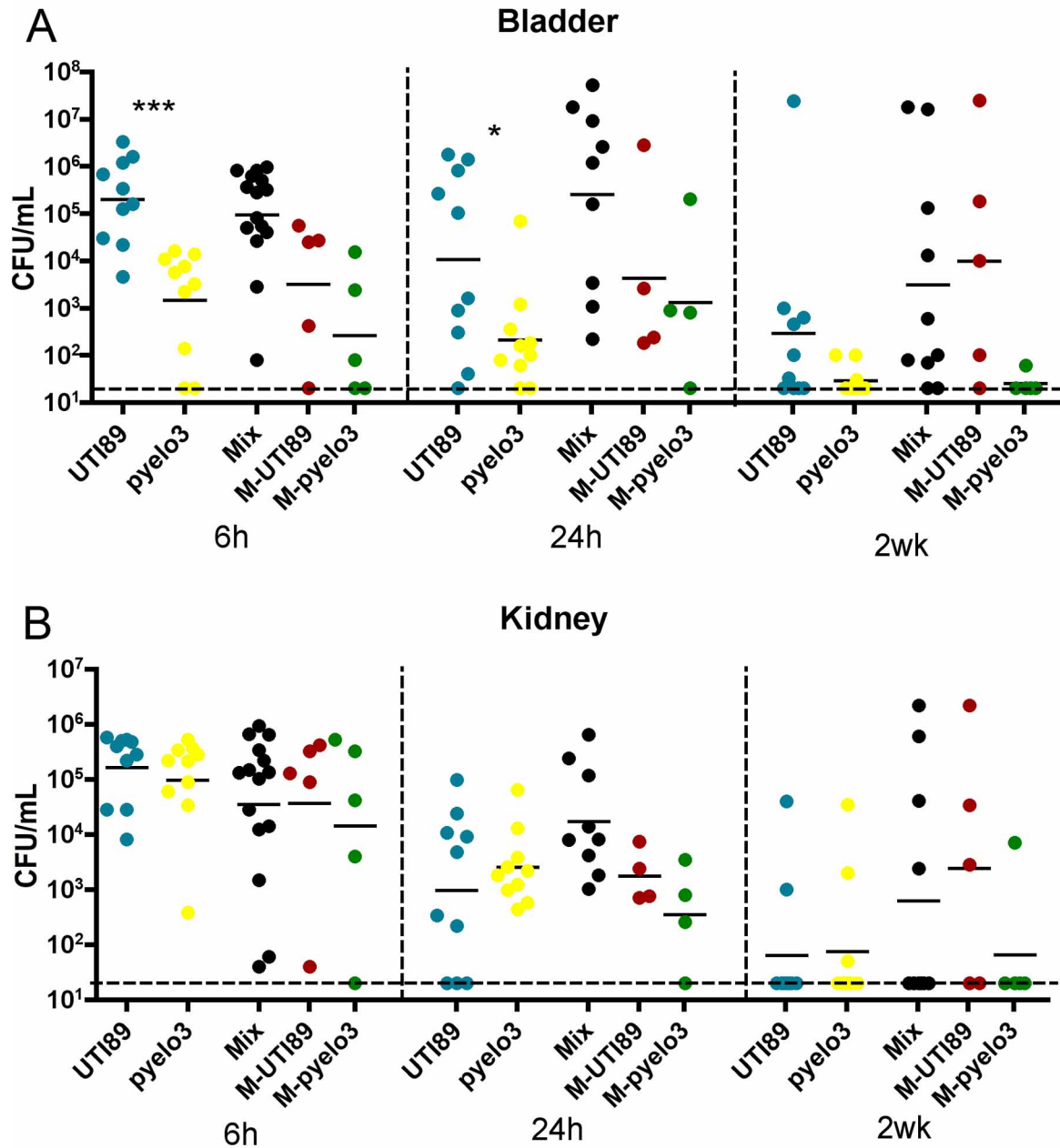


Figure 1. Bacterial load in the bladder and kidney of UTI89 and pyelo3 in single and mixed infections. (A) At 6h and 24h post-infection, bacterial load was significantly lower in the pyelo3-infected bladders than in the UTI89-infected bladders (** $p < 0.001$ and * $p < 0.05$ by Mann-Whitney). Total titers in the mixed infection more closely resembled UTI89 infected bladders. (B) There was no significant difference at any timepoint between any infection in the kidneys.

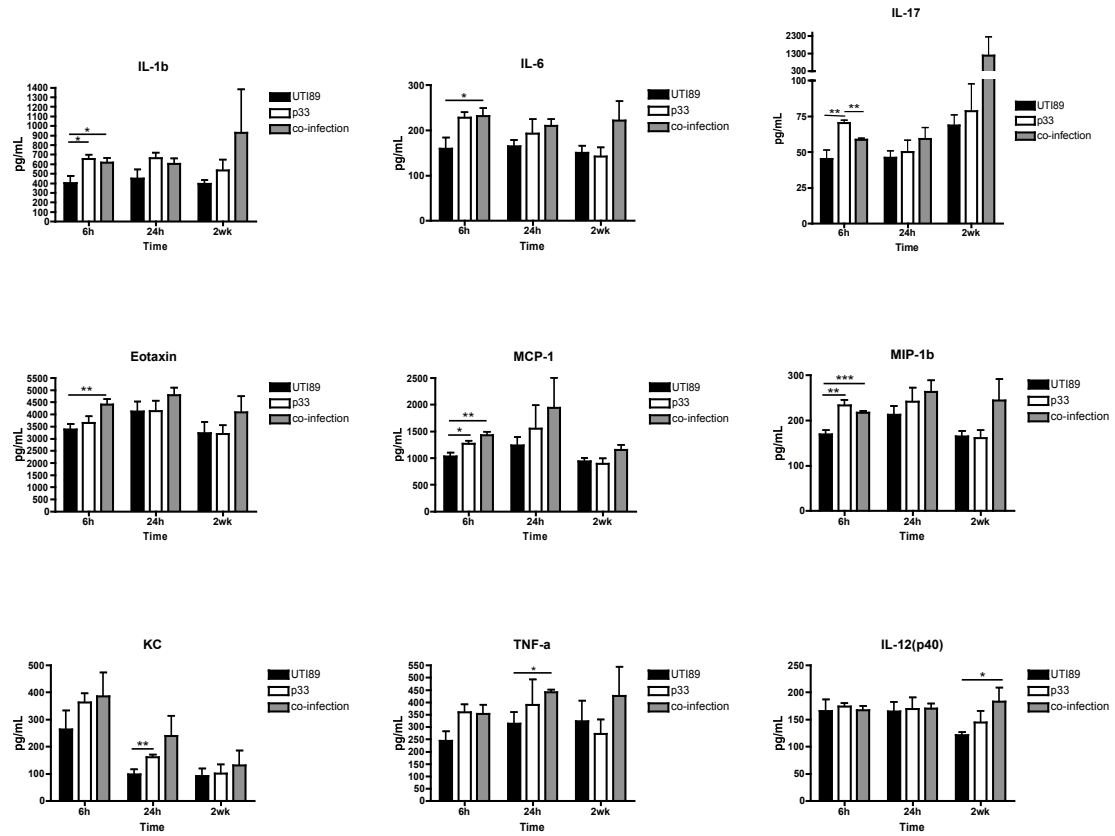


Figure 2. Cytokine levels in the kidney of UTI89, pyelo3 and co-infections.

Cytokines IL-1 β , IL-6, MCP-1 and MIP-1 β were elevated in pyelo3- and co-infected kidneys relative to UTI89-infected kidneys. Thus, co-infection immune response more closely mimics pyelo3 immune response.

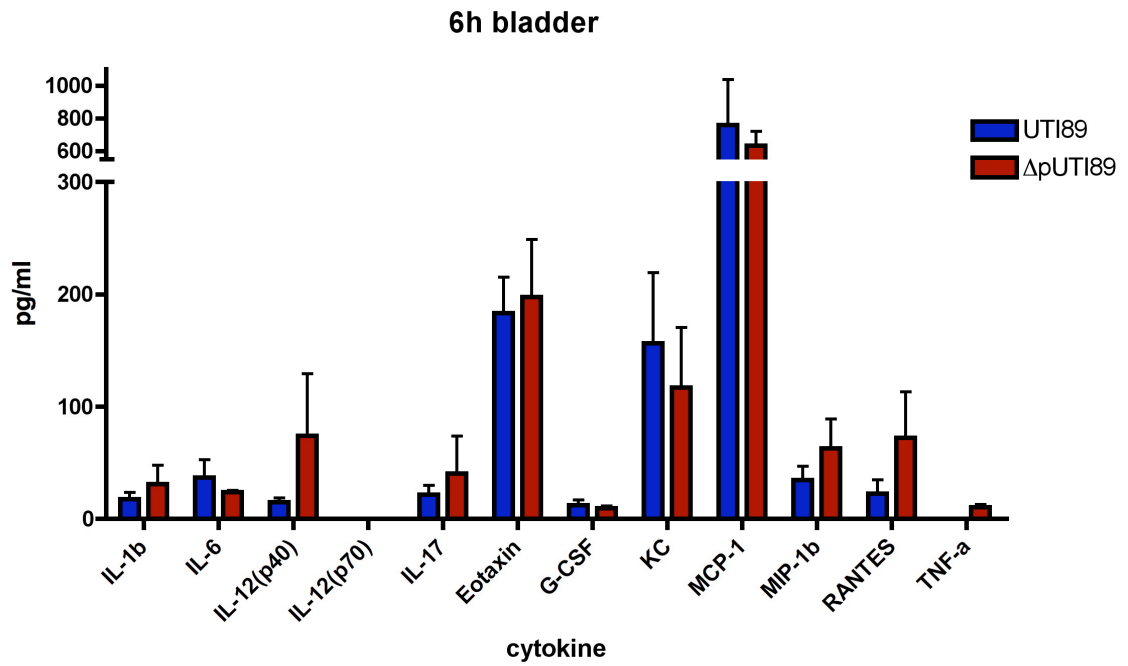


Figure 3. Immune response at 6h in UTI89 and Δ pUTI89 infected bladders. There was no significant difference among any of the cytokines tested in UTI89-infected versus Δ pUTI89-infected bladders.

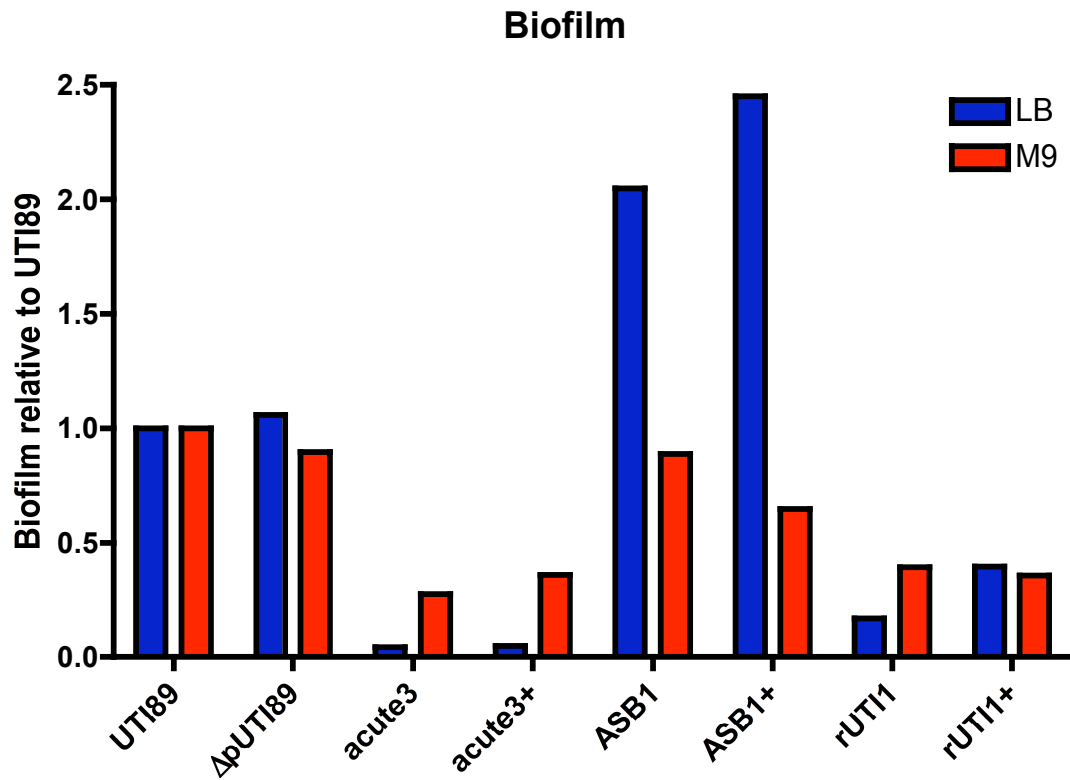


Figure 4. Biofilm formation in the presence or absence of pUTI89. Blue bars represent biofilm formed in LB and red bars represent biofilm formed in M9 + 10 μ g/ml niacin. Acute3+, ASB1+ and rUTI+ all represent strains that have received pUTI89. In the presence of pUTI89 there was difference in biofilm formation in LB or M9 media. Additionally, there was no difference in biofilm formation in either media in the absence of pUTI89 from UTI89.

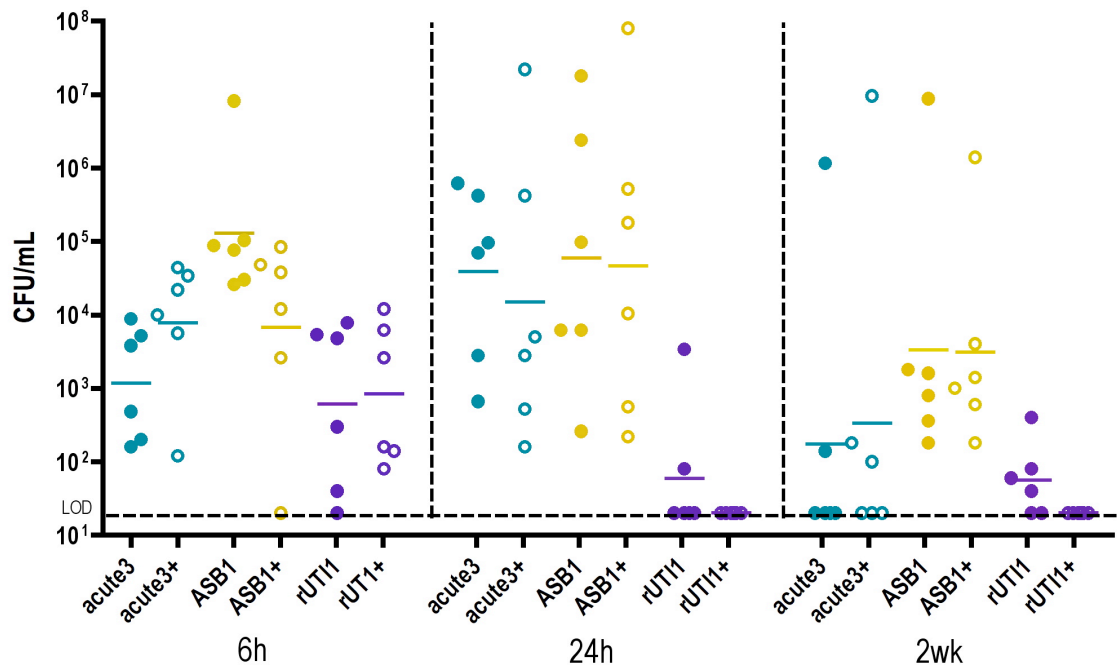


Figure 5. Bacterial load in the bladder of clinical isolates with and without pUTI89.

Acute3+, ASB1+ and rUTI1+ represent strains that received pUTI89. At 6 h, 24 h, and 2 wk post-infection there was no significant difference in bacterial load of each isolate with their pUTI89+ counterpart.

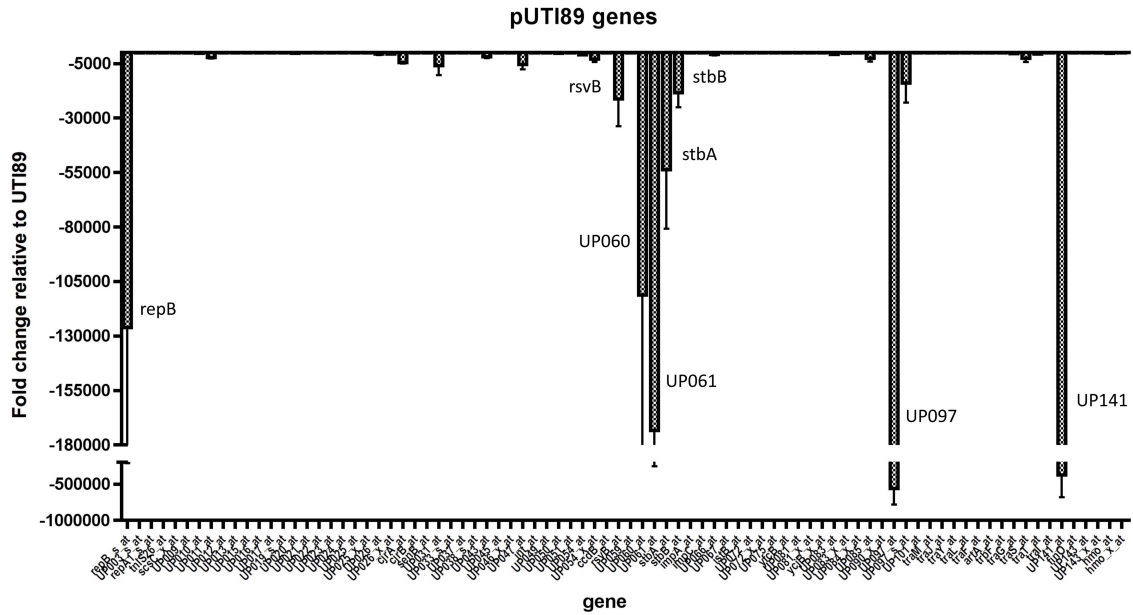


Figure 6. Plasmid genes demonstrating greater than two-fold change in Δ pUTI89 signal compared UTI89 signal. *repB*, *rsvB*, *stbA* and *stbB* were all down suggesting they are expressed *in vitro* and encode plasmid replication and maintenance proteins. *UP060*, *UP061*, *UP097* and *UP141* were also down suggesting their expression *in vitro* and are all hypothetical proteins requiring further study.

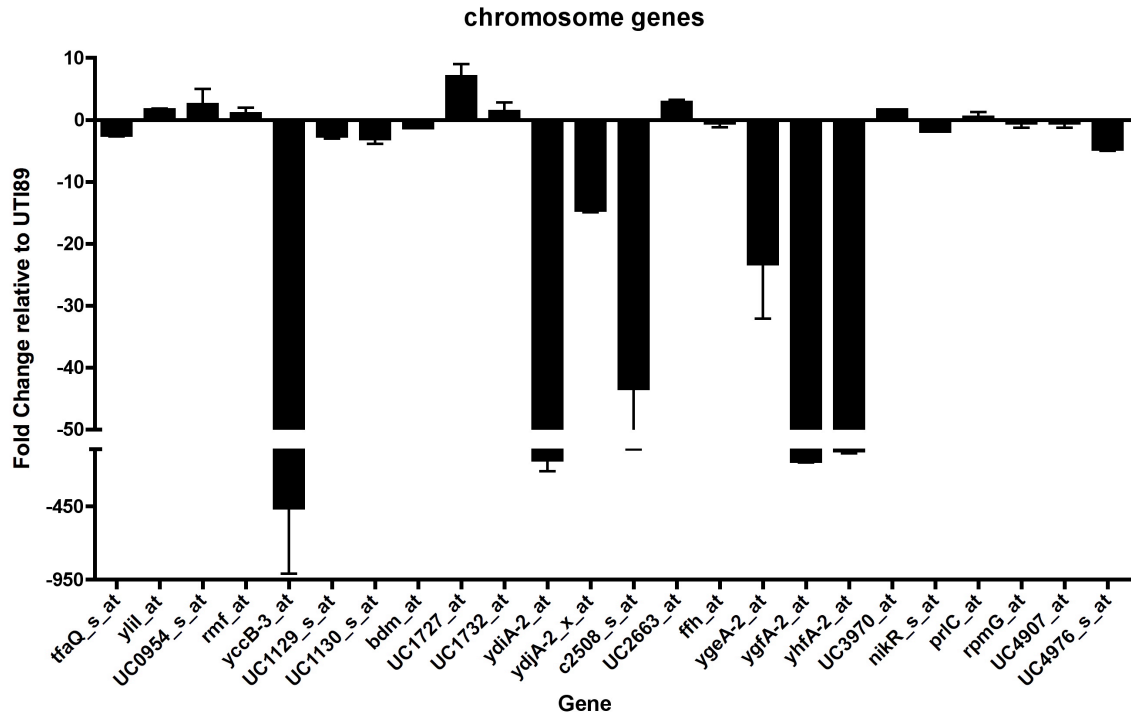


Figure 7. Chromosomal genes demonstrating greater than two-fold change in Δ pUTI89 signal compared UTI89 signal. In the absence of pUTI89 24 chromosomal genes showed significantly altered regulation. The most significantly different expression levels were down in the absence of pUTI89.

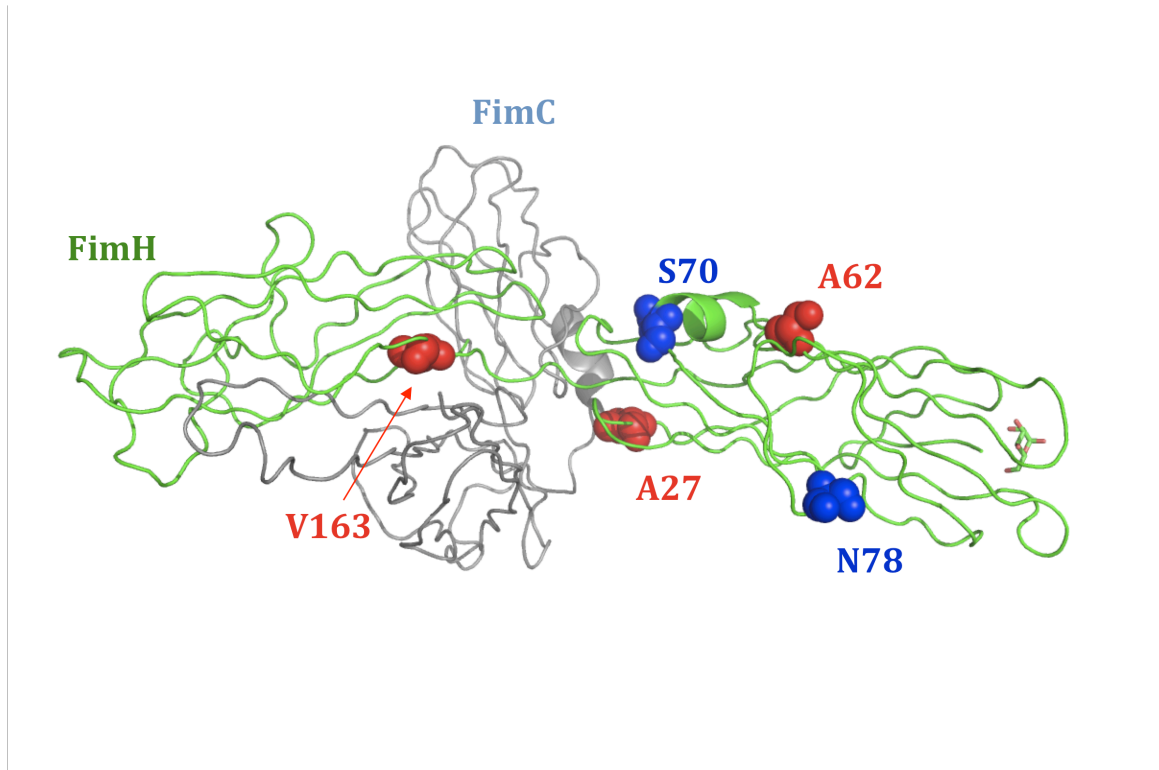


Figure 8. FimH residues under positive selection. FimH is in green and FimC (the chaperone) is in gray. In red are residues under positive selection. In blue are residues not under selection. Mannose is bound at the tip of FimH. All of the positively selected residues are located outside the mannose-binding pocket.

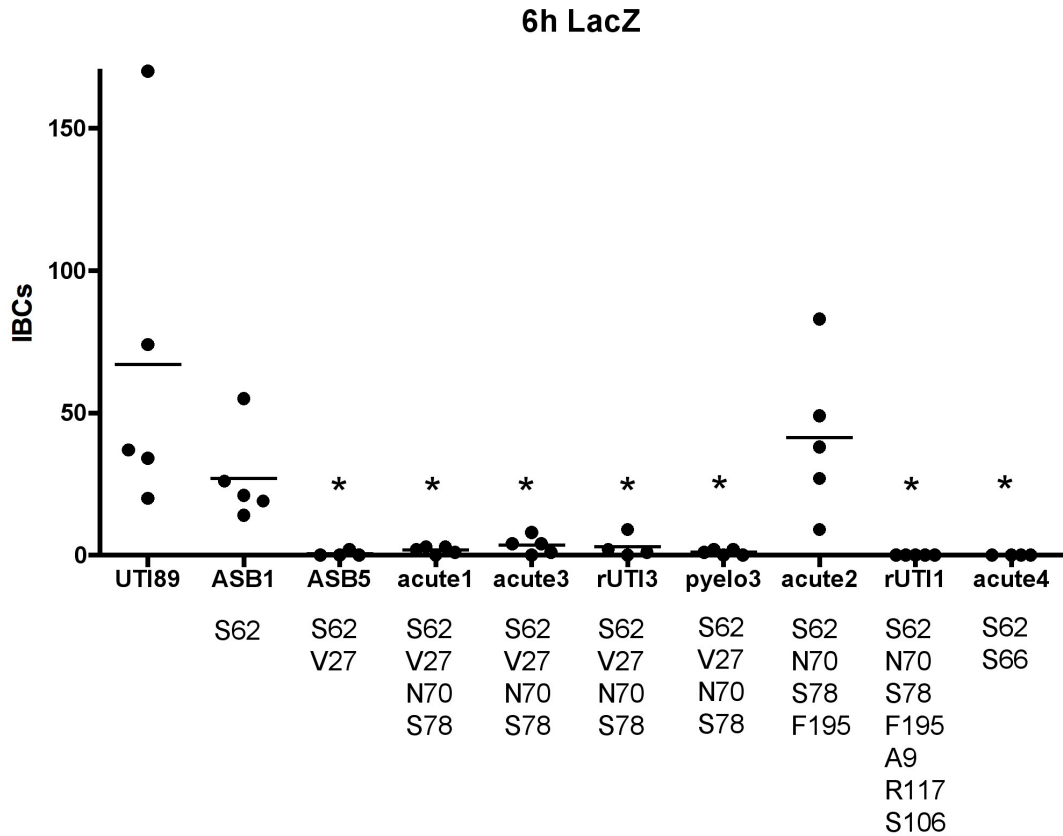


Figure 9. Quantification of IBCs at 6h post-infection from bladders infected with clinical isolates. Below each isolate is listed the amino acids that differ from UTI89.

Amino acids at position 27, 62 and 66 are under positive selection. Isolates with * had significantly fewer IBCs than UTI89 ($p < 0.05$ by Mann-Whitney). Five of the 7 isolates that were significantly different from UTI89 had a valine at position 27 instead of the alanine that is in UTI89.

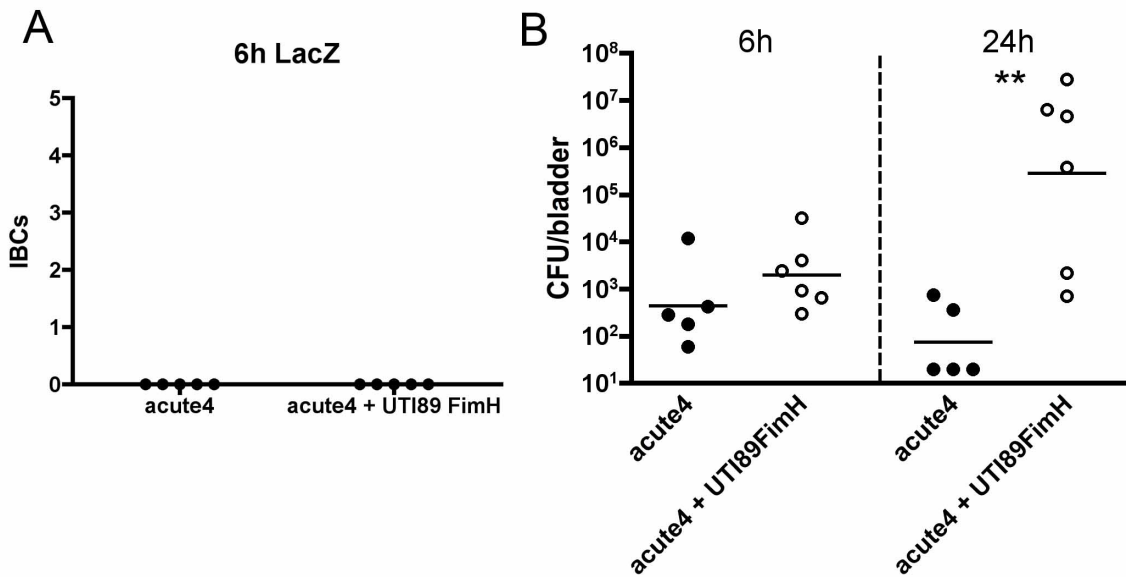


Figure 10. acute4 + UTI89 FimH alters colonization but not IBC formation. (A) IBC quantification at 6h post-infection showed no difference in acute4 and acute4 + UTI89 FimH. (B) Tissue titers at 6h post-infection revealed equal levels of colonization. However, at 24h post-infection, acute4 + UTI89 FimH significantly colonized bladders better than acute4 ($p < 0.01$ by Mann-Whitney).

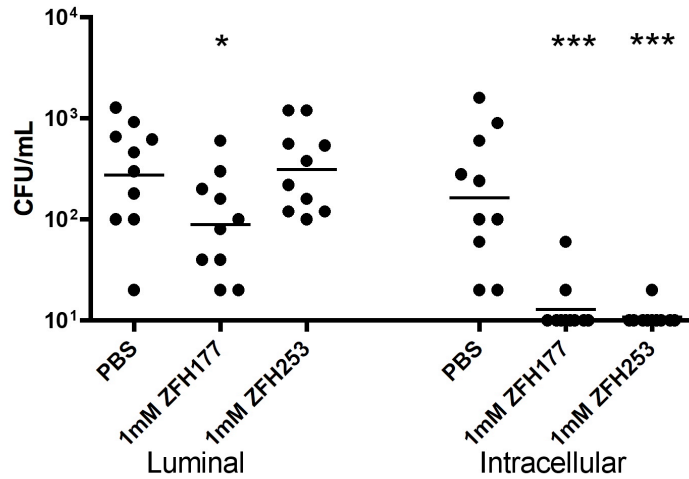


Figure 11. Mannosides ZFH177 and ZFH253 reduced intracellular bacteria at 1 hour post-infection. A 1 hour gentamicin protection assay was used to evaluate the amount of bacteria present in the luminal versus intracellular fraction in the presence of mannosides ZFH177 and ZFH253. A small decrease was seen in the luminal fraction in the presence of ZFH177 ($p < 0.05$) whereas a significant decrease was seen in the intracellular fraction in the presence of either mannoside ($p < 0.0001$).

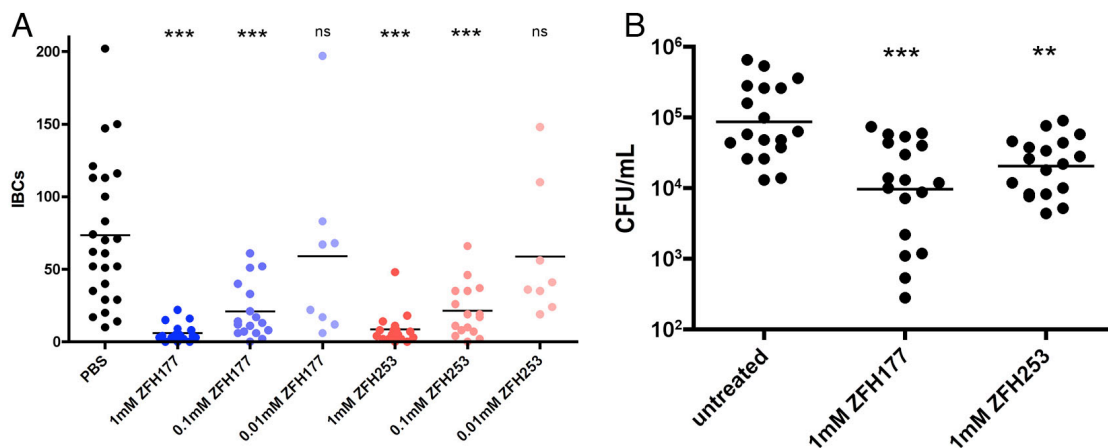


Figure 12. Mannosides ZFH177 and ZFH253 reduce infection capacity *in vivo*. (A) 6 hour LacZ reveals significantly reduced IBCs at 1mM and 0.1mM mannoside for both ZFH177 and ZFH253 ($p < 0.0001$). (B) 6 hour bacterial load quantification reveals significantly reduced colonization with 1mM ZFH177 and 1mM ZFH253 treated bacteria, $p < 0.001$ and $p < 0.01$, respectively.

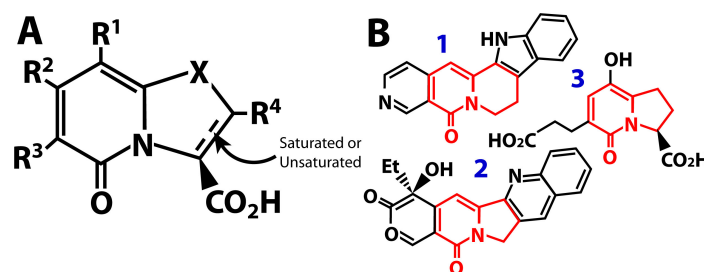


Figure 13. Structures of 2-pyridone compounds. (A) Chemical structure of a ring-fused 2-pyridone with substituent addition sites (R¹-R⁴). (B) Chemical structures of biologically active ring-fused 2-pyridone compounds. Naucietine (1), Camptothecin (2) and A58365A (3). The 2-pyridone core is shown in red.

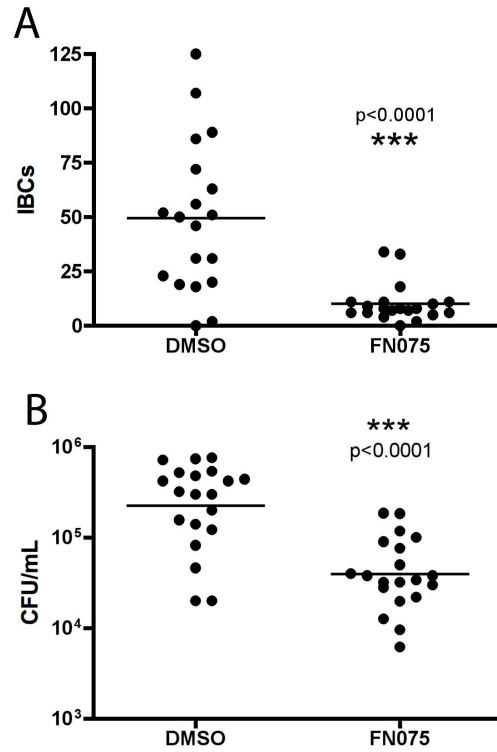


Figure 14. FN075 has an effect on UTI89 bladder colonization *in vivo*. When inoculated in the presence of FN075, UTI89 makes significantly less IBCs in the bladder (A) and has a significantly reduced bacterial load within the bladder at 6 hours post-infection (B). $p < 0.0001$

1. **Aberg, V., F. Norman, E. Chorell, A. Westermark, A. Olofsson, A. E. Sauer-Eriksson, and F. Almqvist.** 2005. Microwave-assisted decarboxylation of bicyclic 2-pyridone scaffolds and identification of Abeta-peptide aggregation inhibitors. *Org Biomol Chem* **3**:2817-2823.
2. **Abreu, P., and A. Pereira.** 2001. New indole alkaloids from *Sarcocephalus latifolius*. *Nat Prod Lett* **15**:43-48.
3. **Ashkar, A. A., K. L. Mossman, B. K. Coombes, C. L. Gyles, and R. Mackenzie.** 2008. FimH adhesin of type 1 fimbriae is a potent inducer of innate antimicrobial responses which requires TLR4 and type 1 interferon signalling. *PLoS Pathog* **4**:e1000233.
4. **Bahrani-Mougeot, F. K., E. L. Buckles, C. V. Lockett, J. R. Hebel, D. E. Johnson, C. M. Tang, and M. S. Sonnenberg.** 2002. Type 1 fimbriae and extracellular polysaccharides are preeminent uropathogenic *Escherichia coli* virulence determinants in the murine urinary tract. *Mol Microbiol* **45**:1079-1093.
5. **Bai, G., E. Smith, A. Golubov, J. Pata, and K. A. McDonough.** 2007. Differential gene regulation in *Yersinia pestis* versus *Yersinia pseudotuberculosis*: effects of hypoxia and potential role of a plasmid regulator. *Adv Exp Med Biol* **603**:131-144.
6. **Berry, R. E., D. J. Klumpp, and A. J. Schaeffer.** 2009. Urothelial cultures support intracellular-bacterial community formation by uropathogenic *Escherichia coli*. *Infect Immun*.
7. **Bishop, B. L., M. J. Duncan, J. Song, G. Li, D. Zaas, and S. N. Abraham.** 2007. Cyclic AMP-regulated exocytosis of *Escherichia coli* from infected bladder epithelial cells. *Nat Med* **13**:625-630.

8. **Bourgogne, A., M. Drysdale, S. G. Hilsenbeck, S. N. Peterson, and T. M. Koehler.** 2003. Global effects of virulence gene regulators in a *Bacillus anthracis* strain with both virulence plasmids. *Infect Immun* **71**:2736-2743.
9. **Bran, J. L., M. E. Levison, and D. Kaye.** 1972. Entrance of bacteria into the female urinary bladder. *N Engl J Med* **286**:626-629.
10. **Buckley, R. M., Jr., M. McGuckin, and R. R. MacGregor.** 1978. Urine bacterial counts after sexual intercourse. *N Engl J Med* **298**:321-324.
11. **Carlson, J. H., W. M. Whitmire, D. D. Crane, L. Wicke, K. Virtaneva, D. E. Sturdevant, J. J. Kupko, 3rd, S. F. Porcella, N. Martinez-Orengo, R. A. Heinzen, L. Kari, and H. D. Caldwell.** 2008. The *Chlamydia trachomatis* plasmid is a transcriptional regulator of chromosomal genes and a virulence factor. *Infect Immun* **76**:2273-2283.
12. **Chen, S. L., C. Hung, J. Pinkner, J. N. Walker, C. K. Cusumano, Z. Li, J. Bouckaert, J. I. Gordon, and S. J. Hultgren.** 2009. Positive selection identifies an in vivo role for FimH during urinary tract infection in addition to mannose binding. *Proc Natl Acad Sci U S A* **Accepted**.
13. **Clive, D. L., D. M. Coltart, and Y. Zhou.** 1999. Synthesis of the Angiotensin-Converting Enzyme Inhibitors (-)-A58365A and (-)-A58365B from a Common Intermediate. *J Org Chem* **64**:1447-1454.
14. **del Pozo, J. L., and R. Patel.** 2007. The challenge of treating biofilm-associated bacterial infections. *Clin Pharmacol Ther* **82**:204-209.
15. **Elliott, T. S., L. Reed, R. C. Slack, and M. C. Bishop.** 1985. Bacteriology and ultrastructure of the bladder in patients with urinary tract infections. *J Infect* **11**:191-199.

16. **Eto, D. S., J. L. Sundsbak, and M. A. Mulvey.** 2006. Actin-gated intracellular growth and resurgence of uropathogenic *Escherichia coli*. *Cell Microbiol* **8**:704-717.
17. **Foxman, B.** 2002. Epidemiology of urinary tract infections: incidence, morbidity, and economic costs. *Am J Med* **113 Suppl 1A**:5S-13S.
18. **Garofalo, C. K., T. M. Hooton, S. M. Martin, W. E. Stamm, J. J. Palermo, J. I. Gordon, and S. J. Hultgren.** 2007. *Escherichia coli* from urine of female patients with urinary tract infections is competent for intracellular bacterial community formation. *Infect Immun* **75**:52-60.
19. **Ghigo, J. M.** 2001. Natural conjugative plasmids induce bacterial biofilm development. *Nature* **412**:442-445.
20. **Hacker, J., G. Blum-Oehler, I. Muhldorfer, and H. Tschape.** 1997. Pathogenicity islands of virulent bacteria: structure, function and impact on microbial evolution. *Mol Microbiol* **23**:1089-1097.
21. **Hacker, J., and J. B. Kaper.** 2000. Pathogenicity islands and the evolution of microbes. *Annu Rev Microbiol* **54**:641-679.
22. **Hedges, S. R., M. Bjarnadottir, W. Agace, L. Hang, and C. Svanborg.** 1996. Immunoregulatory cytokines modify *Escherichia coli* induced uroepithelial cell IL-6 and IL-8 responses. *Cytokine* **8**:686-697.
23. **Henderson, J. P., J. R. Crowley, J. S. Pinkner, J. N. Walker, P. Tsukayama, W. E. Stamm, T. M. Hooton, and S. J. Hultgren.** 2009. Quantitative metabolomics reveals an epigenetic blueprint for iron acquisition in uropathogenic *Escherichia coli*. *PLoS Pathog* **5**:e1000305.
24. **Hooton, T. M., S. Hillier, C. Johnson, P. L. Roberts, and W. E. Stamm.** 1991. *Escherichia coli* bacteriuria and contraceptive method. *JAMA* **265**:64-69.

25. **Hooton, T. M., D. Scholes, A. E. Stapleton, P. L. Roberts, C. Winter, K. Gupta, M. Samadpour, and W. E. Stamm.** 2000. A prospective study of asymptomatic bacteriuria in sexually active young women. *N Engl J Med* **343**:992-997.
26. **Hung, C. S., J. Bouckaert, D. Hung, J. Pinkner, C. Widberg, A. DeFusco, C. G. Auguste, R. Strouse, S. Langermann, G. Waksman, and S. J. Hultgren.** 2002. Structural basis of tropism of *Escherichia coli* to the bladder during urinary tract infection. *Mol Microbiol* **44**:903-915.
27. **Hunstad, D. A., S. S. Justice, C. S. Hung, S. R. Lauer, and S. J. Hultgren.** 2005. Suppression of bladder epithelial cytokine responses by uropathogenic *Escherichia coli*. *Infect Immun* **73**:3999-4006.
28. **Justice, S. S., C. Hung, J. A. Theriot, D. A. Fletcher, G. G. Anderson, M. J. Footer, and S. J. Hultgren.** 2004. Differentiation and developmental pathways of uropathogenic *Escherichia coli* in urinary tract pathogenesis. *Proc Natl Acad Sci U S A* **101**:1333-1338.
29. **Justice, S. S., D. A. Hunstad, P. C. Seed, and S. J. Hultgren.** 2006. Filamentation by *Escherichia coli* subverts innate defenses during urinary tract infection. *Proc Natl Acad Sci U S A* **103**:19884-19889.
30. **Kaper, J. B., J. P. Nataro, and H. L. Mobley.** 2004. Pathogenic *Escherichia coli*. *Nat Rev Microbiol* **2**:123-140.
31. **Kessel, D.** 1971. Some determinants of camptothecin responsiveness in leukemia L1210 cells. *Cancer Res* **31**:1883-1887.
32. **King, S. S., D. A. Young, L. G. Nequin, and E. M. Carnevale.** 2000. Use of specific sugars to inhibit bacterial adherence to equine endometrium in vitro. *Am J Vet Res* **61**:446-449.

33. **Marrs, C. F., L. Zhang, P. Tallman, S. D. Manning, P. Somsel, P. Raz, R. Colodner, M. E. Jantunen, A. Siitonen, H. Saxen, and B. Foxman.** 2002. Variations in 10 putative uropathogen virulence genes among urinary, faecal and peri-urethral *Escherichia coli*. *J Med Microbiol* **51**:138-142.
34. **Martinez, J. J., M. A. Mulvey, J. D. Schilling, J. S. Pinkner, and S. J. Hultgren.** 2000. Type 1 pilus-mediated bacterial invasion of bladder epithelial cells. *EMBO J* **19**:2803-2812.
35. **May, T., and S. Okabe.** 2008. *Escherichia coli* harboring a natural IncF conjugative F plasmid develops complex mature biofilms by stimulating synthesis of colanic acid and Curli. *J Bacteriol* **190**:7479-7490.
36. **McEwan, N. A., G. Kalna, and D. Mellor.** 2005. A comparison of adherence by four strains of *Staphylococcus intermedius* and *Staphylococcus hominis* to canine corneocytes collected from normal dogs and dogs suffering from atopic dermatitis. *Res Vet Sci* **78**:193-198.
37. **Mulvey, M. A., Y. S. Lopez-Boado, C. L. Wilson, R. Roth, W. C. Parks, J. Heuser, and S. J. Hultgren.** 1998. Induction and evasion of host defenses by type 1-piliated uropathogenic *Escherichia coli*. *Science* **282**:1494-1497.
38. **Nataro, J. P., J. Seriwatana, A. Fasano, D. R. Maneval, L. D. Guers, F. Noriega, F. Dubovsky, M. M. Levine, and J. G. Morris, Jr.** 1995. Identification and cloning of a novel plasmid-encoded enterotoxin of enteroinvasive *Escherichia coli* and *Shigella* strains. *Infect Immun* **63**:4721-4728.
39. **Pinkner, J. S., H. Remaut, F. Buelens, E. Miller, V. Aberg, N. Pemberton, M. Hedenstrom, A. Larsson, P. Seed, G. Waksman, S. J. Hultgren, and F. Almqvist.** 2006. Rationally designed small compounds inhibit pilus biogenesis in uropathogenic bacteria. *Proc Natl Acad Sci U S A* **103**:17897-17902.

40. **Porter, M. E., P. Mitchell, A. J. Roe, A. Free, D. G. Smith, and D. L. Gally.** 2004. Direct and indirect transcriptional activation of virulence genes by an AraC-like protein, PerA from enteropathogenic *Escherichia coli*. *Mol Microbiol* **54**:1117-1133.
41. **Reigstad, C. S., S. J. Hultgren, and J. I. Gordon.** 2007. Functional genomic studies of uropathogenic *Escherichia coli* and host urothelial cells when intracellular bacterial communities are assembled. *J Biol Chem* **282**:21259-21267.
42. **Rosen, D. A., T. M. Hooton, W. E. Stamm, P. A. Humphrey, and S. J. Hultgren.** 2007. Detection of intracellular bacterial communities in human urinary tract infection. *PLoS Med* **4**:e329.
43. **Russo, T. A., and J. R. Johnson.** 2000. Proposal for a new inclusive designation for extraintestinal pathogenic isolates of *Escherichia coli*: ExPEC. *J Infect Dis* **181**:1753-1754.
44. **Smajs, D., and G. M. Weinstock.** 2001. The iron- and temperature-regulated *cjrBC* genes of *Shigella* and enteroinvasive *Escherichia coli* strains code for colicin Js uptake. *J Bacteriol* **183**:3958-3966.
45. **Svensson, A., A. Larsson, H. Emtenas, M. Hedenstrom, T. Fex, S. J. Hultgren, J. S. Pinkner, F. Almqvist, and J. Kihlberg.** 2001. Design and evaluation of pilicides: potential novel antibacterial agents directed against uropathogenic *Escherichia coli*. *Chembiochem* **2**:915-918.
46. **Wellens, A., C. Garofalo, H. Nguyen, N. Van Gerven, R. Slattegard, J. P. Hernalsteens, L. Wyns, S. Oscarson, H. De Greve, S. Hultgren, and J. Bouckaert.** 2008. Intervening with urinary tract infections using anti-adhesives based on the crystal structure of the FimH-oligomannose-3 complex. *PLoS ONE* **3**:e2040.

47. **Wright, K. J., P. C. Seed, and S. J. Hultgren.** 2007. Development of intracellular bacterial communities of uropathogenic *Escherichia coli* depends on type 1 pili. *Cell Microbiol* **9**:2230-2241.
48. **Wu, X. R., T. T. Sun, and J. J. Medina.** 1996. In vitro binding of type 1-fimbriated *Escherichia coli* to uroplakins Ia and Ib: relation to urinary tract infections. *Proc Natl Acad Sci U S A* **93**:9630-9635.

APPENDIX I

BACTERIAL ADHESION – A SOURCE OF ALTERNATE ANTIBIOTIC TARGETS

Manuscript in preparation: Cusumano and Hultgren (2009) *iDrugs*.

Corinne K Cusumano¹ and Scott J Hultgren^{1*}

¹Washington University School of Medicine, Department of Molecular Microbiology and Microbial Pathogenesis, 660 S. Euclid Ave, St. Louis, MO 63110, USA

*To whom correspondence should be addressed

Author contributions: CKC and SJH wrote the paper.

Abstract

The prevalence of antibiotic resistance among microorganisms that cause infectious diseases has necessitated the use of new strategies for the development of novel therapeutics. In an effort to thwart this resistance, novel therapeutics are being developed that target bacterial virulence factors as an alternative to the traditional antibiotics which target essential microbial processes promoting bacterial evolution resulting in resistance. While many anti-virulence targets exist, this feature will discuss adhesion as an anti-virulence target using pili of uropathogenic *E. coli* as a model system. The two strategies of drug development discussed in this review involve inhibition of bacterial binding to the host tissue by the addition of exogenous sugars and the disruption of chaperone-usher (CU) pilus assembly through disruption of protein-protein interactions. However, the commonality of adhesion to infectious disease processes and CU pili to many pathogens makes these strategies discussed here translatable to a multitude of organisms.

Keywords

Antibiotic resistance, drug discovery, microbial adhesion, novel therapeutics, biofilm

Introduction

More than a century ago, the discovery of Penicillin marked a significant, albeit not immediately recognized, advance in the field of medicine. By the middle of the 20th century this naturally occurring fungal antibiotic had single-handedly vanquished the biggest wartime killer -- infected wounds. Just four years after the mass production of penicillin began in 1943, resistant microbes started to appear beginning with *Staphylococcus aureus*, followed shortly thereafter by *Streptococcus pneumoniae* and *Neisseria gonorrhoeae*. Today this list includes antibiotic resistant *Enterococcus*, *Salmonella*, *Mycobacterium tuberculosis* and *Escherichia coli*, to name just a few. The bacterial infections which contribute most to human disease are also those in which emerging and microbial resistance is most evident: diarrheal diseases, respiratory tract infections, urinary tract infections, meningitis, sexually transmitted infections, and hospital acquired infections. Thus, there is dire need for new therapeutics to save the lives and ease the suffering of millions of people.

Rising antibiotic resistance

The antibiotics that are available today are primarily variations on a single theme—bacterial eradication based on inhibition of essential molecular processes required for bacterial growth (bacteriostatic) or cellular maintenance (bactericidal). Some target cell-wall biosynthesis, whereas others inhibit protein synthesis or DNA replication. These life or death treatments put selective pressure on the bacteria to adapt or die, selecting for antibiotic resistance. Second generation drugs were developed to combat the resistances that arose, however, they employed the same general mechanism of action. In addition, while some last resort drugs have minimal resistance thus far, they are much more expensive, often are more toxic and typically unavailable to many countries around the world. Consequences of treatment failure due

to antibiotic resistance are high with greater morbidity, mortality and transmission of the resistant organism. Even if pharmaceutical companies increased efforts to develop next generation replacement drugs, bacterial evolution is outpacing drug development for these classes of antibiotics. We are nearing an end to the seemingly endless flow of antimicrobial drugs. We are now faced with a long list of microbes that have found ways to circumvent different structural classes of drugs and are no longer susceptible to most, if not all, therapeutic regimens. New tactics and weapons are needed to combat bacteria that are, owing to evolution and selection, moving targets.

Alternative antibiotic targets

Targeting bacterial virulence is an alternative approach to the development of new classes of antimicrobials that can be used to specifically target and disarm pathogens in the host, while leaving commensal bacteria unperturbed. Prevention of the activity of virulence factors will render the bacteria less able to colonize and give beneficial symbionts and the host immune system time to eradicate the disease causing pathogen prior to colonization or facilitate clearing of an established infection. Furthermore, stripping microorganisms of their virulence properties without threatening their existence may offer a reduced selective pressure for drug-resistant mutations and provide increased potency. Upon exposure to the host, bacteria respond by the production of an arsenal of virulence factors to combat host immune responses and facilitate persistence in their desired niche. There are many examples of virulence factors that represent potential therapeutic targets. Polysaccharide capsules prevent phagocytosis. Siderophores facilitate iron acquisition. Flagella promote motility and chemotaxis. Some bacterial species secrete toxins that alter and disrupt the eukaryotic host cell resulting in disease. Yet another strategy employed by bacteria is the production of a molecular syringe, known as a type three secretion system, that injects

effectors into the host cell causing disease. Another fundamental virulence property of nearly all microbes is their ability to adhere to host cells. This step is typically crucial in pathogenesis and without it bacteria are more likely to be eradicated by the host. Bacterial adhesins typically mediate attachment to a specific receptor with stereochemical specificity, a process that is thought to determine the host and tissue tropisms of a pathogen. While many virulence factors may represent attractive therapeutic targets, this review will focus on two strategies to develop anti-virulence therapeutics based on targeting adhesive pili using uropathogenic *E. coli* (UPEC) as the model system. The first strategy depends on competitively inhibiting bacterial binding to host cells through addition of exogenous carbohydrates that mimic host ligands. The second strategy targets the mechanism by which adhesive pili are assembled thus inhibiting bacterial adhesion to host cells. Thus, both strategies could be used in synergy: the first compound prevents bacterial attachment and colonization by occupying the binding pocket of the bacterial adhesin while the second compound enters the cell and prevents future pilus production. Such a two-pronged approach could eliminate adherence to host cells and promote clearance of the bacteria.

Pili in bacteria

Pathogens are capable of presenting multiple adhesins that can be expressed differentially to permit binding in specific sites and at particular times over the course of a complex infectious cycle. To achieve this, many bacterial species possess long filamentous structures known as pili or fimbriae extending from their surfaces. Pili are extracellular polymers that also have been shown to play a role in invasion, biofilm formation, cell motility, and protein and DNA transport across membranes. Pilus formation is common to many pathogenic bacteria, both Gram-negative and Gram-positive pathogens. Despite the diversity in pilus structure and biogenesis, assembly

mechanisms among Gram-negative and Gram-positive bacteria are conserved within each group. Gram-positive pili are formed by covalent polymerization of pilin subunits in a process that requires a dedicated sortase enzyme. In contrast, Gram-negative pili are typically formed by non-covalent homopolymerization of major pilus subunit proteins. This review will focus on a major family of adhesive pili in Gram-negative bacteria that are classified by their mechanism of assembly; the so-called chaperone/usher (CU) pili (Table 1).

In Gram-negative bacteria, one of the best-characterized pilus assembly systems is the CU pathway. Hundreds of operons encoding CU systems have been reported in a plethora of pathogenic organisms with as many as twelve encoded by a single organism. Examples of CU-assembled adhesive virulence fibers include: Type 1 and P pili predominately on UPEC that cause urinary tract infection (UTI), S pili of *E. coli* strains that cause sepsis, meningitis and UTI and Hif pili of *Haemophilus influenza* which causes otitis media. The causative agents of whooping cough (*Bordetella pertussis*), gastroenteritis (*Salmonella typhimurium*), and pneumonia (*Klebsiella pneumoniae*) also assemble fibers through the CU pathway. Additionally there are 'non-pilus adhesins' assembled by the CU pathway that are generally homopolymers composed of a single protein subunit, like the Afa/Dr family of adhesins of *E. coli* and the polymeric F1 capsular antigen of *Yersinia pestis*. The ubiquitous nature of this pathway paves the way for a potentially broad-spectrum anti-virulence therapeutic that disrupts the assembly of the pilus fibers thus eliminating bacterial colonization.

Pili in UTI

Of the CU pathway assembled pili, P and type 1 pili are the most extensively characterized. Type 1 pili are expressed throughout the *Enterobacteriaceae* family but have been shown to be essential for UPEC in colonization of the urinary epithelium.

UPEC is the leading causative agent for greater than 80% of UTIs which is one of the most common bacterial infections in industrialized countries. UTIs are a significant burden, resulting in more than 8 million outpatient visits per year in the United States and expended costs of US \$3.5 billion annually for evaluation and treatment. Women are the most frequent sufferers – a female has a 60% chance of suffering from at least one UTI in her lifetime. Additionally, up to 44% of women who present with an initial episode of UTI will experience recurrence. While the increased likelihood of recurrence is not entirely understood, data suggests that bacteria can persist within bladder tissue despite antibiotic treatments, and may serve as bacterial reservoirs for recurrent infections.

Type 1 pili are expressed by virtually all UPEC isolates. The FimH adhesin at the tip of type 1 pili achieves specific binding to host cells within the urinary tract. FimH specifically binds mannose groups that abundantly decorate uroplakins on the luminal surface of the bladder. A deep, negatively charged pocket in the N-terminal receptor-binding domain of FimH accommodates the mannose with stereochemical specificity. Once bound, a pathogenic cascade is initiated that involves several distinct phases as examined in the murine cystitis model and human UTIs. Numerous innate defenses are activated early in an attempt to stem off the infection. These defenses include, cytokine induction followed by inflammation, iron sequestering, exfoliation of the colonized epithelial cells and sheer forces elicited by urine flow. Even if UPEC successfully invade into a bladder epithelial cell, the bladder cell has been shown to be able to expel UPEC, potentially serving as an additional innate defense. However, if UPEC are able to escape into the cytoplasm of superficial umbrella cells, they are able to rapidly replicate to form tightly packed intracellular bacterial communities (IBCs) with biofilm-like qualities. Within the urothelial cells, the bacteria are protected from the flow of urine and host defenses. Eventually UPEC detach from the IBC, disperse and initiate new rounds of

IBC formation. This represents a mechanism by which a single invasion event dependent on type 1 pili adhesion can lead to rapid bacterial expansion and colonization of the urinary tract. IBC formation occurs in the acute states of infection. One long-term outcome of infection is that UPEC are also able to form a quiescent intracellular reservoir (QIR) within the bladder. Bacteria in the QIR do not rapidly replicate, but remain dormant, hidden from the immune system and antibiotics. They are then able to reestablish an infection at later timepoints post-treatment resulting in a recurrence. Due to this alternative pathway of continuous colonization, UTIs are more frequently being identified as chronic infections. Detailed analysis of the UPEC pathogenic cascade has identified several potential targets to inhibit virulence, such as siderophores, capsule and flagella. However, type 1 pili represent a particularly attractive drug target because they are ubiquitous among UPEC, and are required to initiate a pathogenic cascade that evades the host immune system and can lead to acute, chronic, persistent or asymptomatic infection. Disruption of type 1 pili function could break the cycle of chronic infection.

New drug development strategies to inhibit pilus mediated function

Carbohydrates of various forms are abundantly expressed on the animal cell surface. Microbes have taken advantage of this property and evolved with the ability to adhere to sugar receptors in an organ-specific manner for colonization and infection. Sugars are commonly involved in cell recognition and communication playing important roles in microbial adherence and uptake, colonization and biofilm formation, and in virulence. Since bacterial adhesion to host cells is extremely specific, exogenous sugars can block binding to carbohydrate receptors and competitively displace or inhibit bacteria from attachment to cells. The ability to impair bacterial adhesion represents an ideal strategy to combat bacterial pathogenesis because it targets an important early step in

the infectious process, and would also be suitable for use as a prophylactic to prevent infection. In the case of UPEC, knowledge of the structural basis of how FimH recognizes the mannose receptor, has led to the development of a ligand-based antagonist, termed mannoside, that mimics the natural receptor for FimH but with increased affinity and avidity. Mannosides effectively block the adhesive properties of type 1 pili by inhibiting bacterial colonization, invasion, IBC formation and disease. Furthermore, the sequence of approximately 300 *fimH* genes of clinical UPEC isolates showed that the mannose-binding pocket is invariant. Thus mannosides are a powerful new class of therapeutics that could have a potent therapeutic effect by preventing UPEC pathogenesis and disease. This approach can be readily extended to other adherent organisms by tailoring the anti-adhesive compounds to antagonize their specific receptor-ligand interactions (Figure 1). Indeed, sugars designed to target adhesive structures of organisms such as *Pseudomonas aeruginosa*, *Staphylococcus* and *Streptococcus* have already proved efficacious at inhibiting adherence *in vitro*.

The goal of the second strategy is to interrupt pilus assembly, which, like the first strategy, blocks pilus-mediated adhesion and subsequent disease. To disrupt pilus assembly, one must first understand the mechanisms employed by bacteria to form fibers. Chaperone-usher mediated assembly prevents premature subunit aggregation and facilitates the ordered secretion, folding and assembly of hundreds of thousands of subunits into fibers on the surface of a bacterium. Components of the pilus are secreted through the general secretory pathway into the periplasm. Once in the periplasmic space, a specific chaperone binds each pilus subunit to facilitate proper folding and prevent premature assembly of subunits. Each subunit consists of six of the seven strands of a standard immunoglobulin (Ig)-fold and an N-terminal extension (Nte) (Figure 2A). In order to form a stable structure prior to incorporation into the growing fiber, the chaperone donates structural information to each subunit, its G1 β strand, to

compensate for the missing seventh strand of the subunit in a process called donor strand complementation (DSC) (Figure 2B). DSC prevents aggregation of the subunits prior to fiber formation. The pilin/chaperone complex is then delivered to the usher, which is a pore in the outer membrane and serves as a platform for pilus assembly. During pilus assembly, the free Nte of one subunit displaces the chaperone bound to another subunit and serves as the seventh strand of the Ig-like fold in a process called donor strand exchange (DSE) (Figure 2C). DSE leads to the polymerization of the fiber extending from the bacterium. Since chaperone-usher systems are necessary for the assembly of extracellular adhesive organelles in a wide range of pathogens, inhibitors may serve as broad-range anti-virulence therapeutics, an attractive feature that would enhance the marketability of an effective drug.

Pilicides are a class of pilus inhibitors that target chaperone function and inhibit pilus biogenesis. A recent study (Pinkner JS *et al*: PNAS (2006) **103**(47):17897-17902) identified a new class of pilicides based on a bi-cyclic 2-pyridone chemical scaffold that inhibit pilus assembly by binding to the chaperone and disrupting the chaperone-usher interaction. As a result, pilicides inhibit pilus dependent activities such as colonization, invasion and biofilm formation. Biofilms are structured communities of microorganisms encapsulated within a self-developed polymeric matrix that defends them against antibiotics and the host immune system. They are of great medical importance, accounting for over 80% of microbial infections in the body. Pilicides target regions on the chaperone that are highly conserved among chaperone-usher pathways and are thus able to inhibit assembly of multiple pilus systems (type 1 and P pili of *E. coli*) (Figure 1). Pyridinones also avoid the severe drawbacks observed for peptide-based drugs; poor absorption after oral administration, rapid enzymatic degradation, and quick excretion.

Another distinct mechanism of adhesive fiber assembly among Gram-negative bacteria is fibers assembled by the extracellular nucleation/precipitation pathway (curli). Curli are proteinaceous fibers found on enteric bacteria such as *E. coli* and *Salmonella* spp. Despite curli's unclear role in pathogenesis, their biochemical and structural properties resemble eukaryotic amyloid fibers found in neurodegenerative diseases, such as Alzheimer's, Parkinson's, and prion diseases making them an ideal model system to study amyloid biogenesis. Curli are heteropolymers that consist of a major subunit, CsgA, and minor subunit, CsgB. CsgA and CsgB are secreted into the extracellular milieu via the outer membrane pore, CsgG. With the help of two chaperone-like proteins, CsgE and CsgF, CsgA is nucleated into a fiber by CsgB. Curli fibers have been implicated in biofilm formation, environmental survival and resistance to sanitizing agents. A recent study (Cegelski L *et al*: submitted) showed that derivatives of the 2-pyridone compounds mentioned above were able to inhibit curli assembly giving them the name curlicides. The lack of curli fibers prevented curli-dependent biofilm formation and reduced infection load *in vivo* as measured by the murine model of UTI. Pilicides and curlicides selectively disrupt a protein-protein interaction required for the biogenesis of a bacterial virulence factor instead of targeting a process essential for survival.

Employing both anti-virulence strategies, inhibition of receptor binding and disruption of pilus assembly, could result in very potent anti-adhesive therapeutics. For example, synergistic effects could be obtained by inhibiting pre-existing type 1 pilus function through mannosides while also eliminating the ability to produce new pili through pilicides. Furthermore, if infection is not entirely controlled by the two-pronged approach, antibiotics can be added, however, at much lower concentration to reduce the opportunity to develop resistance. Type 1 pili are an essential virulence factor for colonization of the urinary tract and are the most extensively studied chaperone-usher

fimbrial system. Thus, they have been described in this review as an excellent target resulting in the development of new prototypic therapeutics to treat UTIs. This new drug class could translate into a multitude of other therapies for Gram-negative infections.

Conclusion

While this review focuses on the development of therapeutics to inhibit adhesion, there are many other virulence factors employed by bacteria to colonize and persist within the host. The general strategy of inhibiting virulence factors rather than essential growth factors changes the paradigm of drug development and reduces the evolutionary pressure for bacteria to develop resistance. Bacteria can survive in the presence anti-virulence drugs, but will be eliminated by the host immune system prior to establishing a foothold. Furthermore, since a complex virulence mechanism is targeted, if mutants arise, they will most likely be avirulent. If the host immune system cannot resolve any residual infection, it is possible to couple anti-virulence therapeutics with traditional antibiotics although at lower doses thus reducing resistance potential. A commitment to developing therapeutics that target virulence requires a serious change in our perspective for treating infectious diseases and increased efforts should be focused on bringing these new therapeutics from bench to bedside.

Chaperone-usher assembled pili

Adhesive fiber	Major pilin	chaperone/usher	Adhesin	Organisms	Disease
Type 1	FimA	FimC/FimD	FimH	<i>Escherichia coli</i> , <i>Klebsiella pneumoniae</i> , <i>Salmonella</i> species	cystitis, sepsis, meningitis
P	PapA	PapD/PapC	PapG	Uropathogenic <i>E. coli</i> (UPEC)	pyelonephritis
Prs	PrsA	PrsD/PrsC	PrsG	<i>E. coli</i>	cystitis
S	SfaA	SfaE/SfaF	SfaS	<i>E. coli</i>	UTI, meningitis, sepsis
Hif	HifA	HifB/HifC	HifE	<i>Haemophilus influenzae</i>	otitis media, meningitis
Type 2 and 3	Fim2 & Fim3	FimB/FimC	FimD	<i>Bordetella pertussis</i>	whooping cough
Pef	PefA	PefD/PefC	unknown	<i>Salmonella typhimurium</i>	gastroenteritis
Long polar fimbriae	LpfA	LpfB/LpfC	unknown	<i>S. typhimurium</i>	gastroenteritis
MR/K	MrkA	MrkB/MrkC	MrkD	<i>K. pneumoniae</i>	pneumonia
Myf fimbriae	MyfA	MyfB/MyfC	unknown	<i>Yersinia enterocolitica</i>	enterocolitis
PMF	PmfA	PmfC/PmFD	PmfF	<i>Proteus mirabilis</i>	UTI
Dr	DraA	DraB/DraC	DraE	UPEC Diffuse adhering <i>E. coli</i> (DAEC)	pyelonephritis cystitis
Afa	AfaA	AfaB/AfaC	AfaE	UPEC	cystitis, diarrhea
F1	Caf1	Caf1M/Caf1A		<i>Yersinia pestis</i>	plague

Alternative chaperone pathway

Adhesive fiber	Major pilin	Assembly proteins	Adhesin	Organism	Disease
CS1 pili	CooA	CooB/CooC	CooD	<i>E. coli</i>	diarrhea

Extracellular nucleation-precipitation pathway

Adhesive fiber	Assembly proteins	Adhesin	Organism	Disease
Curli	CsgB (nucleator), CsgE and CsgF (assembly) and CsgG (secretion)	CsgA (major subunit)	<i>E. coli</i>	sepsis
			<i>Salmonella</i> spp.	gastroenteritis, sepsis

Table 1. Representative adhesive fibers, fiber classification and disease association

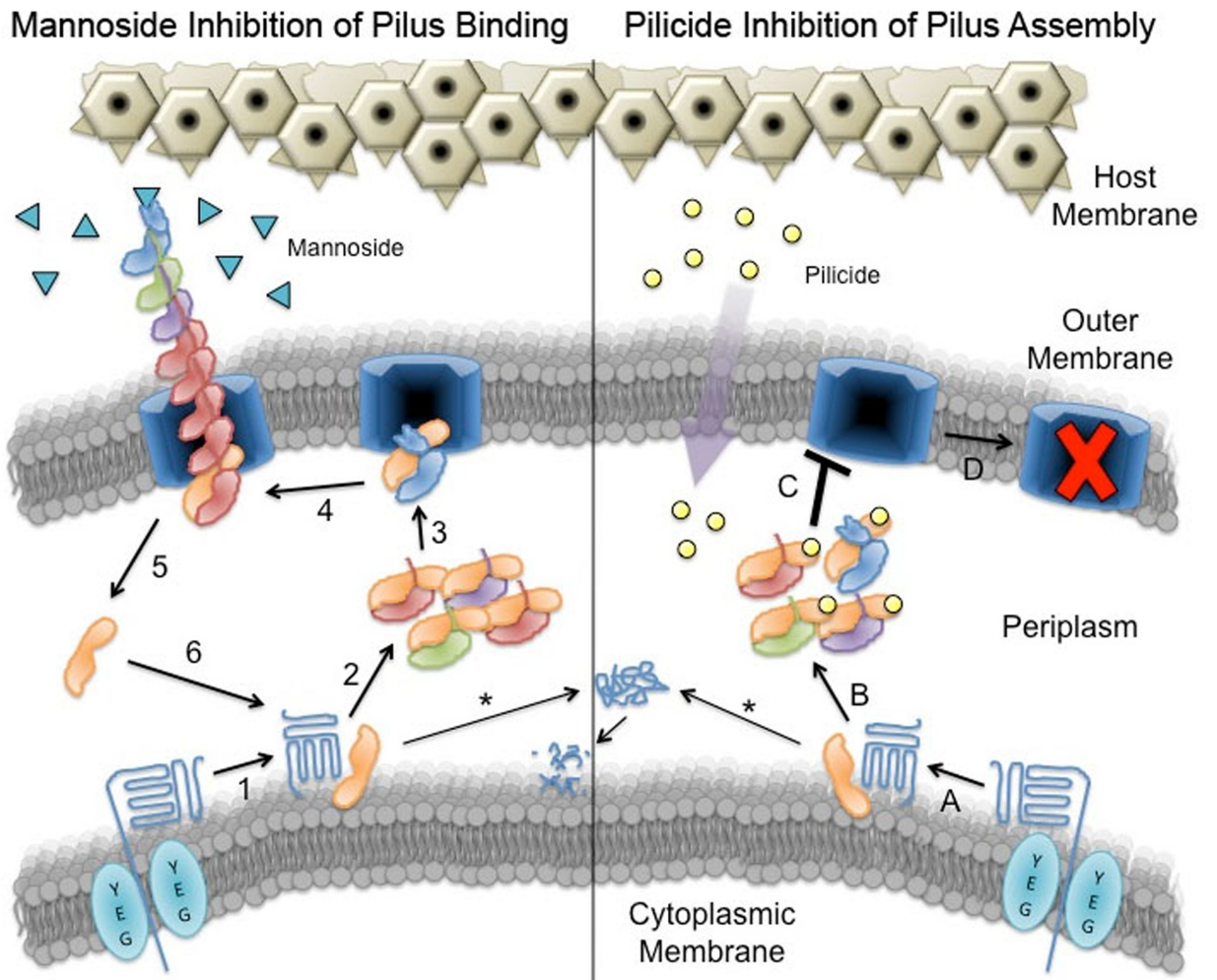


Figure 1. Two strategies to inhibit bacterial binding to host cells. The schematic diagram shows the model of chaperone-assisted pilus assembly and the mode of mannoside (left panel) and pilicide (right panel) action. During normal pilus biogenesis, newly synthesized pilus subunits cross into the periplasm via the Sec secretion pathway. These pilus subunits bind to their periplasmic chaperone proteins (orange molecules) and fold into correct conformations (1). In the absence of the chaperones, pilus subunits are degraded (*). Chaperone-subunit complexes (2) are transported to the outer membrane usher proteins (blue cylinders) for assembly (3). Pilus assembly follows an ordered process with the chaperone-adhesin complexes as the initiators (4). As subunits are assembled into the growing pilus, accompanying chaperones disassociate from the membrane complexes (5), which could potentially be recycled to bind newly synthesized subunits. Mannosides (teal triangles) interact with the pilus adhesin and prevent binding to mannose residues (light brown triangles) on the surface of epithelial cells. Pilicides (yellow circles) can cross freely through bacterial outer membranes and bind to periplasmic chaperones (B). Pilicides block the interaction of chaperone-subunit complexes with the outer membrane usher (C) and prevent pilus assembly (D).

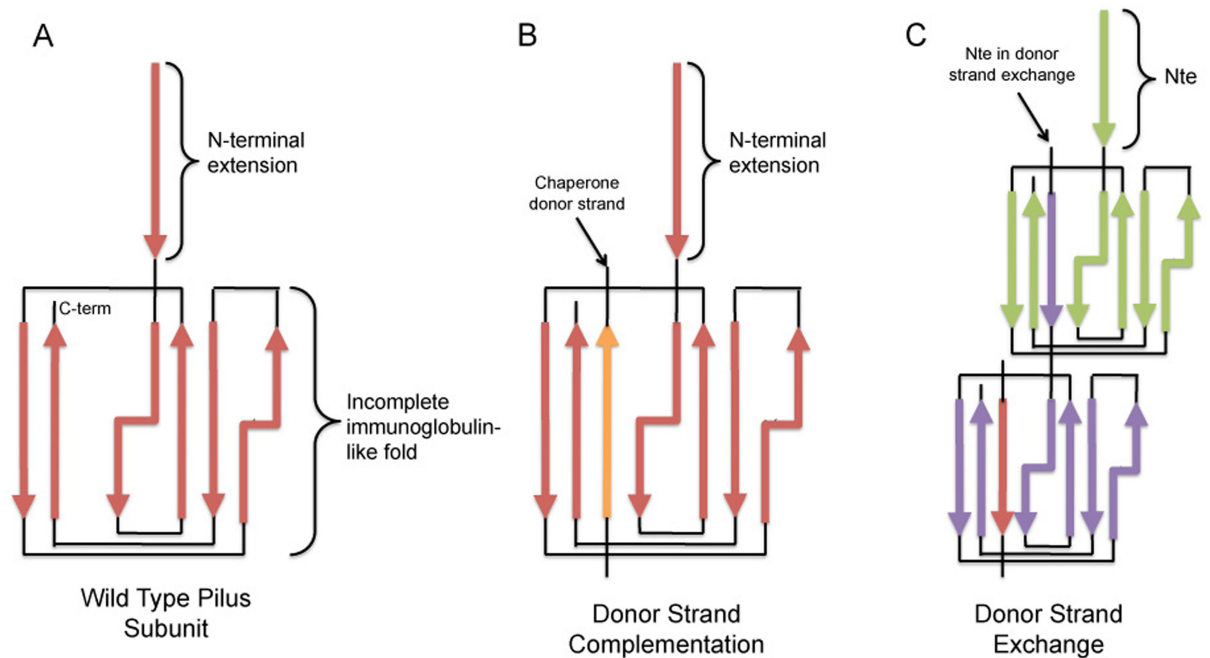


Figure 2. Chaperone-subunit donor strand exchange (DSE) and donor strand complementation (DSC). (A) Each subunit consists of six of the seven strands of a standard immunoglobulin (Ig)-fold and an N-terminal extension (Nte). (B) In order to form a stable structure prior to incorporation into the growing fiber, the chaperone donates the missing seventh strand of the subunit in a process called donor strand complementation (DSC). (C) During pilus assembly, the free Nte of one subunit displaces the chaperone bound to another subunit and serves as the seventh strand of the Ig-like fold in a process called donor strand exchange (DSE).

Further Reading

1. Åberg V, Almquist F: **Pilicides—small molecules targeting bacterial virulence.** *Org Biomol Chem* (2007) **5**:1827-1834.
2. Arkin MR, Wells JA: **Small-molecule inhibitors of protein-protein interactions: progressing towards the dream.** *Nat Rev Drug Discov* (2004) **3**(4):301-317.
3. Barnhart MM, Chapman MR: **Curli biogenesis and function.** *Annu Rev Microbiol* (2006) **60**: 131-147.
4. Cegelski L, Marshall GR, Eldridge GR, Hultgren SJ: **The biology and future prospects of antivirulence therapies.** *Nat Rev Microbiol* (2008) **6**(1): 15-27.
5. Foxam B: **Epidemiology of urinary tract infections: incidence, morbidity, and economic costs.** *Dis Mon* (2003) **49**(2): 53-70.
6. Justice SS, Hung C, Theriot JA, Fletcher DA, Anderson GG, Footer MJ, Hultgren SJ: **Differentiation and developmental pathways of uropathogenic Escherichia coli in urinary tract pathogenesis.** *Proc Natl Acad Sci USA* (2004) **101**(5): 1333-1338.
7. Lloyd DH, Viac J, Werling D, Reme CA, Gatto H: **Role of sugars in surface microbe-host interactions and immune reaction modulation.** *Vet Dermatol* (2007) **18**(4): 197-204.
8. Proft T, Baker EN: **Pili in Gram-negative and Gram-positive bacteria – structure, assembly and their role in disease.** *Cell Mol Life Sci* (2009) **66**(4): 613-635.
9. Sauer FG, Barnhart M, Choudhury D, Knight SD, Waksman G, Hultgren SJ: **Chaperone-assisted pilus assembly and bacterial attachment.** *Curr Opin Struct Biol.* **10**(5): 548-556.
10. **Understanding antimicrobial (drug) resistance:** NIAID, Washington, D.C. (2009). www.niaid.nih.gov/topics/antimicrobialresistance.htm.